RICE UNIVERSITY

Enabling QoS Controls in Modern Distributed Storage Platforms

By

Yuhan Peng

A THESIS SUBMITTED
IN PARTIAL FULFILLMENT OF THE
REQUIREMENTS FOR THE DEGREE

Doctor of Philosophy

APPROVED, THESIS COMMITTEE

T. S. Eugene Ng
T. S. Eugene Ng (Apr 15, 2020)

Eugene Ng

Eugene Ng

Ang Chen
Ang Chen (Apr 16, 2020)

Ang Chen

Ang Chen

Peter Varman

Peter Varman

Peter Varman

HOUSTON, TEXAS

April 2020

ABSTRACT

Enabling QoS Controls in Modern Distributed Storage Platforms

by

Yuhan Peng

Distributed storage systems provide a scalable approach for hosting multiple clients on a consolidated storage platform. The use of shared infrastructure can lower costs but exacerbates the problem of fairly allocating the IO resources. Providing performance Quality-of-Service (QoS) guarantees in a distributed storage environment poses unique challenges. Workload demands of clients shift unpredictably between servers as their locality and IO intensities fluctuate. This complicates the problem of providing QoS controls like reservations and limits that are based on aggregate client service, as well as providing differentiated tail latency guarantees to the clients.

In this thesis, we present novel approaches for providing bandwidth allocation and response time QoS in distributed storage platforms. For bandwidth allocation QoS, we develop a token-based scheduling framework to guarantee the maximum and minimum aggregate throughput of different clients. We introduce a novel algorithm called *pTrans* for solving the token allocation problem. *pTrans* is provably optimal and has better theoretical and empirical scalability than competing approaches based on linear-programming or max-flow formulations. For the response time QoS, we introduce *Fair-EDF*, a framework that extends the earliest deadline first (*EDF*) scheduler to provide fairness control while supporting latency guarantees.

Acknowledgments

Firstly, I would like to thank my advisor, Professor Peter Varman, for advising my PhD research. He provided me excellent guidance in developing research ideas and conducting research in the field of distributed storage systems and QoS. Professor Varman also offered a lot of help in publishing the research papers based on the thesis, as well as in revising this thesis document. I also express my appreciation to Professor Eugene Ng and Professor Ang Chen for serving on my PhD thesis committee and providing valuable feedback before and during my PhD defense.

In addition, I thank my teammate, Qingyue Liu, for help in performing the experiments, and in providing useful feedback for paper revisions. I also thank my 4-year roommate, Peng Du, as well as other friends, for offering me a warm and harmonious life environment to conduct my PhD research.

Finally, I would like to thank my parents and other family members for their support and love. Without them, I could not imagine how could I achieve the accomplishments in my research.

Contents

Illustrations

Tables

Chapter 1

Introduction and Overview

1.1 Introduction

Distributed storage systems are widely deployed in today's datacenters, to scalably manage the ever-increasing volume of persistent data. Providing **Quality of Service (QoS)** performance guarantees to clients sharing system resources in an important requirement of such systems. Performance QoS involves two aspects: *resource allocation* that sets policies and mechanisms to divvy up system resources among competing clients, and *request scheduling* to enforce the allocation. In general, QoS guarantees can be for physical resources like network bandwidth and CPU time, or derived metrics like request throughput and response time. In this thesis, the I/O request throughput (number of I/O requests per second or IOPS) and tail-latency guarantees (percentage of requests meeting a specified response time target) will be used as the QoS measures.

The thesis is motivated by the need to provide *bucket* QoS in distributed storage systems, an important requirement that has not been addressed by existing works. A **bucket** is a collection of related stored objects that are treated as a single logical entity for purposes of QoS. In practice, a bucket will consist of several directories, program or data files, or file chunks, belonging to a designated owner. The bucket objects may be accessed by multiple clients authorized by the owner. For instance, the bucket owner may be a department within an organization, and the clients could

be departmental team members. The owner of the bucket is responsible for paying for the storage services for the bucket objects by the different authorized clients. A bucket can be distributed across multiple storage nodes based on the data allocation policies of the storage system.

Although many existing QoS studies have been proposed over the past two decades, most approaches focused on providing QoS in a centralized server environment rather than a distributed server cluster. A few approaches to QoS for distributed systems that have been proposed, impose strong restrictions that make them unsuitable for providing bucket QoS (see Section 1.3.1).

Providing bucket QoS in a distributed environment is challenging, because of the spatial and temporal variability in demand and capacity distributions across the servers. Firstly, since a bucket's objects are distributed by the storage system across multiple servers, the aggregate bucket demand can be distributed unevenly on different servers. In addition, the rate at which a server can perform I/Os (referred to as the server *capacity*), may also depend on the workload characteristics. Finally, requests for multiple buckets may overload some servers, raising the questions of which requests to serve, which to defer, and which to drop, in order to meet QoS requirements.

In this thesis, we introduce novel QoS algorithms for the QoS support in distributed storage platforms. We focus on bandwidth allocation QoS and response time QoS. For bandwidth QoS, we focus on providing reservations and limits, which represent the minimum and maximum I/Os per second allowed for the bucket. We present **bQueue**, a token-based framework for bandwidth QoS, and **pTrans**, a scalable algorithm for dynamic token distribution. For response time QoS, we focus on meeting the tail-latency requirements of the buckets, in which each bucket specifies

the percentage of requests that must meet a specified latency bound. We introduce **Fair-EDF**, which provides support for differentiated latency guarantees. The proposed algorithms can be applied for both conventional client QoS and bucket QoS *. We also present empirical evaluation results of the proposed QoS algorithms, and show that they provide reliable QoS support.

1.2 Distributed Storage Platform Overview

1.2.1 Clustered Storage Systems

Clustered storage systems such as Ceph [1], GlusterFS [2], Amazon's Cloud Storage [3], FAB [4], Kudu [5], Dynamo [6], Cassandra [7], HDFS [8], vSAN [9] and VMWare storage DRS [10], provide a scalable and economical approach for the storage of huge data sets over multiple storage servers. When deployed in a datacenter these systems are shared among multiple clients, each representing tens to hundreds of users. Clients require predictable performance typically codified in *service-level objectives* (SLOs) such as guaranteed throughput (averaged over a specified duration) or a maximum response time for a specified percentage of its requests.

Object-based storage decouples namespace management from the underlying hardware, facilitating the use of decentralized scale-out architectures spread over multiple storage servers (even geographical regions), and supports APIs for remote access to stored data. Multiple related objects can be encapsulated within logical containers called **buckets** and accessed using object identifiers. Amazon S3, for instance, treats buckets and objects as controllable resources and provides APIs to create or delete buckets and upload objects. The storage system is responsible for storage and access

*To maintain generality, we use the term *client* as the entity for the QoS support. When providing bucket QoS, *clients* refer to the owners of the buckets.

of objects. Objects may be sharded for manageability, and distributed over multiple storage nodes for fault tolerance and performance, while decentralized protocols provide concurrency control and manage object consistency. A cluster manager monitors the performance of nodes and links and is responsible for recovery from failures.

The focus of this thesis is on sharing the storage subsystem. In this scenario, the storage server must provide explicit controls for service differentiation to prevent some clients from unfairly monopolizing system resources, and favoring preferred customers with better service when there is resource contention. In addition, service differentiation is also necessary to prioritize system usage over client needs. For instance, I/O traffic to rebuild a failed node on a replacement server competes with normal application traffic; QoS policies must permit rebuilding to proceed quickly while avoiding unreasonable application slowdowns.

1.2.2 Chip-level Distributed Storage Devices

A new generation of non-volatile memory devices and interfaces are changing the traditional storage landscape made up of SSA/SATA based hard disks (HDs) and solid-state devices (SSDs). The adoption of the NVMe interface, a purpose-crafted protocol to access SSDs using the PCIe bus standard, has increased the performance of modern SSDs by orders of magnitude, while new memory-bus connected persistent memory devices like Optane DC promise to further blur the performance gap between volatile DRAM memory and non-volatile storage. NVMe over Fabric protocols based on Remote Direct Memory Access (RDMA) and Fiber Channel (FC) technologies are poised to bring the latency and parallelism advantages of NVMe to distributed storage. These hardware innovations have raised questions about how to structure storage system software to exploit their unique characteristics and handle newly-

exposed performance bottlenecks.

Datacenter storage is a shared resource that is accessed by hundreds or thousands of concurrent users. Performance isolation techniques are usually deployed at the OS layer to allocate I/O bandwidth fairly and prevent aggressive workloads, with high request rates or large request sizes, from grabbing excessive resources. This approach has been fairly successful in host-centered I/O request schedulers accessing traditional HD/SSD devices. In this scenario, the storage device is typically treated as a black box and assumed to handle its internal requests fairly; average read and write times are often used to characterize its I/Os.

These simple models that underly traditional storage software become increasingly untenable for modern SSD devices that provide a multiplicity of parallel data channels to access (multibit encoded) NAND flash cells arranged in multiple planes, chips, and dies that provide large amounts of internal concurrency. In NVMe SSDs, the host-side I/O request queues bypass the OS and are directly exposed to the SSD controller, which can make better scheduling decisions based on informed knowledge of the internal device state. However, there is a considerable gap between the commercially available MQ-SSDs and the models used for their evaluation. A recent study [11] of real-world MQ-SSDs highlighted the performance loss arising from internal interference between workloads and contention for internal resources that are not captured by currently used models. In fact, only recently has an accurate and extensible simulator, MQSim [12] become broadly available for conducting research on MQ-SSDs.

1.3 QoS Overview

1.3.1 Bandwidth QoS

With shared storage becoming the norm in cloud and datacenter deployments, QoS controls are becoming an increasingly important requirement of storage systems. There has been considerable past research [13–21] on providing such controls for virtual machines sharing a single storage-attached server or a SAN-attached storage array. These QoS controls typically take the form of reservations and limits on the I/Os of a single virtual machine. Each VM is guaranteed a minimum number of IOPS (I/O requests per second) as well as an upper limit on the number of IOPS it should be allowed. These controls are provided by a storage QoS module within the hypervisor running on a host. The I/Os of all VMs go through the hypervisor module, which controls the order and timing of requests dispatched to the storage backend to enforce fine-grained QoS guarantees.

Providing QoS in distributed storage creates new challenges not addressed in most previous work. In one scenario, each client contracts for a minimum and maximum number of I/Os (over a specified time interval) on objects stored in the distributed system. The **QoS period** refers to the time interval over which the performance guarantees are enforced. Early policies had QoS periods of days or weeks, and mainly concentrated on billing and limit enforcement. In our model, the **reservation** guarantees a minimum number of I/Os for the client in every QoS period, aggregated over all servers, *i.e.* a lower bound on the IOPS averaged over a QoS period. Similarly, the **limit** places an upper bound on the maximum number of I/Os allowed for the client, aggregated over all servers over a QoS period.

Since the requests of a client are distributed over multiple storage nodes, the QoS

mechanism must account for the service received at multiple servers for each client. Furthermore, since I/O requests to objects follow independent paths from the client to the destination servers, there is no single control point that sees all the requests of even a single client. Providing QoS guarantees in this distributed environment is a challenging problem that has not been addressed in its full generality before. In contrast, existing distributed solutions [18, 20, 22] considered a restricted model where requests from a client are funneled through a single ingress point and then dispersed to distributed servers. The single ingress point allows global information to be collected about a client's requests before they are forwarded to the appropriate storage node. The requests carry meta-information added by the ingress node that are then used by the node scheduler. These server node schedulers are sophisticated fine-grained QoS schedulers (like mClock [20]) that use request-level real-time tags to guarantee reservations and limits, and arbitrate among the requests of different clients.

1.3.2 Response Time QoS

The problem of guaranteeing latencies in storage systems has been extensively studied over the years. Many solutions like [23–33] combine workload shaping and real-time deadline scheduling algorithms to meet QoS latency bounds, based on two-sided SLOs. Others [34–40] present a variety of different system techniques to reduce average or tail latencies.

In order to make strong response time QoS guarantees, two-sided SLOs are employed; the client receives the agreed-upon latency guarantees provided its input meets specified constraints on its arrival rates and the sizes and frequency of its bursts [29]. Admission control is used to limit the mix of clients in the system to a sustainable

set, regulators police client traffic for compliance with input SLOs, and schedulers order the requests in a globally expedient manner to meet guarantees. However, in distributed storage, requests belonging to a client are directed to different storage servers based on the internal placement and replication policies of the system. Clients are typically unaware of the data placement, making it hard to predict the dynamic runtime demands on any particular server. Hence, the traffic seen by an individual server is highly dynamic and difficult to limit using traffic regulators like token-bucket controllers. While SLO policing may be used to regulate the *aggregate* client traffic characteristics, it is unreasonable (and impractical) to require these at the individual server level.

A recent work, MittOS [41], describes a novel driver-level model and implementation that predicts whether an arriving request can meet its deadline, and drops (or redirects) the arriving request if it cannot. In this thesis, we propose an orthogonal dimension to this solution: we describe an algorithm for deciding when to discard a request and which request to drop based on the QoS requirements. If the estimates of the service time are accurate then the algorithm drops the provably minimum number of requests possible.

1.4 Motivation

In many datacenter deployment scenarios, QoS needs to be provided at the granularity of buckets. For instance, an organization may lease a bucket of raw storage on behalf of its departments, or an application service provider may group its application files and user data sets in a bucket. In these cases, the storage provider may be asked to guarantee the owner of the bucket a certain minimum average I/O throughput (in MB/s or IOPS) aggregated over all accesses to the bucket's objects. Similarly

to enforce pay-for-service fairness, IOPS to a bucket may be limited to a maximum contractually-agreed-upon amount. Fine-grained QoS that enforced I/O reservations and limits for VMs within a host was introduced in VMWare's vSphere 5.5 [42], and for multiple hosts sharing a SAN-based array in VMWare storage DRS [10]. However, providing bucket QoS in distributed storage systems with multiple, independent storage nodes has been largely lacking.

In the distributed environment considered in this thesis, it is impractical to force all requests made to a bucket through a single ingress node. This makes approaches to distributed QoS based on global tagging [20, 43, 44] of requests of a client infeasible. Furthermore, it is desirable to use simple request schedulers at the nodes that do not rely on real-time, request-level synchronization, and are less CPU intensive than those used in conjunction with global tagging. Moreover, while the existing schedulers provide very fine-grained QoS guarantees, in a distributed environment coarse-grained guarantees are adequate, due to significant jitter in the latencies of other system components.

Providing response time QoS in the distributed model considered in this thesis, raises the following question: how to provide reasonable differential response time guarantees for clients sharing a server when the traffic cannot be predicted or controlled at the ingress to the server? One simple approach to provide latency QoS is to use a two-level scheduling scheme: the server capacity is divided among the clients (using a fair scheduler) in a specified ratio based on the client SLOs, and each client orders its own requests (using *EDF* for instance) within its capacity allocation. As discussed in [45], this approach requires significant capacity overestimation and, in any case, cannot work when the server load is not known. This motivates the *Fair-EDF* scheduling algorithm proposed in this thesis.

1.5 Thesis Statement

The thesis statement is stated below:

Modern distributed storage platforms are shared by multiple concurrent clients with different performance QoS requirements. This thesis introduces new efficient algorithms to provide bandwidth and tail-latency QoS in distributed storage platforms, with provable performance guarantees.

1.6 Contributions

This thesis makes the following contributions:

- We developed a framework called **bQueue** [46] for providing bandwidth reservation and limit guarantees in distributed systems. The framework uses *tokens* to control the scheduling of requests, and dynamically adjusts the number of tokens allocated in response to changes in client demands and server capacities.

- We introduced a scalable algorithm called **pTrans** [47] [48] for dynamic token allocation in the *bQueue* framework. *pTrans* models the token allocation procedure using a novel graph data structure, and iteratively applies an operation called *prudent transfer* to drive the token distribution towards a maximal allocation. We proved that *pTrans* always finds the optimal token allocation, and terminates in a polynomial number of steps. Empirically, *pTrans* is shown to have much smaller runtime than other approaches like *integer linear programming* (ILP) and *max-flow*, and can be further optimized with parallelization and approximation.

- We designed a QoS algorithm **Fair-EDF** [49] [50] for providing fairness in the tail latencies of client requests. *Fair-EDF* uses a data structure called *occupancy*

chart to detect potential server overload; it selects a request to drop from a set of candidate requests identified by the occupancy chart, so as to meet tail-latency guarantees. In order to avoid unnecessary dropped requests when the service time is overestimated, *Fair-EDF* incorporates a second-chance mechanism that performs *best-effort scheduling* of these requests.

- We run the proposed QoS algorithms in both simulated and Linux distributed storage platforms, and the experimental results show these algorithms can provide reliable QoS support.

1.7 Thesis Organization

The rest of the thesis is organized as follows. In Chapter 2 we introduce the *bQueue* framework, which handles bandwidth reservations and limits in a distributed storage cluster. Chapter 3 presents several approaches to the token allocation problem, including the *pTrans* algorithm that performs token allocation in a scalable manner. Chapter 4 gives a formal proof of the optimality and polynomial bound of the *pTrans* algorithm. Chapter 5 presents the results of empirical evaluation of the *bQueue* framework using the *pTrans* algorithm for token allocation. Chapter 6 describes the *Fair-EDF* algorithm for ensuring tail-latency fairness. Chapter 7 shows the results of empirical evaluation of *Fair-EDF*. Finally, Chapter 8 summarizes the thesis and discusses open problems.

Chapter 2

Bandwidth Allocation QoS

2.1 Chapter Overview

In this chapter, we describe the *bQueue* framework for providing reservation and limit QoS in a distributed storage system. *bQueue* uses *tokens* to represent the QoS requirements of clients. It is made up of two components: a global token allocator and a scheduler at each server node. The token allocator periodically computes new token allotments and distributes them to the storage servers to guide their scheduling. The details of the token allocation problem will be discussed in Chapter 3. Compared to the schedulers used for fine-grained QoS, the *bQueue* scheduler does not require request-level tag computation and uses simple round-robin based scheduling. Moreover, *bQueue* does not require the requests of a client to be funneled through a common ingress node, and uses only a small amount of overhead communication for periodic status updates.

2.2 Problem Statement

In this section, we formalize the bandwidth allocation QoS problem in distributed storage systems. The storage system consists of **servers** (storage nodes) that collectively store and manage data collections for the **clients**. At runtime, the servers receive read and write I/O requests from clients for their stored objects. Each server has a certain service **capacity** equal to the number of requests it can process in a

given time interval. A client can be an entity like an organization or one of its departments, that represents multiple users who directly send their I/O requests to the storage system. In a specified time interval a server receives some number of requests from a client, referred to as the **demand** of the client on the server. The demands of a client may not be evenly distributed across servers, and the demands can also be time-varying. QoS is provided at the granularity of **clients**. Each client specifies **QoS requirements** for the storage system based on its Service-Level Objectives (SLOs). For bandwidth allocation, we focus on two QoS requirements: **reservations** and **limits**. These are the lower-bound and upper-bound respectively on the I/O bandwidth to be allocated to the client in a given time interval. We will use the number of I/Os per second (IOPS) as the measure of I/O bandwidth. This is based on a fixed-size I/O request, usually 4KB. Larger I/Os can be considered as being composed of several 4KB blocks and treated as multiple I/O requests.

Example 2.2.1. An example of a distributed storage system for bandwidth QoS allocation is shown in Figure 2.1. There are two servers and two clients (*green* and *purple*) with two active users for each client. Both servers have service **capacity** of 100 IOPS. The *green* client has a **reservation** of 50 IOPS and a **limit** of 100 IOPS, meaning that in every second, the number of I/O requests serviced for the *green* client at *all* servers should be *at least* 50 and *at most* 100. Similarly, the **reservation** and **limit** for the *purple* client are 50 IOPS and 150 IOPS, respectively.

Both clients consist of two active users that independently send their requests to any of the servers. Currently, the number of queued requests for the *green* and *purple* clients on server 1 are 100 and 120 respectively, *i.e.* the unsatisfied **demands** of the *green* and *purple* clients on server 1 are 100 and 120 respectively. Similarly, the pending **demands** of the *green* and *purple* clients on server 2 are 100 and 80,

respectively. □

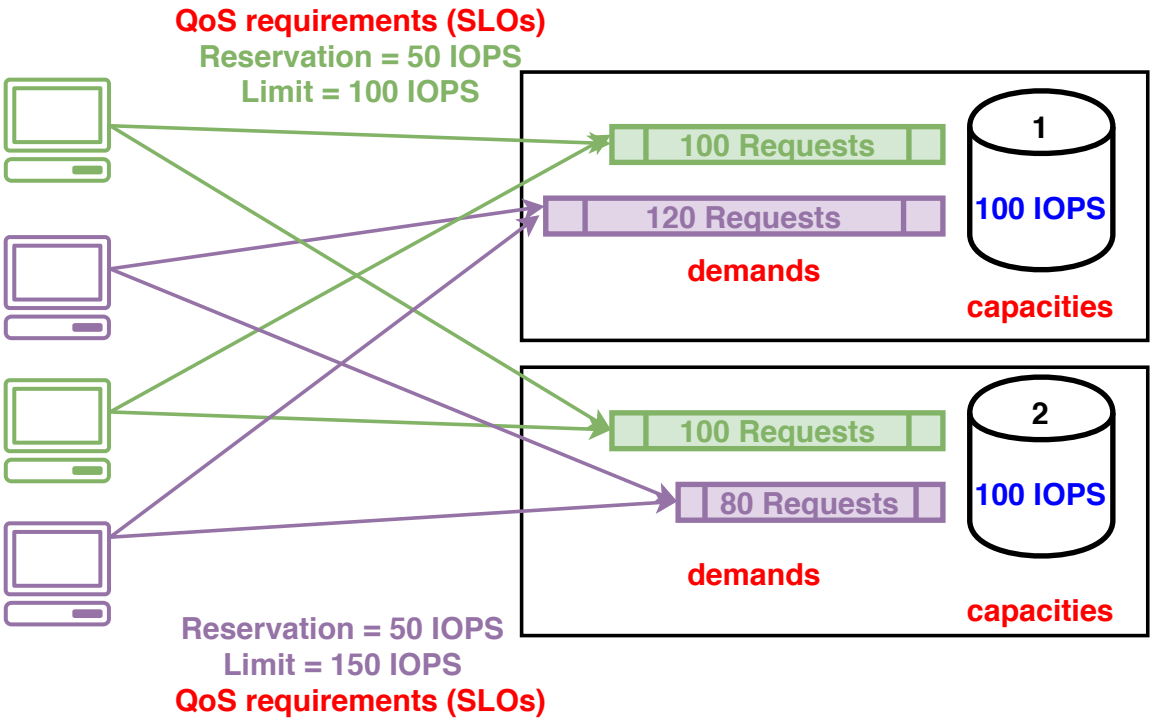

Figure 2.1 : An illustration of the distributed storage system for the bandwidth allocation QoS in Example 2.2.1.

The system model we propose can also support the bucket QoS model discussed in Section 1.4. To provide bandwidth allocation QoS for buckets, each bucket has to specify its **reservation** and **limit**. However, to make the definitions consistent, we still use the term **client** for the QoS specification, where the word **client** can be treated as the owner of a bucket. That is, each client owns a bucket whose contents (files or objects) are distributed across the servers. An external *user* sends I/O requests to the server holding the data it requires. The I/O is charged to the owner of the bucket associated with that data. Hence we can use the same terms as demand of a client on a server, bucket reservation, and bucket limit without change.

Example 2.2.2. An example of a distributed storage system for providing bandwidth allocation QoS for buckets is shown in Figure 2.2. The setup is similar to Example 2.2.1. However, we have two buckets, a *green* bucket and a *purple* bucket, distributed across the servers, and the QoS requirements are defined on the buckets (or the owners of the buckets, *i.e.* the **clients**). The external users can send I/O requests to any bucket; depending on the server on which the requested data has been placed, the request is routed to that server. □

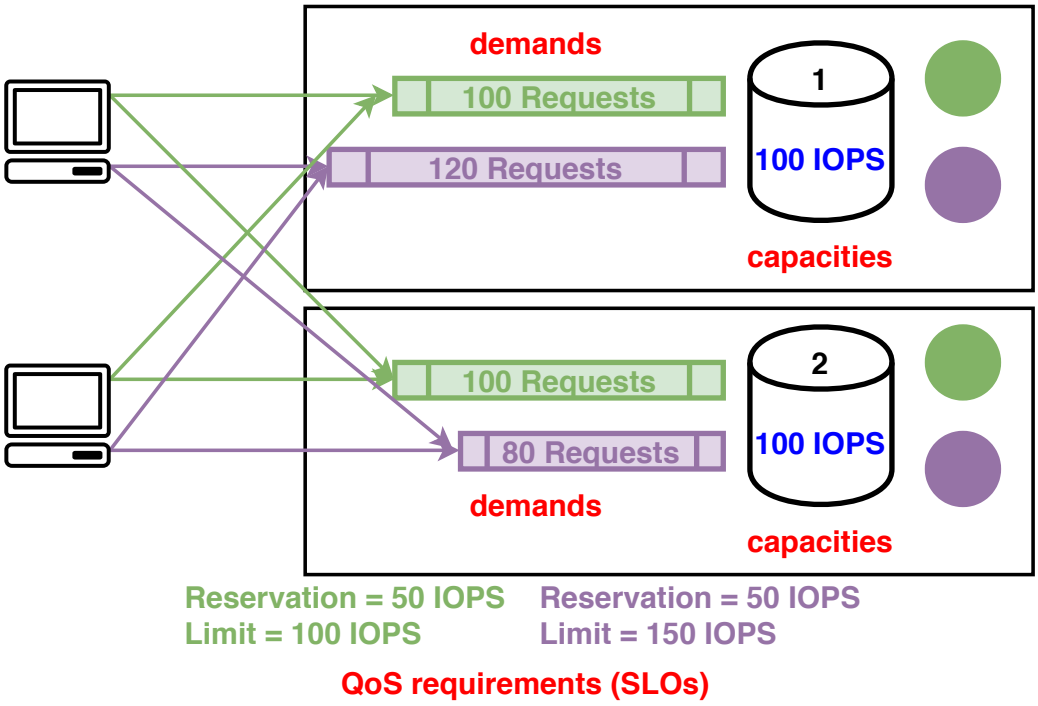

Figure 2.2 : An illustration of the distributed storage system for the bandwidth allocation QoS for buckets in Example 2.2.2.

2.2.1 Challenges for Distributed Bandwidth Allocation

Providing bandwidth allocation in a distributed environment can be hard. The first challenge arises because a client's accesses are distributed among multiple server nodes

and its run-time access patterns (both the servers it contacts and the intensity of requests to that server) change dynamically. A server cannot independently decide how much service to give a client so that the aggregate number of I/Os meets its reservation or stays below its limit. If the aggregate demand on a server does not exceed its capacity then each server can simply perform all its requests. This strategy ensures that the reservations of all clients that have sufficient demand will be met, provided the total reservation of the clients does not exceed the aggregate system capacity*. However, this may violate the limit QoS specification if many servers perform uncontrolled numbers of I/Os for the same client. If a server does not have enough capacity, then the scheduler on the server must decide how many I/Os of each client to perform. A client with a high reservation that is not receiving sufficient service at other servers should be prioritized over those that can meet their reservation with the service received at other servers.

In principle, fine-grained approaches like dSFQ [22] and dClock [18] can be modified to perform distributed bandwidth allocation in our model. These algorithms assume that all requests from a client are made to a single ingress node, the **gateway** node, for that client. The gateway node tags each request with metadata reflecting the aggregate service that the client has received, which is then used by the scheduler on the servers to prioritize the requests. We can emulate the behavior of a gateway by funneling all requests from a client through a single server that does the metadata computation before forwarding the request to the server holding the data. An illustration is shown in Figure 2.3. However, this requires additional communication bandwidth and adds an additional communication hop and processing time on the request path. Further to control the QoS accuracy, these fine-grained solutions limit

*In practice, this requirement is enforced by an admission control module.

the number of outstanding requests at a server; this reduces the concurrency available at the storage node and also requires frequent fine-grained communication between the server and the gateway. Finally, the fine-grained solutions also require sophisticated schedulers at the servers that use request metadata to select the order in which requests are dispatched, increasing scheduling overheads. The overhead problem will get more severe as new, low latency storage devices begin the dominate the back-end. A recent open-source [43, 44] project implemented dmClock in Ceph, but no deployment on Ceph has yet been announced.

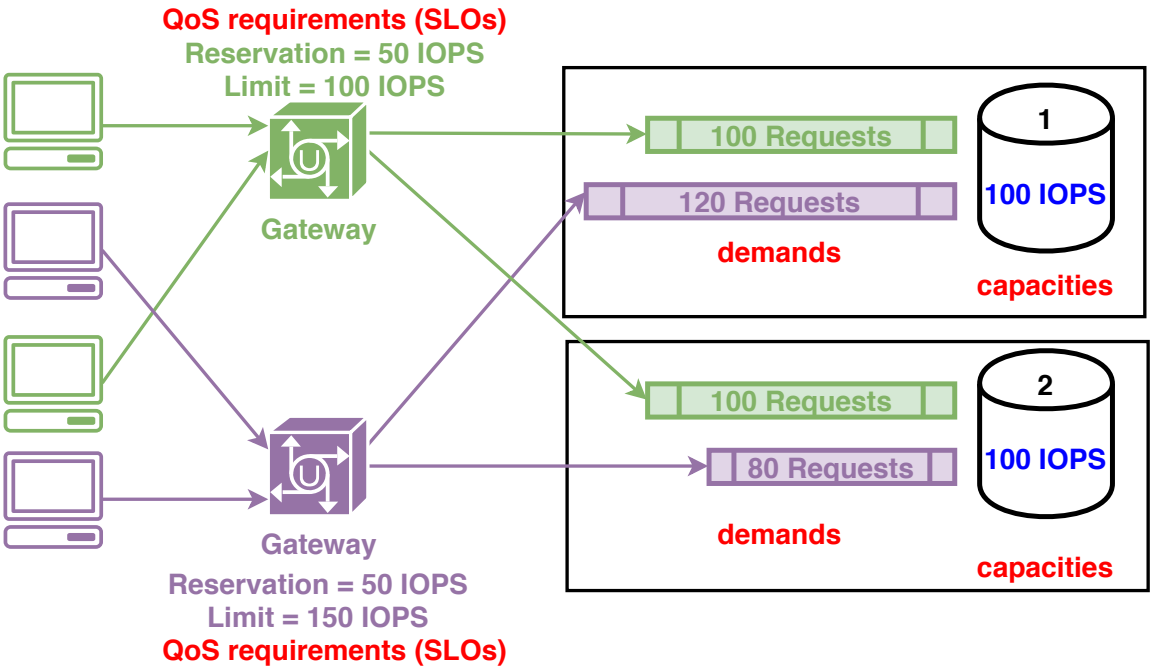

Figure 2.3 : The model extending existing fine-grained approaches to support bandwidth allocation QoS in our distributed model. Comparing to the framework shown in Figure 2.1, it requires gateway nodes to collect all the requests of a client and compute the metadata needed by the scheduler to control the QoS.

These considerations motivate us to develop a *coarse-grained* scheduling framework for distributed bandwidth allocation. The goal is to maximize the servers'

utilizations while fulfilling the reservation and limit requirements of the clients.

2.3 *bQueue* Framework

In this section, we give an overview of our *bQueue* framework. *bQueue* uses **tokens** to control the scheduling of requests at individual servers; the details of using tokens to control the QoS will be given in Section 2.3.1. At runtime, the I/O requests are queued at the server in client-specific queues and dispatched to the backend devices by a QoS scheduler called the **token scheduler**. A **token controller** process running on a dedicated computing node (or one of the server nodes) periodically receives status information from the storage nodes and pushes dynamic QoS control parameters (encoded as **tokens**) back to them for use by their respective token schedulers.

Example 2.3.1. Figure 2.4 shows an example of *bQueue* system hierarchy. There are 4 clients indicated by different colors, sending I/O requests to 3 server nodes. Node 1 receives I/O requests from *red* and *green* clients; node 2 receives I/O requests from *red*, *orange* and *blue* clients; and node 3 receives I/O requests from *red*, *green* and *orange* clients. □

2.3.1 QoS Model

The bandwidth allocation QoS is specified for each client i using two QoS requirements: **reservation** R_i and **limit** L_i in a *coarse-grained* manner. Time is divided into equal-sized non-overlapping intervals called **QoS periods**; QoS reservations and limits are guaranteed at the granularity of a QoS period. The total number of I/Os aggregated across all servers for client i done in a QoS period must be *at least* R_i and must *not exceed* L_i.

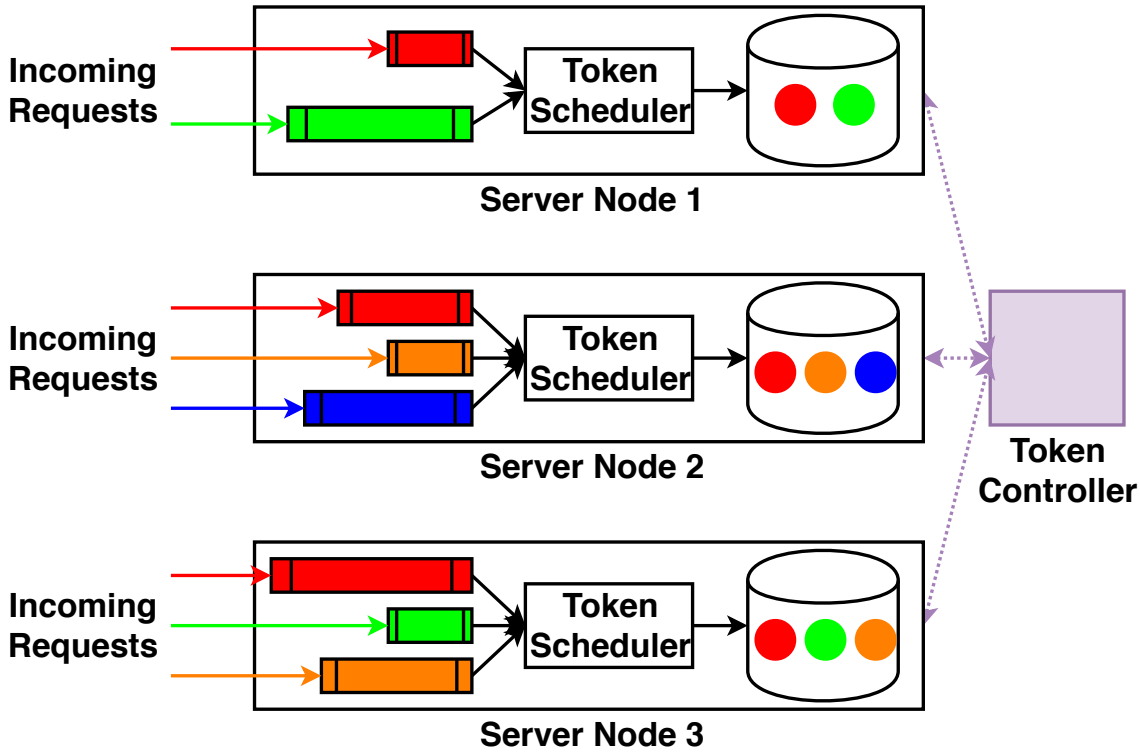

Figure 2.4 : *bQueue* system hierarchy in Example 2.3.1.

In the *bQueue* framework, there are two types of tokens associated with a client: *reservation tokens* (**R-tokens**) and *limit tokens* (**L-tokens**). An R-token for a client implies priority in scheduling the requests of that client. A client without any R-tokens at a server will only receive service when there are no pending requests for clients with R-tokens at the server. L-tokens control the total number of I/Os for a client serviced at the storage nodes. A client without L-tokens at a server will not be scheduled at a server.

The token controller periodically allocates R-tokens and L-tokens to the servers. During a QoS period, the distribution and intensity of requests to servers (**demands**) can change and varying workload patterns can result in servers running at different speeds (**capacities**). Hence the token controller recomputes the token allocation at

fixed intervals based on feedback information received from the servers. In particular, each QoS period is divided into multiple **redistribution intervals**. At the end of a redistribution interval, each server reports summary information about the server behavior in this interval to the controller. The controller uses such information to compute new token allocation and pushes them out to the servers.

Example 2.3.2. Figure 2.5 shows an example of the *coarse-grained* bandwidth allocation QoS. The QoS period is 5 seconds; hence, the reservations and limits for each client represent the minimum and maximum number of its I/O requests that must be serviced every 5 seconds. Moreover, there are 5 redistribution intervals per QoS period, *i.e.* each redistribution interval is 1 second. Thus, in each QoS period, at the beginning of every 1 second, the controller interacts with all servers for the runtime status information and computes the new token allocations, which it then pushes to the servers. □

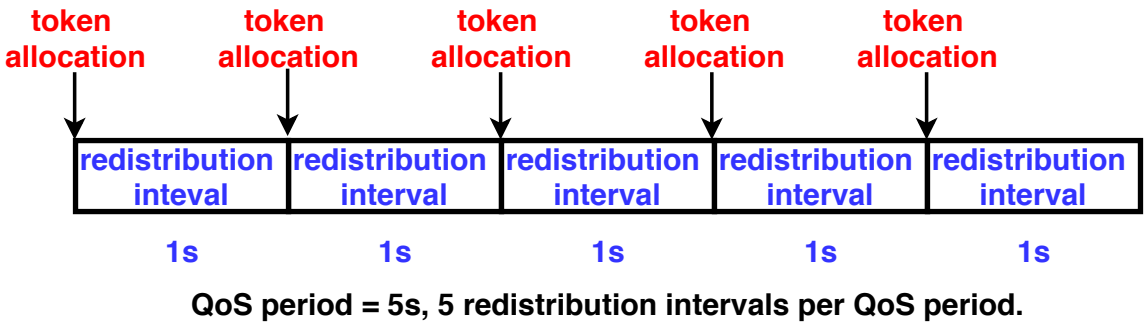

Figure 2.5 : The illustration of *coarse-grained* bandwidth allocation QoS in Example 2.3.2.

2.3.2 Token Controller

The most important component of the *bQueue* framework is the **token controller**, which periodically determines the token allocation based on the current status of the system: current service rates (IOPS) of the servers, demand distribution of the clients at the servers, and the number of unconsumed tokens of a client (representing unfulfilled reservation or available slack in the limit). In this section, we give a high-level description of the token allocation problem, and details of our approaches will be discussed in Chapter 3.

2.3.2.1 Specifications for Token Allocation

The token allocation algorithm has the following inputs for each client i and server j:

- **Residual reservation** (RR_i): The number of additional requests of i that must be serviced in the remainder of the QoS period to meet its reservation. RR_i is initialized to R_i (the reservation for i). In every redistribution interval, it is reduced by the *total number* of requests for i serviced at *all* the nodes during the previous interval, until it reaches 0.

- **Residual limit** (RL_i): The maximum number of additional requests of i that can be serviced in the remainder of the QoS period without exceeding its limit. RL_i is initialized to L_i (the limit for i). In every redistribution interval, it is reduced by the *total number* of requests for i serviced at *all* the nodes during the previous interval, until it reaches 0.

- **Residual capacity** (RC^j): An estimate of the number of requests that can be processed at the server j in the remainder of the QoS period.

- **Residual demand** (RD_i^j): An estimate of the number of requests for i at server j in the remainder of the QoS period.

Sometimes, we omit the term *'residual'* when discussing the token allocation problem.

The outputs of the token allocation algorithm are the number of reservation tokens and limit tokens for client i allocated to server j for the next redistribution interval, denoted by RT_i^j and LT_i^j, respectively.

In practice, reservations requirements are more important than limit constraints. Therefore, the primary goal of the token allocation is to distribute the maximum number of reservation tokens, subject to the constraints $1(a)$, $2(a)$ and $3(a)$ below. For a given distribution of R-tokens, the secondary goal is to distribute the largest number of limit tokens, subject to the constraints $1(b)$, $2(b)$, $3(b)$ and 4.

1. (a) The number of reservation tokens of each client i allocated to *all* servers should not exceed its residual reservation, *i.e.* $\forall i, \sum_j RT_i^j \leq RR_i$.

   (b) The number of limit tokens of client i allocated to *all* servers should not exceed its residual limit, *i.e.* $\forall i, \sum_j LT_i^j \leq RL_i$.

2. (a) The number of reservation tokens of *all* clients allocated to any server j should not exceed its residual capacity, *i.e.* $\forall j, \sum_i RT_i^j \leq RC^j$.

   (b) The number of limit tokens of *all* clients allocated to any server j should not exceed its residual capacity, *i.e.* $\forall j, \sum_i LT_i^j \leq RC^j$.

3. (a) The number of reservation tokens of client i allocated to any server j should not exceed the corresponding residual demand, *i.e.* $\forall i, \forall j, RT_i^j \leq RD_i^j$.

   (b) The number of limit tokens of client i allocated to any server j should not exceed the corresponding residual demand, *i.e.* $\forall i, \forall j, LT_i^j \leq RD_i^j$.

4. The number of reservation tokens of client i allocated to any server j should not exceed the corresponding number of its limit tokens, *i.e.* $\forall i, \forall j, RT_i^j \leq LT_i^j$.

2.3.2.2 Two Phase Token Allocation Approach

Our token allocation procedure works in two phases. In the first phase we distribute reservation tokens RT_i^j to maximize their allocation, subject to the constraints $1(a)$, $2(a)$ and $3(a)$ mentioned above. These allocations, RT_i^j, also serve as a *lower bound* on the number of limit tokens LT_i^j of client i at each server.

To make the allocation of limit tokens fit the same problem model as allocating reservation tokens, we proceed as follows. We treat the current allotment of reservation tokens of a client as the base number of limit tokens at a server. We then distribute the remaining limit tokens (*i.e.* $RL_i - \sum_j RT_i^j$) among the servers while satisfying the constraints $1(b)$, $2(b)$, and $3(b)$ above. Since any allocated amount is in excess of the allocated reservation RT_i^j, condition 4 will be automatically satisfied, as we can assume that $RL_i \geq RR_i$ for all clients i, *i.e.* a client always has a limit no smaller than its reservation.

In particular, for a given allocation of reservation tokens, we further make the following definitions:

- We define the number of *excess limit tokens* of client i on server j as $XLT_i^j = LT_i^j - RT_i^j$.
- We define the *excess residual limit* of client i as $XRL_i = RL_i - \sum_j RT_i^j$.
- We define the *excess residual capacity* on server j as $XRC^j = RC^j - \sum_i RT_i^j$.
- We define the *excess residual demand* of client i on server j as $XRD_i^j = RD_i^j - RT_i^j$.

We can then rewrite constraints $1(b)$, $2(b)$, $3(b)$ and 4 to get:

1. $\sum_j LT_i^j \leq RL_i$ implies that $\sum_j (XLT_i^j + RT_i^j) \leq RL_i$, so Condition $1(b)$ can be rewritten as $\forall i, \sum_j XLT_i^j \leq RL_i - \sum_j RT_i^j = XRL_i$.

2. $\sum_i LT_i^j \leq RC^j$ implies that $\sum_i (XLT_i^j + RT_i^j) \leq RC^j$, so Condition $2(b)$ can be rewritten as $\forall j, \sum_i XLT_i^j \leq RC^j - \sum_i RT_i^j = XRC^j$.

3. $LT_i^j \leq RD_i^j$ implies that $(XLT_i^j + RT_i^j) \leq RD_i^j$, so Condition $3(b)$ can be rewritten as $XLT_i^j \leq RD_i^j - RT_I^j = XRD_i^j$.

4. $LT_i^j \geq RT_i^j$ implies that $XLT_i^j + RT_i^j \geq RT_i^j$, so Condition 4 can be rewritten as $XLT_i^j \geq 0$.

Therefore, we can use the same procedure used to allocate reservation tokens to allocate excess limit tokens XLT_i^j using the modified constraints 1, 2 and 3 derived above. The limit token allocations LT_i^j are then computed as $LT_i^j = XLT_i^j + RT_i^j$.

Thus, the allocation of both reservation and limit tokens can be handled in the same way. In Chapter 3, we will use the model for allocating reservation tokens.

2.3.2.3 Demand and Capacity Estimation

The servers provide feedback to the token controller at the end of every redistribution interval. Specifically, for each client i, server j sends:

- Unconsumed reservation and limit tokens of i: $\hat{RT}_i^j$ and $\hat{LT}_i^j$.

- The number of requests for i arriving at j during last redistribution interval: N_i^j.

- The number of requests for i served by j during last redistribution interval: R_i^j.

- The number of pending requests for i on j at the end of last redistribution interval: M_i^j.

The residual reservation and residual limit can be directly obtained at the controller by summing up the values at individual servers, *i.e.*, $RR_i = \sum_j \hat{RT}_i^j$ and $RL_i = \sum_j \hat{LT}_i^j$. However, the controller needs to estimate the residual capacities and demands.

In this thesis, we give a simple but effective approach called **linear extrapolation**. In particular, the controller estimates the residual capacity of j by extrapolating the average service rate achieved in the last redistribution interval to the remaining intervals in the QoS period *i.e.* $RC^j = \sum_i R_i^j \times Q$, where Q denotes the number of remaining intervals. Similarly, the demands are estimated using a linear combination of the extrapolated arrival rate during the interval and the pending number of requests: *i.e.* $RD_i^j = N_i^j \times Q + M_i^j$. Figure 2.6 shows the linear extrapolation approach for demand and capacity estimation.

The demand and capacity estimator described above adapts well to sudden bursts and changes in the request arrival rate. Although arrival rates may fluctuate, the estimator is able to be self-correct. When the demand is underestimated (because there were too few requests in the previous interval) then fewer tokens will be allocated in this interval. If however, there is a burst of requests in this interval, the unavailability of tokens may result in an increase in its backlog. This backlog causes the estimated demand of the next interval to be high, resulting in more tokens in the next and subsequent intervals (even if there are no additional arrivals) till the backlog is cleared.

Similarly, if the demand is overestimated, then more tokens will be given for one interval consuming any pending requests and reducing subsequent estimates. Similar

considerations apply to capacity estimation. It should be noted that unless there is severe contention at a server, an error in the token count is not necessarily fatal. If a server has unused capacity after serving reservation requests, it will serve the pending requests as normal requests which will still count towards fulfilling the reservations. We also found in practice, our approach can effectively handle abnormal demand changes at runtime, and the related evaluation results are shown in Section 5.5.

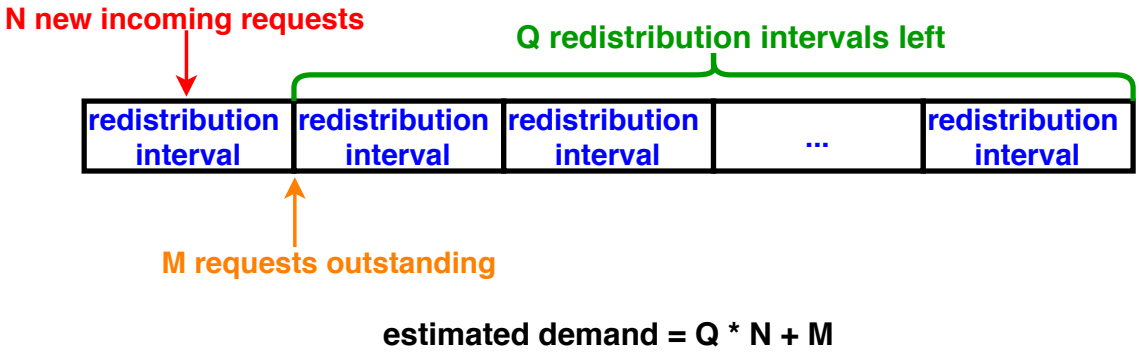

(a) Demand estimation.

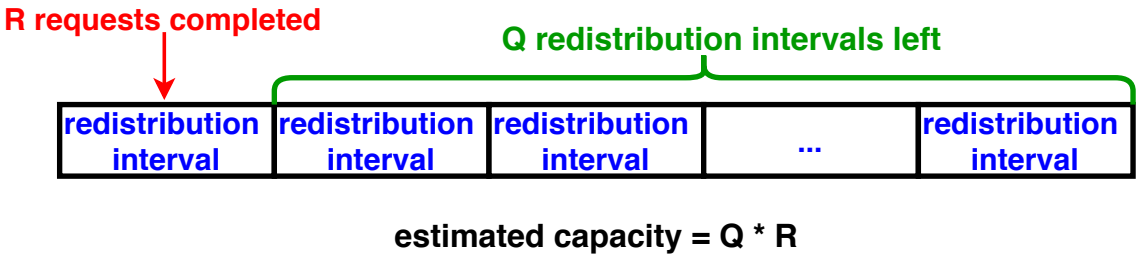

(b) Capacity estimation.

Figure 2.6 : The illustration of linear extrapolation approach for demand and capacity estimation.

2.3.3 Token Scheduler

The second component of the *bQueue* framework is the **token scheduler** at a server node. Requests arriving at a server are placed in a client-specific queue, one queue

for each client. Each server runs a local token scheduler that selects requests based on its token allocations and dispatches the requests to the storage devices.

The scheduler categories its requests into two types:

- **Reservation requests** (high priority): requests done to fulfill the reservation requirement of the client; requires a reservation token for the client to service this request.
- **Normal requests** (low priority): requests done after fulfilling the reservation before reaching the limit.

Algorithm 1: Request scheduling algorithm of Token Scheduler.

next = 0;
while *(TRUE)* **do**
  Step 1*a*: Search the **client queues** in round-robin order starting from *next* for the first queue that has both pending requests and reservation tokens;
  if *there is no such queue* **then**
    Go to **Step** 2
  Step 1*b*: Schedule a request from the **client queue** found in Step 1*a*, decrement the number of reservation and limit tokens for this queue by 1, update *next*; **continue**;
  Step 2*a*: Search the **client queue** in round-robin order starting from *next* for the first queue that has both pending requests and limit tokens;
  if *there is no such queue* **then**
    Go to **Step** 3
  Step 2*b*: Schedule a request from the **client queue** found in Step 2*a*, decrement the number of limit tokens for this queue by 1, update *next*; **continue**;
  Step 3: Delay a small amount; **continue**;

The token scheduler at a server uses its current allocation of R-tokens and L-tokens received from the controller in scheduling its requests. Algorithm 1 shows the

request scheduler. The scheduler will not idle if there are any requests pending in its queues, unless all clients with pending requests have reached their limit for the QoS period. It gives priority to clients with non-zero R-tokens (*reservation requests*) over those without any reservation tokens (*normal requests*). It chooses requests fairly among pending reservation requests by serving them in a *round-robin* order. If there are no reservation requests it chooses among normal requests that have not exceeded their limit, again in a round-robin manner. If there are no pending requests or if the only pending requests are for clients that have reached their limit, the scheduler will wait for a short interval and try again. One R-token and one L-token of a client will be consumed for each reservation request of the client that is scheduled. For each normal request scheduled one L-token is consumed.

2.4 Case Study

In this section, we present a simple example to illustrate how the token allocations are useful to control QoS.

Example 2.4.1. See Figure 2.7. Client A sends requests to servers 1 and 2 while client B only sends requests to server 2. Both clients are fully backlogged with requests on their servers, and the server capacities are both 100 IOPS. The reservations of A and B are 120 and 80 IOPS respectively. The QoS period is 1 second.

Case 1: Consider a naive policy that distributes the reservation tokens of a client equally among its servers. Both servers will get 60 reservation tokens for A, and server 2 will get all 80 reservations tokens for B. Server 1 will first do 60 requests of A (in 600ms) and consume all its reservation tokens. Since no clients have any reservation tokens it will serve normal requests of A for the remaining 400ms. Hence client A gets 100 requests at server 1.

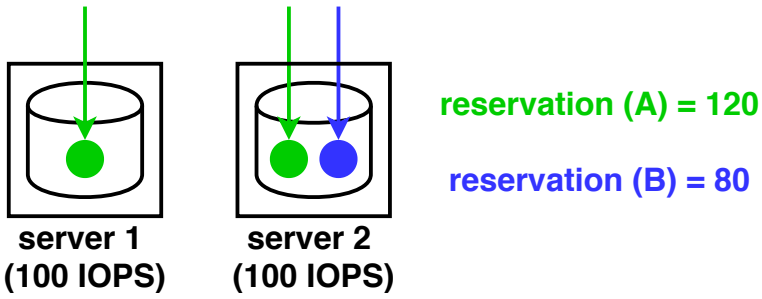

Figure 2.7 : Illustration of Example 2.4.1.

In contrast, server 2 is over-committed: it received 140 reservation tokens (60 for A and 80 for B), exceeding its capacity of 100 IOPS. Its scheduler will serve A and B in a round-robin fashion as long as both have reservation tokens. Hence both clients get 50 requests. As a result, A gets 150 requests (100 at server 1 and 50 at server 2) and exceeds its reservation. However, B gets only 50 requests serviced in total and fails to meet its reservation. Both servers are 100% utilized and do a total of 200 requests, but the naive token allocation fails to meet the reservation of B.

Case 2: An optimal token distribution will allocate all 80 reservation tokens for B to server 2 (as before), but will only allocate 20 reservation tokens for A to it. The remaining 100 tokens of A will be allocated to server 1. Now server 2 will complete 80 requests of B and 20 requests of A before it runs out of reservation tokens, while server 1 will do 100 reservation requests of A. Both clients will now meet their reservation requirements, and both servers are 100% utilized. □

2.5 Chapter Summary

In this chapter, we presented the *bQueue* framework for providing reservation and limit controls in distributed storage systems. We use tokens to control the number of reservation requests done for a client at a server, and to cap the maximum num-

ber of serviced requests. To accommodate variations in demand and capacity due to workload changes, token allocations are recomputed at fixed intervals using run-time estimates of the demand and capacity. The servers use a token-based round-robin scheduling algorithm to schedule the requests. Compared to fine-grained QoS solutions, we do not have extra overhead for generating metadata with each request at a centralized ingress node, and require only a simple round-robin scheduler at the servers. In the next chapter, we formalize the token allocation problem and present our solutions including the novel *pTrans* algorithm.

Chapter 3

Token Allocation

3.1 Chapter Overview

In this chapter, we formalize the process of token allocation as an optimization problem. We first present two natural formulations for the problem: an Integer Linear Program (ILP) and finding the maximum flow (max-flow) in a directed graph. This is followed by the description of a novel formulation called *pTrans*. In particular, *pTrans* uses a directed graph with vector edge attributes to model the token allocation problem. It uses an iterative algorithm that successively identifies feasible token distributions with higher total allocation. A detailed proof in Chapter 4 shows that *pTrans* terminates with a globally optimal allocation, and that it has a worst-case polynomial-time upper bound. Moreover, *pTrans* can be easily parallelized using multiple threads, and can be further accelerated using a simple approximation approach.

3.2 Problem Description

We first present a precise description of the token allocation problem. We use the term **client** to refer to the entity that receives QoS guarantees, which must be satisfied within a **QoS period** as defined in Section 2.2. A client may represent an organization with multiple users accessing the storage system or, when applied to bucket QoS, a client may represent a bucket owner who is paying for accesses made to the objects in the bucket.

We use **C** and **S** to denote the sets of clients and servers, respectively. A client $i \in \mathbf{C}$ may make requests to multiple servers; the **demand** d_i^j is the number of requests made by client i to server j. The aggregate demand of client i across all servers is $D_i = \sum_{\mathbf{j} \in \mathbf{S}} d_i^j$. Each client i specifies its **reservation requirement** R_i as the minimum number of its requests that must receive service in the colorred QoS period. Without loss of generality, we assume that $D_i \geq R_i$ for all $i \in \mathbf{C}$, *i.e.* a client has sufficient aggregate demand to meet its reservation. If not, the best the system can do is to match its demand, so we will temporarily set $R_i = D_i$. Finally, each server has a **capacity** upper bound T^j equal to the number of requests it can service during the QoS period.

For each client i, the algorithm allocates some number, a_i^j, of **tokens** to server j. The availability of a token implies that the server will serve one request for that client. We distribute as many of the R_i tokens of client i among the servers based on capacity and demand constraints. When a server does a request for client i, it *consumes* one of its tokens. We assume that servers use a scheduling method that prioritizes clients with available tokens; these clients are served requests evenly using a round-robin scheduling policy. If all R_i tokens of client i are consumed, its reservation requirement will be met.

There are two situations when a server j may have unconsumed tokens. Firstly, if j is allocated more tokens for client i than its demand (*i.e.* $d_i^j < a_i^j$), then at most d_i^j tokens of i can be consumed on server j. Secondly, if the total number of tokens allocated to server j (*i.e.* $\sum_{i \in \mathbf{C}} a_i^j$) exceeds its capacity T^j, then some tokens will not be consumed. In the first case, we say that server j has **strong excess tokens** for client i, and in the second case we say that server j has **weak excess tokens**. A server having weak excess tokens is also said to be **overloaded**.

The goal of the algorithm is to distribute the tokens so as to maximize the total

number of tokens that will be consumed. However, the distribution of demands on servers may preclude meeting all reservations *irrespective* of the scheduling or token allocation method. For instance, a server may become overloaded if all the demands of several clients are concentrated on it. One cannot redistribute the tokens to other servers since they do not have demand from these clients. In this case, it is fundamentally impossible to meet all reservations, and we settle for maximizing the total number of tokens consumed.

We refer to a **configuration** of the system by its demand distribution, server capacities, and token allocations: $\{[d_i^j, T^j, a_i^j] : i \in \mathbf{C}, j \in \mathbf{S}\}$. For a given configuration μ, we define the **effective server capacity**, $\phi^j(\mu)$, to be the number of tokens that server j will consume: $\phi^j(\mu) = min(T^j, (\sum_{i \in \mathbf{C}} min(a_i^j, d_i^j))$. The **effective system capacity**, $\Phi(\mu)$, is the sum of the effective capacities of individual servers, *i.e.* $\Phi(\mu) = \sum_{\mathbf{j} \in \mathbf{S}} \phi^j(\mu)$. For different configurations, the effective system capacities Φ may be different, and the goal is to find an allocation that maximizes Φ, which we call an **optimal** allocation. Note that the optimal allocation may not be unique.

Example 3.2.1. Table 3.1 shows a system of 2 servers with capacity 100, and two clients (*red* and *blue*) with reservations of 100 each. The demands and token allocations are shown in the table. Server 1 receives a total of 125 tokens that exceeds its capacity, so it is overloaded with 25 weak excess tokens. Server 2 has only 75 tokens so is **underloaded**. Note that the allocation of a client on any server does not exceed the corresponding demand on that server, so there are no strong excess tokens. The effective capacity of server 1 is $min(100, (min(75, 150) + min(50, 50))) = 100$ which is its I/O capacity. Similarly, the effective capacity of server 2 is $min(100, (min(25, 50) + min(50, 50))) = 75$. The effective system capacity of the configuration is 175. The *blue* client meets its reservation but the *red* client gets only 75 requests served. □

	d_1	d_2	a_1	a_2
Red	150	50	75	25
Blue	50	50	50	50

Table 3.1 : Configuration of Example 3.2.1, 3.3.1, 3.3.2 and 3.4.1. Servers 1 and 2 have capacity 100 each. The *red* and *blue* clients have reservation of 100 each. d_i and a_i are demand and token allocation on server i.

3.3 Direct Problem Formulations

The preliminary approaches directly model token allocation as a constrained optimization problem, with constraints $1(a)$, $2(a)$ and $3(a)$ discussed in Section 2.3.2.1. We present an integer linear programming (ILP) approach that directly specifies the constraints, and a max-flow approach that models the constraints as edge capacities of a flow graph.

3.3.1 Integer Linear Programming Approach

The token allocation problem can be directly modeled as an *integer linear programming* (ILP) optimization as described in Algorithm 2.

Algorithm 2: Integer linear-programming formation for the token allocation problem

Maximize $\sum_{\mathbf{j}\in\mathbf{S}} \sum_{i\in\mathbf{C}} a_i^j$
subject to $\forall i \in \mathbf{C}, \forall j \in \mathbf{S}, a_i^j \in \mathbb{Z}^+$ // integer constraints
and $\forall i \in \mathbf{C}, \sum_{\mathbf{j}\in\mathbf{S}} a_i^j \leq R_i$ // reservation specifications
and $\forall j \in \mathbf{S}, \forall i \in \mathbf{C}, a_i^j \leq d_i^j$ // demand constraints
and $\forall j \in \mathbf{S}, \sum_{\mathbf{i}\in\mathbf{C}} a_i^j \leq T^j$ // capacity constraints

Example 3.3.1. The linear programming formalism for Example 3.2.1 is shown in Algorithm 3. There are two reservation constraints (one for each client), four demand

constraints (per client per server), and two capacity constraints (one for each server).

□

Algorithm 3: Integer linear programming formation for the token allocation of Example 3.2.1

Maximize $a^1_{red} + a^2_{red} + a^1_{blue} + a^2_{blue}$
subject to $a^1_{red}, a^2_{red}, a^1_{blue}, a^2_{blue} \in \mathbb{Z}^+$
and $a^1_{red} + a^2_{red} \leq 100$
and $a^1_{blue} + a^2_{blue} \leq 100$
and $a^1_{red} \leq 150$
and $a^2_{red} \leq 50$
and $a^1_{blue} \leq 50$
and $a^2_{blue} \leq 50$
and $a^1_{red} + a^1_{blue} \leq 100$
and $a^2_{red} + a^2_{blue} \leq 100$

Since ILP is NP-complete [51], one can try to approximate the solution by relaxing the integer constraints to obtain a near-optimal solution. Algorithm 4 shows one possible approximation using integer relaxation. It first solves a Linear Programming (LP) formulation of the problem by removing the integer constraints in Algorithm 2. Then it allocates the tokens by taking the floor of the result of the LP optimization. Finally, the remaining unallocated tokens are allocated to servers with spare demands* in a greedy manner. Since LP can be solved in polynomial time [52–54], Algorithm 4 is polynomial-time. However, even the LP solution was found to perform very slow in practice (see Section 5.3.1).

*We refer $d^j_i - a^j_i$ as the *spare demand* of client i on server j. The formal definition will be given later in Section 3.4.2.

Algorithm 4: Linear-programming approximation for the token allocation problem using integer relaxation.

// **Solve the LP by removing the integer constraints in Algorithm 2.**
Maximize $\sum_{\mathbf{j}\in\mathbf{S}} \sum_{i\in\mathbf{C}} f_i^j$
and $\forall i \in \mathbf{C}, \sum_{\mathbf{j}\in\mathbf{S}} f_i^j \leq R_i$ // reservation specifications
and $\forall j \in \mathbf{S}, \forall i \in \mathbf{C}, f_i^j \leq d_i^j$ // demand constraints
and $\forall j \in \mathbf{S}, \sum_{\mathbf{i}\in\mathbf{C}} f_i^j \leq T^j$ // capacity constraints

// **Allocate the tokens by taking the floor of the LP solution.**
// **For the remaining tokens, allocate them to servers with spare demands*.**
for *each client* i **do**
  for *each server* j **do**
    $a_i^j = \lfloor f_i^j \rfloor$;
  $res_i = R_i - \sum_{\mathbf{j}\in\mathbf{S}} a_i^j$;
  Allocate res_i tokens to servers with spare demands of client i;

3.3.2 Max-flow Approach

We developed a model for token allocation based on a max-flow [55] approach, as part of the initial *bQueue* framework [46]. The algorithm first constructs a **token allocation graph**, which is a weighted, directed bipartite graph with a vertex for each client and each server plus a single SOURCE vertex and a single SINK vertex. The edges of the graph are defined below.

- A directed edge from the SOURCE vertex to each client vertex i, where the weight of the edge is the reservation R_i.
- A directed edge from each client vertex i to all server vertices j, where the weight of the edge is the demand d_i^j.
- A directed edge from each server vertex j to the SINK vertex, there the weight of the edge is the capacity T^j.

Then by running the max-flow algorithm, flow f_i^j on edge $\{i, j\}$ represents the number of tokens to be allocated for client i on server j. Since all edges in the token allocation graph have integer weights, based on the *integral flow theorem* [55], there always exists a maximum flow for which the flow on every edge is an integer. This implies that we can always find an optimal token allocation indicated by flow f_i^j.

Example 3.3.2. Figure 3.1a shows the token allocation graph for the scenario described in Example 3.2.1. The weights on the edges from SOURCE to nodes *Red* and *Blue* represent reservations of 100 for both clients. The edges of weight 100 from servers 1 and 2 to SINK are the capacities of the servers. Finally, the edges between the clients and servers indicate the corresponding demands. As shown in Figure 3.1b, the max-flow has a value of 200, and the individual flows between clients and servers are all 50, as shown on the edges. Note the optimal allocation may not be unique, and the max-flow algorithm may give any of them. □

Algorithm 5 shows the pseudo-code of the max-flow approach.

Comparing to the NP-complete ILP approach or LP approximation in Section 3.3.1, the max-flow approach guarantees the optimal solution in polynomial time. However, max-flow algorithms still have high time complexities and cannot be parallelized, which makes it impractical to use in storage systems at large scales. This motivates us to develop a dedicated algorithm for the token allocation problem.

3.4 *pTrans* Algorithm

In this section, we present a polynomial-time algorithm *pTrans* which efficiently solves the token allocation problem. Unlike the LP and max-flow approaches which work on satisfying constraints, *pTrans* uses a directed graph with vector edge attributes to model the allocation problem as a load balancing problem.

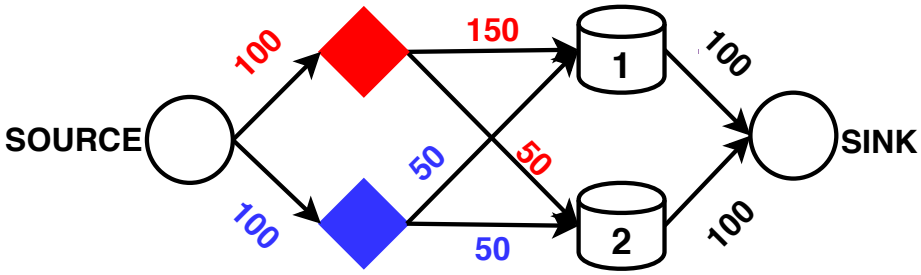

(a) Token allocation graph.

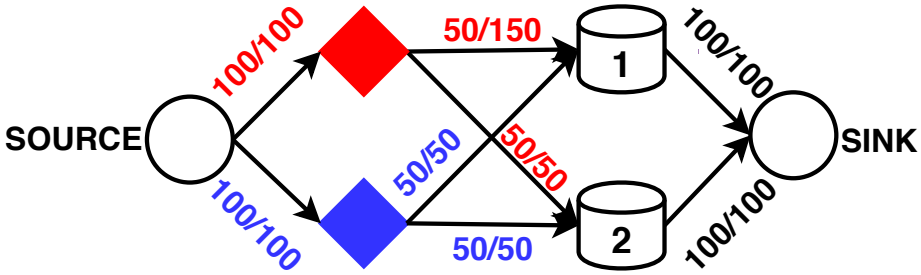

(b) Token distribution given by the max-flow algorithm.

Figure 3.1 : Token allocation determined by max-flow approach for Example 3.3.2.

Algorithm 5: Max-flow approach for the token allocation problem

---

// **Build token allocation graph**.
for *each client* i **do**
  $w(SOURCE, i) = R_i$;
for *each server* j **do**
  $w(j, SINK) = T^j$;
for *each client* i **do**
  for *each server* j **do**
    $w(i, j) = d_i^j$;

// **Determine the token allocation by computing the max-flow**.
Determine the maximum flow from SOURCE to SINK for the token allocation graph.
Let f_i^j denote the flow along the edge from client i to server j computed by the max-flow algorithm.
for *each client* i **do**
  for *each server* j **do**
    Allocate f_i^j tokens for client i to server j;

3.4.1 *pTrans* Algorithm Overview

To find an optimal allocation we only consider **prudent allocations** in which there are no strong excess tokens at any server, *i.e.* the token allocation satisfies $a_i^j \leq d_i^j$ for all $i \in \mathbf{C}, j \in \mathbf{S}$. A prudent allocation always exists since $\sum_{\mathbf{j}\in\mathbf{S}} a_i^j = R_i \leq D_i = \sum_{\mathbf{j}} d_i^j$. It is obvious that an optimal allocation is either prudent or can be transformed to a prudent allocation with the same Φ.

The algorithm operates as follows. An initial prudent allocation is obtained by distributing the R_i tokens of client i among the servers in proportion to its demand on the server, *i.e.* server j gets an **initial allocation** of $a_i^j = R_i \times (d_i^j/D_i)$. Since $D_i \geq R_i$, we always have $a_i^j \leq d_i^j$, so there are no strong excess tokens in the initial allocation. Following this allocation some servers may be overloaded, some may be underloaded, and the rest will exactly match their capacities.

The algorithm then iteratively attempts to find another prudent allocation with higher Φ by moving tokens from an overloaded server to an underloaded one. We refer to such a token movement as a **prudent transfer**. Every token moved in this way increases Φ by 1. The algorithm stops when there are no overloaded servers or there are no prudent transfers from an overloaded to an underloaded server possible. The resulting allocation will be optimal, and the proof is given in Section 4.2.

The pseudo-code in Algorithm 6 shows the overview of *pTrans* algorithm. There are three major steps: initial prudent allocation of tokens to the servers (Algorithm 7); creation of the initial **prudent transfer graph** (Algorithm 8), discussed in Section 3.4.2; iterative improvement of Φ by prudent transfers of tokens from overloaded to underloaded servers (Algorithm 9), discussed in Section 3.4.3.

Algorithm 6: *pTrans* Algorithm Overview

```
InitialAllocation();
MakePrudentTransferGraph();
IterativePrudentTransfers();
```

Algorithm 7: InitialAllocation Function

for *each client* $i \in \mathbf{C}$ **do**
  $D_i = \sum_{j \in \mathbf{S}} d_i^j$;
  $A_i = min(D_i, R_i)$;
for *each client* $i \in \mathbf{C}$ **do**
  $a_i^j = A_i \times d_i^j / D_i$;

3.4.2 Prudent Transfer Graph

We first give a clearer definition of prudent transfers. The prudent transfer of tokens between two servers may be done either directly or indirectly. To effect a *direct transfer*, the donor server must have a sufficient number of tokens of some client and the receiver must have high enough demand for that client to avoid creating strong excess tokens. Specifically, a prudent transfer of $n \geq 1$ tokens of client i from server j to server k requires: (i) $a_i^j \geq n$ and (ii) $d_i^k - a_i^k \geq n$. We refer to $d_i^k - a_i^k$ as the **spare demand** of server k for client i, which indicates the number of tokens of client i that server k can accept in a prudent transfer.

Example 3.4.1. The token distribution of Example 3.2.1 is an initial prudent allocation in which tokens are distributed in proportion to the demands. Server 1 has 50 *blue* tokens that it can donate. However, server 2 cannot accept any *blue* tokens since it has no spare demand. So no *blue* tokens can be transferred from server 1 to server 2. On the other hand, server 1 has 75 *red* tokens it can donate and server 2 has a spare demand of 25 *red* tokens. So $min\{75, 25\} = 25$ *red* tokens can be transferred

	d_1	d_2	d_3	a_1	a_2	a_3
Red	150	50	0	75	25	0
Blue	0	150	50	0	75	25
Green	50	0	50	50	0	50

Table 3.2 : Configuration of Example 3.4.2. All servers have capacity 100 and all clients have reservation of 100. d_i and a_i are the demand and token allocation for server i.

from server 1 to 2 resulting in both servers having 100 tokens each. After the transfer, Φ increases to 200. The reservations of both clients are now satisfied. □

We now describe a more complicated example where a direct token transfer is not possible.

Example 3.4.2. Consider three servers of capacity 100 each and three clients: *red*, *blue* and *green*. The demands and initial token allocations of the clients are shown in Table 3.2. Server 1 is overloaded (125), server 3 is underloaded (75) and server 2 is full (100). The tokens on server 1 and 3 are not compatible: server 1 can donate *red* and *green* tokens but server 3 has no spare demand for either client, and so cannot accept them in a prudent transfer. On the other hand, server 3 has a spare demand of 25 for *blue* tokens but server 1 has no *blue* tokens to donate. Hence direct transferring tokens from 1 to 3 is not possible. We therefore look for an indirect transfer using intermediate servers to act as *token brokers* to create a path of compatible token transfers. In this example, server 1 can donate 25 *red* tokens to server 2 in a prudent transfer; this would make server 2 overloaded, but it can get rid of these 25 weak excess tokens by transferring 25 *blue* tokens to server 3. After this brokered transfer, there are no weak or strong excess tokens and all clients meet their reservations. □

When servers j and k do not have compatible donor and receptor tokens an

indirect transfer may be possible. In an *indirect transfer* of tokens from server j to k, the transfer is effected with the help of intermediate servers $u_1, u_2, \cdots u_s$ (called **brokers**). A broker accepts a token of some client and sends out a token of another client. For each of the n tokens transferred from server j to k: j moves a token of client c_0 to server u_1 that in turn moves a token of another client c_1 to server u_2. Each server u_i, $2 \leq i < s$, accepts a token of a client c_{i-1} from u_{i-1} and sends a token of client c_i to u_{i+1}. Finally, u_s sends a token of client c_s to server k. If the source server j is overloaded by at least n tokens and the sink server k is underloaded by at least n then the above transfer will increase Φ by n.

In the *pTrans* algorithm, we maintain a data structure called the **prudent transfer graph (PTG)**, which is a weighted directed graph in which each vertex represents a server. For each pair of servers j and k, there is an associated vector $\mathbf{PT}_{j,k}$ called a **prudent transfer vector** with $|C|$ components, one for each client. The i^{th} component of the vector specifies the number of tokens of client i that can be moved from j to k directly. From the previous discussion, $\mathbf{PT}_{j,k}[i] = min(a_i^j, d_i^k - a_i^k)$. We also define the **weight** of the edge between servers j and k as $\mathbf{PTS}_{j,k} = \sum_{i \in C} \mathbf{PT}_{j,k}[i]$, the total number of tokens of all clients that can be moved between the servers directly. We omit the edge if its weight is 0.

Example 3.4.3. Table 3.3 shows the **PT** vectors and **PTS** between each pair of servers for the configuration of Example 3.4.2. For instance, server 1 can only transfer 25 *red* tokens to server 2 and cannot transfer any tokens to server 3, hence $\mathbf{PT}_{1,2} = [25, 0, 0]$ and $\mathbf{PTS}_{1,2} = 25$. An illustration of the corresponding prudent transfer graph is shown in Figure 3.2. Note the edges between vertices 1 and 3 have zero weight and are not shown. □

Algorithm 8 shows the initialization of the prudent transfer graph, and the collec-

	1	2	3
1	-	[25, 0, 0] / **25**	[0, 0, 0] / **0**
2	[25, 0, 0] / **25**	-	[0, 25, 0] / **25**
3	[0, 0, 0] / **0**	[0, 25, 0] / **25**	-

Table 3.3 : Prudent transfer graph for configuration of Table 3.2. Each entry is $\mathbf{PT}_{j,k}$ vector / $\mathbf{PTS}_{j,k}$ from server j (row) to server k (column).

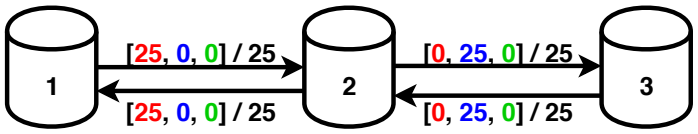

Figure 3.2 : Illustration of prudent transfer graph in Example 3.4.3.

tion of the prudent transfer vectors $\mathbf{PT}_{j,k}$ and $\mathbf{PTS}_{j,k}$, for all pairs of servers $j, k \in \mathbf{S}$.

Algorithm 8: MakePrudentTransferGraph Function

```
// Create a prudent transfer vector for each pair of servers
for each j ∈ S do
    for each k ∈ S, k ≠ j, do
        for each i ∈ C do
            PT_{j,k}[i] = min(a_i^j, d_i^k − a_i^k);
        PTS_{j,k} = Σ_{i∈C} PT_{j,k}[i];
```

3.4.3 Prudent Token Transfer

After the initialization, *pTrans* iteratively makes prudent transfers from an overloaded to an underloaded server until no more prudent transfers can be made, or there are no overloaded servers. The prudent transfer graph models the prudent transfers we can do with the current configuration. If there is a directed edge with weight $\mathbf{PTS}_{j,k} = w > 0$ from an overloaded server j to an underloaded server k, then it is

possible to move w tokens from server j to server k so Φ will be increased by w, while not creating strong excess tokens (*i.e.* in a direct prudent transfer).

We extend this observation to a *simple path* of length $l \geq 2$ from overloaded server j to underloaded server k going through intermediate vertices $u_1, u_2, \cdots u_{l-1}$. Let the nonzero weights of the edges in this path be $w_1, w_2 \cdots w_l$. Denote the *smallest weight* on this path by w_{min}. Then it is always possible to construct a prudent transfer that moves w_{min} tokens from j to the k, by moving w_{min} tokens across each edgein the path *i.e.* from j to u_1, from u_i to u_{i+1}, $i = 1, \cdots l-2$, and from u_{l-1} to k. We call such a path a **transfer path**, and an illustration is shown in Figure 3.3. Transfer paths can be found using *breadth-first search (BFS)* on the prudent transfer graph.

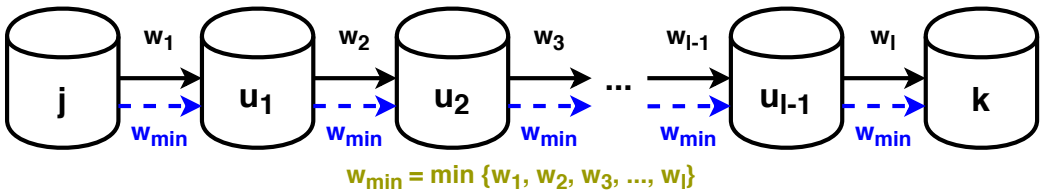

Figure 3.3 : Illustration of transfer path.

Note that the number of tokens at any intermediate server u_i is not changed by the prudent transfer, so no weak excess tokens are created at u_i. Also, since the transfer is prudent, no strong excess tokens are created. Hence the effective server capacity ϕ^{u_i} of an intermediate server u_i does not change.

The effective capacity ϕ^j of the source server j will not decrease so long as it does not become underloaded due to the tokens moved from it. Correspondingly, the effective capacity ϕ^k of the destination server k will increase so long as it does not become overloaded due to the tokens transferred into it. As a consequence, the effective system capacity Φ will increase if j is an overloaded server and k is an underloaded server, and the number of tokens transferred does not cause either j to

become underloaded or k to become overloaded.

Therefore, given a transfer path from an overloaded server j to an underloaded server k, we denote the amount of overload on j (i.e. $\sum_{i \in \mathbf{C}} a_i^k - T^j$) by γ^j, and the amount of underload on k (i.e. $T^k - \sum_{i \in \mathbf{C}} a_i^k$) by θ^k. Let w_{min} denote the smallest weight of the edges in a chosen transfer path from j to k. We define the **transfer size** $\Omega = \min\{\gamma^j, w_{min}, \theta^k\}$. The algorithm will move Ω tokens along the transfer path. By construction, the resulting allocation will be prudent and Φ will increase by Ω.

Moving tokens along the transfer path changes the configuration. Specifically, each server w in the transfer path may have a change in the allocation a_i^w for one or more clients $i \in \mathbf{C}$. This requires recalculating the prudent transfer vectors of all outgoing and incoming edges from and to w for those clients $i \in \mathbf{C}$ whose token allocations have changed, *i.e.* $\mathbf{PT}_{w,k}[i]$ and $\mathbf{PT}_{k,w}[i]$, $\forall k \in \mathbf{S}$. This also means that some edge with zero weight (*i.e.* not present in the current graph) may have non-zero weight after the transfer, and will now appear in the graph representing the new configuration. To bound the complexity of the algorithm we will need to bound the number of times an edge can (re)appear in the graph.

Algorithm 9 gives a pseudo-code of the iterative prudent transfer function. For each overloaded server P, it iteratively moves tokens from P to underloaded servers by exploring transfer paths in increasing order of length. We can show that making a transfer from P will never generate a shorter transfer path from P to an underloaded server. Hence, by performing transfers in increasing order of path lengths, we can derive a polynomial upper bound on the number of transfers made from P (see Section 4.3). The algorithm for overloaded server P ends when P is no longer overloaded or no transfer path can be found from P. For the latter case, we show in Section 4.2 that when making prudent transfers from other overloaded servers, we

Algorithm 9: IterativePrudentTransfers Function

```
for each overloaded server P do
    for l from 1 to (|S| − 1) do
        while P is still overloaded and a transfer path from P with length l
          exists do
            Find a transfer path (u_0, u_1, ··· u_{l−1}, u_l) from server P = u_0 to an
              underloaded server u_l = Q with length l using BFS;
            if no transfer path found then
                break;
            Ω = min(γ^P, θ^Q);
            for each pair of adjacent servers (u_i, u_{i+1}) on the transfer path do
                Ω = min(Ω, w_i);
            for each pair of adjacent servers (u_i, u_{i+1}) on the transfer path do
                Select Ω tokens on u_i to move to u_{i+1};
                Update prudent transfer graph for all edges into and out of u_i
                  and u_{i+1};
```

will never generate new transfer paths from P.

The algorithm terminates either when there are no overloaded servers or when there is no transfer path. Since moving tokens along a transfer path will increase Φ, it is obvious that a globally optimal allocation should not contain any transfer path in its prudent transfer graph. On the other hand, it can be shown (Section 4.1) that the converse is also true: *i.e.* an allocation with no transfer path is optimal. Therefore, the iterative prudent transfer function will terminate with a globally optimal solution that maximizes Φ.

3.4.4 Performance Optimizations

3.4.4.1 Parallelizing *pTrans*

pTrans has the opportunity to achieve better scalability by parallelization. The two most time-consuming functions are *MakePrudentTransferGraph* and *IterativePru-*

dentTransfers, and both can be parallelized. The function *MakePrudentTransfer-Graph* shown in Algorithm 8, has execution time complexity of $O(|\mathbf{S}|^2|\mathbf{C}|)$. Since this function is simply initializing a 2D array of vectors whose entries are independent, this step can be fully parallelized. For instance, we can evenly divide one dimension of the array into several parts and have different threads working on different subarrays.

In the function *IterativePrudentTransfers* shown in Algorithm 9, the most time-consuming step is the update of the *Prudent Transfer Graph* for each affected server. The update has a complexity of $O(|\mathbf{S}||\mathbf{C}|)$. However, the updates can be parallelized by evenly partitioning the clients, and letting different threads work on updating entries in its partition.

3.4.4.2 Approximation Approach

Another opportunity to accelerate the *pTrans* algorithm is to use an approximation approach. This is based on the observation that not all clients contribute equally in causing overload or reducing underload. In particular, clients with a small number of tokens and those with only a small amount of spare demand do not contribute much to increasing Φ.

Therefore, instead of maintaining a vector of size $|\mathbf{C}|$ for each edge, *pTrans* need only consider the clients with the top M (or fraction f) token counts and spare demands. Then the controller only considers the reduced information for the prudent transfers. In practice, we found that in most cases we only need a small fraction of the clients to achieve the optimal or near-optimal Φ (see Section 5.4). We leave for future work an analysis of such an approximation scheme.

3.4.5 Comparing *pTrans* with Preliminary Approaches

In this section, we compare *pTrans* with the LP and max-flow formulations of the problem, and show the advantages of *pTrans*. Furthermore, experimental comparisons of the methods are presented in Section 5.3.1.

The *ILP* approach has the same goal as *pTrans*: maximizing the number of reservations that can be met. However, this formulation requires $O(|\mathbf{S}||\mathbf{C}|)$ inequalities to model the per-client per-server demand constraints. Since ILP is NP-complete it makes an efficient exact solution unlikely. Furthermore, even an approximate *LP* formulation using integer relaxation has a poor running time. In contrast, in Section 4.3, we prove that *pTrans* is able to find the optimal allocation in polynomial-time, and our experiments show that it runs fast in practice.

Similarly, the *max-flow* approach works on graphs with per-server, per-client information simultaneously, which results in a graph of $O(|\mathbf{S}||\mathbf{C}|)$ edges, which is especially poor for the typical situation in which $|C| >> |S|$. In contrast, *pTrans* has a much smaller overhead by modeling the token allocation as a two-level problem. It first works on the prudent transfer graph which only includes servers (whose number of vertices is $O(|\mathbf{S}|)$) to find out the shift path, and then figures out which clients' tokens to move.

3.5 Chapter Summary

In this chapter, we formalized the token allocation problem and presented three token allocation algorithms. Apart from the direct formulations using *ILP* and *max-flow*, the major contribution is a novel approach embodied in *pTrans*, a fast and scalable algorithm for handling token allocation. *pTrans* models the problem as distributing tokens on a small graph (the number of vertices equals the number of servers)

augmented with per-edge vectors with client information. *pTrans* greedily transfers tokens from overloaded to underloaded servers while avoiding the creation of wasteful strong-excess tokens. *pTrans* has a much smaller runtime overhead than the other approaches considered. It can be further accelerated using parallelization and approximation mechanisms.

In the next chapter, we formally prove that *pTrans* always results in an optimal allocation, and converges to the global optimal solution in a polynomial number of steps. In Chapter 5, we experimentally show that *pTrans* handles distributed token allocation effectively, and outperforms the other methods by a large margin.

Chapter 4

Analysis of *pTrans* Algorithm

In this chapter we present formal proofs of correctness and analysis of the time complexity of *pTrans* [48].

4.1 Fundamental *pTrans* Optimality Theorem

In this section, we show the **fundamental pTrans optimality theorem**, which states that *an allocation is optimal if and only if it has no transfer path in its prudent transfer graph.* By using this theorem, we show in the next section that *pTrans* always terminates with the optimal token allocation. To prove this theorem, we show that **an allocation is non-optimal if and only if it has a transfer path in its prudent transfer graph**. Moreover, since the input allocation of *pTrans* is prudent and *pTrans* always keeps the allocations prudent, all allocations in this section will be assumed to be prudent, *i.e.* satisfy $\forall i \in \mathbf{C}, j \in \mathbf{S}, a_i^j \leq d_i^j$.

First of all, the *'if'* part is trivial to show.

Theorem 1. An allocation μ which contains a transfer path in its prudent transfer graph is non-optimal.

Proof. For an allocation μ with a transfer path, we can find another allocation $\mu\prime$ with higher Φ by moving Ω tokens (the transfer size) along the transfer path. This increases Φ by Ω. Thus, the allocation μ is not optimal. □

Next we show the *'only if'* part. We establish some elementary properties of the

token distribution in a non-optimal allocation, followed by an inductive argument in Lemma 6 that a non-optimal allocation must have a transfer path. Firstly, given an allocation μ, we recall the three states of the servers. A server j is said to be

- **overloaded** if the number of tokens allocated to it exceeds its capacity, *i.e.* $\sum_{i \in \mathbf{C}} a_i^j > T^j$.
- **full** if the number of tokens allocated to it equals to its capacity, *i.e.* $\sum_{i \in \mathbf{C}} a_i^j = T^j$.
- **underloaded** if the number of tokens allocated to it is less than its capacity, *i.e.* $\sum_{i \in \mathbf{C}} a_i^j < T^j$.

Lemma 2. For a non-optimal allocation μ, $\exists s \in \mathbf{S}$ where s is overloaded, i.e. $\sum_{i \in \mathbf{C}} a_i^s > T^s$.

Proof. Assume no server is overloaded, i.e. $\forall j \in \mathbf{S}$, we have $\sum_{i \in \mathbf{C}} a_i^j \leq T^j$. Then for any server j, its effective server capacity will be

$$\phi^j(\mu) = min(T^j, \sum_{i \in \mathbf{C}} a_i^j) = \sum_{i \in \mathbf{C}} a_i^j \tag{4.1}$$

i.e. $\phi^j(\mu)$ equals the total number of tokens allocated to server j. Then the effective system capacity will be

$$\Phi(\mu) = \sum_{j \in \mathbf{S}} \phi^j(\mu) = \sum_{j \in \mathbf{S}} (\sum_{i \in \mathbf{C}} a_i^j) = \sum_{i \in \mathbf{C}} (\sum_{j \in \mathbf{S}} a_i^j) = \sum_{i \in \mathbf{C}} R_i \tag{4.2}$$

i.e. $\Phi(\mu)$ equals the sum of the reservations of all clients. This means that all reservations will be met and thus μ is optimal, which contradicts our assumption. □

Lemma 3. For a non-optimal allocation μ, $\exists t \in \mathbf{S}$ where t is underloaded, i.e. $\sum_{i \in \mathbf{C}} a_i^t < T^t$.

Proof. Assume no server is underloaded, i.e. $\forall j \in \mathbf{S}$, we have $\sum_{i \in \mathbf{C}} a_i^j \geq T^j$. Then for any server j, its effective server capacity will be

$$\phi^j(\mu) = min(T^j, \sum_{i \in \mathbf{C}} a_i^j) = T^j \tag{4.3}$$

i.e. $\phi^j(\mu)$ equals the capacity of server j. Then the effective system capacity will be

$$\Phi(\mu) = \sum_{j \in \mathbf{S}} \phi^j(\mu) = \sum_{j \in \mathbf{S}} T^j \tag{4.4}$$

i.e. $\Phi(\mu)$ equals the total capacity of all servers. This means all servers' capacities will be utilized and thus μ is optimal, which contradicts our assumption. □

Hence, according to Lemma 2 and Lemma 3, for a non-optimal allocation μ, the server set $\mathbf{S}$ can be partitioned into two non-empty subsets $\mathbf{S_{OF}}(\mu)$ and $\mathbf{S_U}(\mu)$, where $\mathbf{S_{OF}}(\mu)$ consists of all overloaded and full servers and $\mathbf{S_U}(\mu)$ consists of all underloaded servers in μ. We will refer to the sum of the effective server capacities for a subset of servers W as the **effective capacity** of W.

Lemma 4. Given a non-optimal allocation μ and its corresponding partition $\mathbf{S_{OF}}(\mu)$ and $\mathbf{S_U}(\mu)$, any optimal allocation μ^* will have a higher value for the effective capacity of $\mathbf{S_U}(\mu)$, i.e. $\sum_{j \in \mathbf{S_U}(\mu)} \phi^j(\mu^*) > \sum_{j \in \mathbf{S_U}(\mu)} \phi^j(\mu)$.

Proof. Firstly, since μ^* is optimal and μ is non-optimal, we have

$$\Phi(\mu^*) > \Phi(\mu) \tag{4.5}$$

Then by the definition of effective system capacity, we have

$$\Phi(\mu) = \sum_{j \in \mathbf{S}} \phi^j(\mu) = \sum_{j \in \mathbf{S_{OF}}(\mu)} \phi^j(\mu) + \sum_{j \in \mathbf{S_U}(\mu)} \phi^j(\mu) \tag{4.6}$$

and

$$\Phi(\mu^*) = \sum_{j \in \mathbf{S}} \phi^j(\mu^*) = \sum_{j \in \mathbf{S_{OF}}(\mu)} \phi^j(\mu^*) + \sum_{j \in \mathbf{S_U}(\mu)} \phi^j(\mu^*) \tag{4.7}$$

Moreover, all servers in $\mathbf{S_{OF}}(\mu)$ are fully utilized (hence their effective server capacities are maximized) in μ. Thus, we have

$$\sum_{j \in \mathbf{S_{OF}}(\mu)} \phi^j(\mu) = \sum_{j \in \mathbf{S_{OF}}(\mu)} T^j \geq \sum_{j \in \mathbf{S_{OF}}(\mu)} \phi^j(\mu^*) \tag{4.8}$$

By combining Equations (4.5) (4.6) (4.7) (4.8), we have

$$\sum_{j \in \mathbf{S_U}(\mu)} \phi^j(\mu^*) > \sum_{j \in \mathbf{S_U}(\mu)} \phi^j(\mu) \tag{4.9}$$

□

Using Lemma 4, we can further derive the following lemma, which forms the basic requirement for a prudent transfer.

Lemma 5. Given a non-optimal allocation μ and its corresponding partition $\mathbf{S_{OF}}(\mu)$ and $\mathbf{S_U}(\mu)$, $\exists i \in \mathbf{C}$, $s \in \mathbf{S_{OF}}(\mu)$ and $t \in \mathbf{S_U}(\mu)$, such that in μ, i has token(s) on s and spare demand(s) on t.

Proof. Assume such an i does not exist, *i.e.* all clients having spare demands (if any) in $\mathbf{S_U}(\mu)$ do not have any tokens in $\mathbf{S_{OF}}(\mu)$. Then consider the effective capacity of $\mathbf{S_U}(\mu)$. Since all servers in $\mathbf{S_U}(\mu)$ are underloaded, *i.e.* there are no weak excess tokens, $\sum_{j \in \mathbf{S_U}(\mu)} \phi^j(\mu)$ will be equal to the number of tokens of all clients allocated

in $\mathbf{S_U}(\mu)$,*i.e.* we have

$$\sum_{j \in \mathbf{S_U}(\mu)} \phi^j(\mu) = \sum_{i \in \mathbf{C}} (\sum_{j \in \mathbf{S_U}(\mu)} a_i^j) \tag{4.10}$$

For each client i, there are two cases.

- If i does not have spare demand in $\mathbf{S_U}(\mu)$, which means the number of tokens of i allocated in $\mathbf{S_U}(\mu)$ is exactly same as the total demand of i in $\mathbf{S_U}(\mu)$. Then $\sum_{j \in \mathbf{S_U}(\mu)} a_i^j = \sum_{j \in \mathbf{S_U}(\mu)} d_i^j$, which cannot be increased in any other allocation.
- If i has spare demand in $\mathbf{S_U}(\mu)$, then according to the assumption, there are no tokens of i allocated in $\mathbf{S_{OF}}(\mu)$. This means that all tokens of i are allocated in $\mathbf{S_U}(\mu)$, which implies that $\sum_{j \in \mathbf{S_U}(\mu)} a_i^j = R_i$. This also cannot be increased in any other allocation.

Therefore, for any client i, the value $\sum_{j \in \mathbf{S_U}(\mu)} a_i^j$ in Equation 4.10 cannot be increased in any other allocation. This means $\sum_{j \in \mathbf{S_U}(\mu)} \phi^j(\mu)$ is maximized in the non-optimal allocation μ, which contradicts Lemma 4. □

Now by using induction, we can show a transfer path must exist in the prudent transfer graph of any non-optimal allocation.

Theorem 6. Given a non-optimal allocation μ, a transfer path exists in its prudent transfer graph.

Proof. Let $\mathbf{S_{OF}}(\mu)$ and $\mathbf{S_U}(\mu)$ be the server partitions of μ as defined earlier. We use induction on $|\mathbf{S_{OF}}(\mu)|$ to show that a transfer path must exist.

- If $|\mathbf{S_{OF}}(\mu)| = 1$, then according to Lemma 2, $\mathbf{S_{OF}}(\mu)$ must contain one overloaded server, say s_0. Then by Lemma 5, $\exists i \in \mathbf{C}$ and $s_1 \in \mathbf{S_U}(\mu)$ such that i has token(s) on s_0 and has spare demand(s) on s_1. This implies a transfer path $\{s_0, s_1\}$ exists (*i.e.* a direct transfer) that establishes the base of the induction.

- Suppose a transfer path exists for all non-optimal allocations with $|\mathbf{S_{OF}}| = K$. Consider a non-optimal allocation μ where $|\mathbf{S_{OF}}(\mu)| = K + 1$. Then, by Lemma 5, there are two situations.

  - If $\exists i \in \mathbf{C}$ which has token(s) on an overloaded server $s_0 \in \mathbf{S_{OF}}(\mu)$ and has spare demand(s) on $s_1 \in \mathbf{S_U}(\mu)$, then it implies a direct transfer path $\{s_0, s_1\}$ exists.

  - If $\nexists i \in \mathbf{C}$ that has token(s) on an overloaded server in $\mathbf{S_{OF}}(\mu)$ and has spare demand(s) on a server in $\mathbf{S_U}(\mu)$, then it means $\exists i \in \mathbf{C}$ which has token(s) on a *full* server $s_0 \in \mathbf{S_{OF}}(\mu)$ and has spare demand(s) on $s_1 \in \mathbf{S_U}(\mu)$. Then consider the configuration μ' which is same as μ but in which s_0's capacity is increased by 1. Note μ' should also be non-optimal (otherwise μ will also be optimal since the extra capacity 1 added on s_0 will not help increasing Φ), and s_0 is underloaded in μ', i.e. $\mathbf{S_U}(\mu') = \{s_0\} \cup \mathbf{S_U}(\mu)$ and $|\mathbf{S_{OF}}(\mu')| = K$. According to the induction assumption, a transfer path $\{s'_0, s'_1, \cdots s'_{n-1}, s'_n\}$ exists in μ'. Then we can always find another transfer path in μ:

    * If $\exists k \in \mathbf{C}$ where $s'_k = s_1$, then $\{s'_0, s'_1, \cdots s'_{k-1}, s'_k = s_1\}$ is also a transfer path in μ.

    * If $\nexists k \in \mathbf{C}$ where $s'_k = s_1$, and $s'_n \neq s_0$, then $\{s'_0, s'_1, \cdots s'_{n-1}, s'_n\}$ is also a transfer path in μ.

    * If $\nexists k \in \mathbf{C}$ where $s'_k = s_1$, and $s'_n = s_0$, then we can form a transfer path $\{s'_0, s'_1, \cdots s'_{n-1}, s_0, s_1\}$ in μ.

Therefore, a transfer path always exists for non-optimal allocations. □

Finally, according to Theorems 1 and 6, we have the following conclusion, which

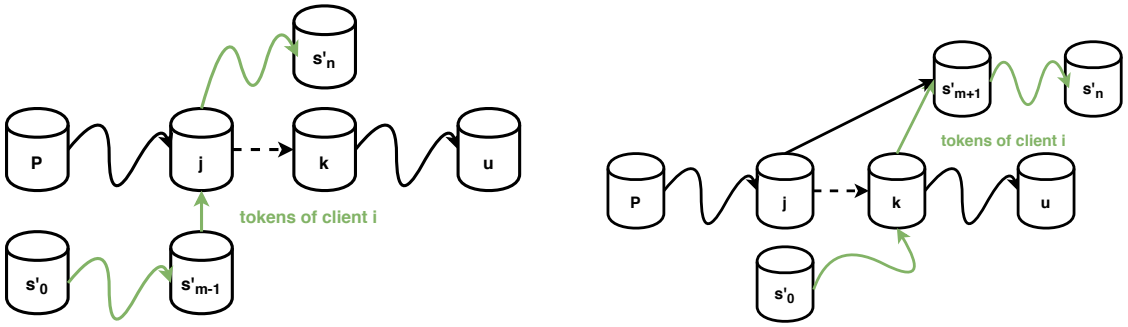

(a) Case (1) and (3). (b) Case (2).

Figure 4.1 : Illustration of base cases in the proof of Theorem 8. The green edges indicate the prudent transfer made, and the dotted edge indicates the new edge $\{j, k\}$ generated after making the transfer.

is the fundamental pTrans optimality theorem.

Theorem 7. An allocation is optimal if and only if it has no transfer path in its prudent transfer graph.

4.2 Correctness of *pTrans*

We now show that when the *pTrans* algorithm specified in Algorithm 9 terminates there will be no transfer paths in the prudent transfer graph. Then Theorem 7 implies that its allocation is optimal. Since Algorithm 9 is performed server by server in the outer loop, we must show that after the algorithm completes its iteration for some overloaded server P, no new transfer paths starting from P will be generated in subsequent iterations. Hence when the algorithm terminates, there are no transfer paths and the allocation is optimal.

Before giving the proof, we first discuss the situations in which new edges can be generated in the prudent transfer graph. Suppose that after making a transfer, a new edge $\{j, k\}$ from server j to server k is generated. Recall the definition of the edge weight: $\mathbf{PTS}_{j,k} = \sum_{i \in \mathbf{C}} \mathbf{PT}_{j,k}[i]$ and $\mathbf{PT}_{j,k}[i] = min(a_i^j, d_i^k - a_i^k)$. Since $\mathbf{PTS}_{j,k}$

changed from 0 to some non-zero value, there must exist a client i for which $\mathbf{PT}_{j,k}[i]$ increased, *i.e.*, $min(a_i^j, d_i^k - a_i^k)$ increased. Then there are three cases:

1. $\exists i \in \mathbf{C}$, whose token allocation on j increased from 0 (*i.e.* a_i^j increased), and the spare demand on k was positive.

2. $\exists i \in \mathbf{C}$, whose token allocation on j was positive, and the spare demand on k increased from 0, (*i.e.* $d_i^k - a_i^k$ increased, hence a_i^k decreased).

3. Both changes in (1) and (2) occurred, *i.e.* a_i^j increased and a_i^k decreased.

The following theorem shows that after Algorithm 9 completes an iteration for an overloaded server P, no new transfer path from P will be subsequently generated. This validates the correctness of the greedy per-server approach.

Theorem 8. Consider an allocation μ in which there is no transfer path with $P \in \mathbf{S}$ as the source. Then making prudent transfers from other overloaded servers will never generate new transfer paths from P.

Proof. We show that no new path from P is generated following a single prudent transfer from some other overloaded server. Suppose, to the contrary, that a new transfer path $\pi = \{s_0 = P, s_1, \cdots s_{n-1}, s_n\}$ is generated after making a prudent transfer from some other overloaded server s_0'. Then there must be at least one new edge in π which did not exist in μ. Let $\{s_i = j, s_{i+1} = k\}$ be the first of such new edges. For each of the three situations identified above we derive a contradiction:

- If case (1) or case (3) occurs, it means tokens of client i were moved to server j in the transfer π' from s_0', shown by
  $\pi' = \{s_0', s_1', \cdots s_{m-1}', j, s_{m+1}', \cdots s_n'\}$ in Figure 4.1a. Then we can form another transfer path from P in μ as
  $\{s_0 = P, \cdots s_{i-1}, j, s_{m+1}', \cdots s_n'\}$, which is a contradiction.

- If case (2) occurs, it means tokens of i were moved out of server k in the transfer π' from s'_0, shown by
  $\pi' = \{s'_0, s'_1, \cdots s'_{m-1}, k, s'_{m+1}, \cdots s'_n\}$ in Figure 4.1b. Since s'_{m+1} is receiving tokens of i from k, it must have spare demand of i in μ. On the other hand, by hypothesis, j has tokens of i in μ: this means the edge from j to s'_{m+1} exists in μ. Then we can form another transfer path $\{s_0 = P, \cdots s_{i-1}, j, s'_{m+1}, \cdots s'_n\}$ in μ, which is a contradiction.

Therefore, no new transfer path from P can be generated after making a prudent transfer from another source. □

Theorems 7 and 8 show that greedily increasing the effective system capacity by exploiting transfer paths in an arbitrary per-server order, does lead to an optimal solution.

4.3 Polynomial Bound of *pTrans*

In this section, we derive a polynomial upper bound for the *pTrans* algorithm. To this end, we show that the transfers from a fixed overloaded source server P (*i.e.* each outermost iteration in Algorithm 9) can be performed efficiently, by bounding the number of times any edge can be regenerated in the prudent transfer graph. Given an allocation μ, we use $\delta_\mu(j, k)$ to denote the shortest distance (*i.e.* the number of edges in the shortest path) between vertices j and k. The following theorem bounds the number of times an edge can be regenerated and hence bounds the number of transfers made by any source server.

Theorem 9. Consider a configuration μ with the source server P. Suppose a prudent transfer π is made and let μ' be the resulting configuration. Then in μ', $\forall q \in \mathbf{S}$, any

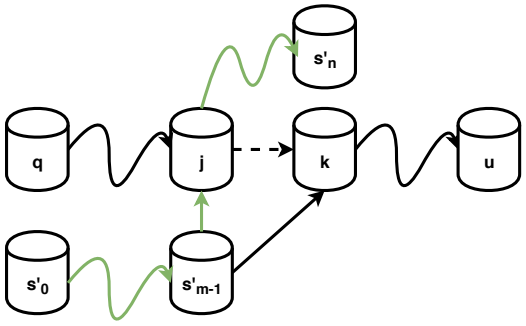

(a) Case (1).

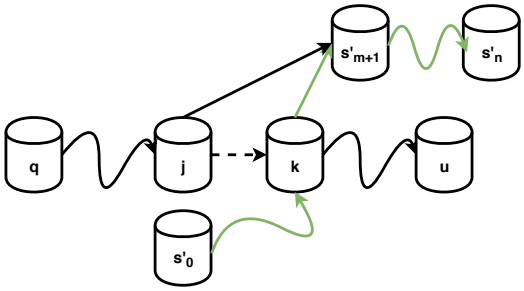

(b) Case (2).

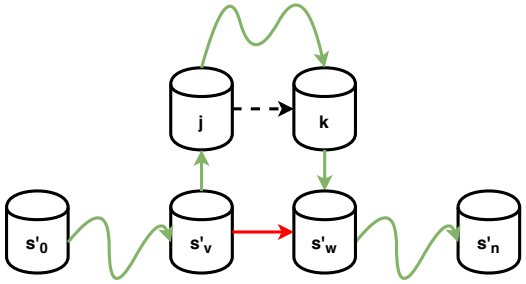

(c) Case (3)-1: the transfer path goes to j then k (not possible when the transfer path is shortest).

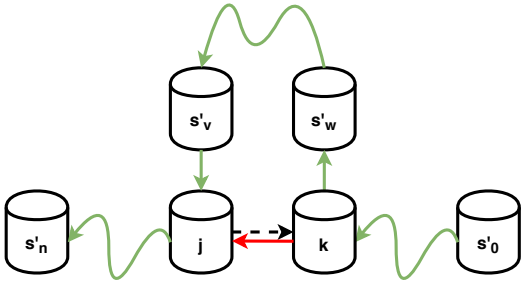

(d) Case (3)-2: the transfer path goes to k then j.

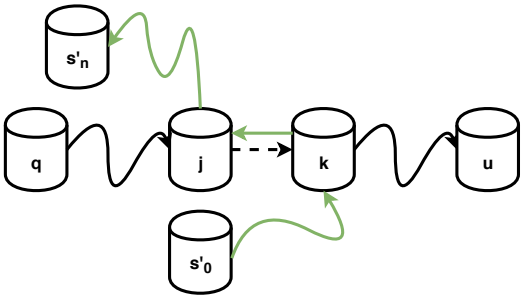

(e) The only possible situation in Case (3)-2.

Figure 4.2 : Illustration the proof of Theorem 9. The green edges indicates the prudent transfer made, and the dotted edge indicates the new edge $\{j, k\}$.

path π' from q to an underloaded server that includes a new edge will have length $> dist_\mu(q)$. Note that π' may not be a transfer path if q is not overloaded.

Proof. We prove the Theorem by induction on the number of new edges in the path π' and we use $\{j, k\}$ to denote the first new edge in π'.

- Base Case: π' contains the only one new edge $\{j, k\}$. In this case, in π', all edges from q to j, as well as k to u, are old edges that also existed in μ. Hence we have:

$$\delta_{\mu'}(q, j) \geq \delta_\mu(q, j) \tag{4.11}$$

and

$$\delta_{\mu'}(k, u) \geq \delta_\mu(k, u) \tag{4.12}$$

Then referring to the analysis of three cases when a new edge was generated (in Section 4.2):

  - If case (1) occurs, it means tokens of some client i were moved to j in π. Then the transfer path of π can be represented as $\{s'_0, \cdots s'_{m-1}, j, s'_{m+1}, \cdots s'_n\}$, as shown in Figure 4.2a. Since s'_{m-1} was sending tokens of i to j, it must have tokens of i in μ. On the other hand, it is assumed that k has spare demand of i in μ, then it means the edge from s'_{m-1} to k exists in μ.
    Then by the definition of $dist$, we have:

$$dist_\mu(q) \leq \delta_\mu(q, j) + \delta_\mu(j, s'_n) \tag{4.13}$$

On the other hand, since the transfer path from s'_{m-1} to s'_n was a shortest one, it means:

$$\delta_\mu(s'_{m-1}, s'_n) = \delta_\mu(j, s'_n) + 1 \leq \delta_\mu(k, u) + 1 \tag{4.14}$$

Then by combining Equations (4.11) (4.12) (4.13) (4.14), we conclude that:

$$dist_{\mu}(q) < \delta_{\mu'}(q, j) + \delta_{\mu'}(k, u) + 1 \tag{4.15}$$

where $\delta_{\mu'}(q, j) + \delta_{\mu'}(k, u) + 1$ is the length of the path π'.

– If case (2) occurs, it means tokens of some client i were moved away from k in the transfer. Then the transfer path of π can be represented as $\{s'_0, \cdots s'_{m-1}, k, s'_{m+1}, \cdots s'_n\}$, as shown in Figure 4.2b. Since s'_{m+1} was receiving tokens of i from k, it must have spare demand of i in μ. On the other hand, it is assumed that j has tokens of i in μ, then it means the edge from j to s'_{m+1} exists in μ.

  Then by the definition of $dist$, we have:

$$dist_{\mu}(q) \leq \delta_{\mu}(q, j) + 1 + \delta_{\mu}(s'_{m+1}, s'_n) \tag{4.16}$$

  On the other hand, since the transfer path from k to s'_n was a shortest one, it means:

$$\delta_{\mu}(k, s'_n) = \delta_{\mu}(s'_{m+1}, s'_n) + 1 \leq \delta_{\mu}(k, u) \tag{4.17}$$

  By combining Equations (4.11), (4.12), (4.16) and (4.17), we conclude that:

$$dist_{\mu}(q) < \delta_{\mu'}(q, j) + \delta_{\mu'}(k, u) + 1 \tag{4.18}$$

  where $\delta_{\mu'}(q, j) + \delta_{\mu'}(k, u) + 1$ is the length of the path π'.

– If case (3) occurs, it means tokens of some client i were moved to j and moved away from k in the transfer. Then the transfer path of π be represented as either

Case$(3)-1$: $\{s'_0, \cdots s'_v, j, \cdots, k, s'_w, \cdots s'_n\}$ (Figure 4.2c), or

Case$(3)-2$: $\{s'_0, \cdots k, s'_w, \cdots, s'_v, j, \cdots s'_n\}$ (Figure 4.2d). Case$(3)-1$ is not possible, because in μ, s'_v has tokens of i and s'_w has spare demand of i, we can form a shorter transfer path $\{s'_0, \cdots s'_v, s'_w, \cdots s'_n\}$. For the same reason, the only possible situation in Case$(3)-2$ is k directly moved tokens of i to j, as shown in 4.2e, because otherwise $\{s'_0, \cdots k, j, \cdots s'_n\}$ is a shorter transfer path.

Then by the definition of $dist$, we have:

$$dist_\mu(q) \leq \delta_\mu(q, j) + \delta_\mu(j, s'_n) \tag{4.19}$$

On the other hand, since the transfer path from k to s'_n) was a shortest one, it means:

$$\delta_\mu(k, s'_n) = \delta_\mu(j, s'_n) + 1 \leq \delta_{\mu'}(k, u) \tag{4.20}$$

By combining Equations (4.11), (4.12), (4.19) and (4.20), we conclude that:

$$dist_\mu(q) < \delta_{\mu'}(q, j) + \delta_{\mu'}(k, u) + 1 \tag{4.21}$$

where $\delta_{\mu'}(q, j) + \delta_{\mu'}(k, u) + 1$ is the length of the path π'.

- Inductive Step: for the induction, suppose the statement is true for all paths from any vertex q to some underloaded server in μ' with K new edges. Then consider a path π' from q to some underloaded server in μ' with $K+1$ new edges. Then since $\{j, k\}$ is the first new edge in π', all edges from q to j are old edges that also existed in μ. Hence we have:

$$\delta_{\mu'}(q, j) \geq \delta_\mu(q, j) \tag{4.22}$$

On the other hand, since the sub-path from k to u contains K new edges, based on the induction hypothesis, we have:

$$\delta_{\mu'}(k,u) > dist_{\mu}(k) \tag{4.23}$$

Again, referring to the analysis of three cases when a new edge was generated (in Section 4.2):

– If case (1) (Figure 4.2a) occurs, by the definition of $dist$, we have:

$$dist_{\mu}(q) \leq \delta_{\mu}(q,j) + \delta_{\mu}(j,s'_n) \tag{4.24}$$

On the other hand, since the transfer path from s'_{m-1} to s'_n was a shortest one, it means:

$$\delta_{\mu}(s'_{m-1},s'_n) = \delta_{\mu}(j,s'_n) + 1 \leq dist_{\mu}(k) + 1 \tag{4.25}$$

By combining Equations (4.22) (4.23) (4.24) (4.25), we conclude that:

$$dist_{\mu}(q) < \delta_{\mu'}(q,j) + \delta_{\mu'}(k,u) + 1 \tag{4.26}$$

where $\delta_{\mu'}(q,j) + \delta_{\mu'}(k,u) + 1$ is the length of the path π'.

– If case (2) (Figure 4.2b) occurs, by the definition of $dist$, we have:

$$dist_{\mu}(q) \leq \delta_{\mu}(q,j) + 1 + \delta_{\mu}(s'_{m+1},s'_n) \tag{4.27}$$

On the other hand, since the transfer path from k to s'_n) was a shortest

one, it means:

$$\delta_\mu(k, s'_n) = \delta_\mu(s'_{m+1}, s'_n) + 1 = dist_\mu(k) \tag{4.28}$$

By combining Equations (4.22), (4.23), (4.27) and (4.28), we conclude that:

$$dist_\mu(q) < \delta_{\mu'}(q, j) + \delta_{\mu'}(k, u) + 1 \tag{4.29}$$

where $\delta_{\mu'}(q, j) + \delta_{\mu'}(k, u) + 1$ is the length of the path π'.

– If case (3) (Figure 4.2e) occurs, by the definition of $dist$, we have:

$$dist_\mu(q) \leq \delta_\mu(q, j) + \delta_\mu(j, s'_n) \tag{4.30}$$

On the other hand, since the transfer path from k to s'_n) was a shortest one, it means:

$$\delta_\mu(k, s'_n) = \delta_\mu(j, s'_n) + 1 = dist_\mu(k) \tag{4.31}$$

By combining Equations (4.22), (4.23), (4.30) and (4.31), we conclude that:

$$dist_\mu(q) < \delta_{\mu'}(q, j) + \delta_{\mu'}(k, u) + 1 \tag{4.32}$$

where $\delta_{\mu'}(q, j) + \delta_{\mu'}(k, u) + 1$ is the length of the path π'.

□

Finally, by treating the source server P as the vertex q in Theorem 9, we can immediately derive Theorem 10.

Theorem 10. Consider a configuration μ with the source server P. Suppose a prudent transfer π is made on a path of length l and let μ' be the resulting configuration.

Then in μ' any new edge generated by the transfer can only occur in a transfer path from P of length greater than l.

Finally, the following theorem can be used to derive a polynomial upper bound of *pTrans* algorithm.

Theorem 11. In *pTrans*, for each source server P, the number of prudent transfers can be made is bounded by $O(|\mathbf{S^3}|)$.

Proof. Each time when making the shortest prudent transfer with length l in μ, one of the following scenarios will happen:

1. P become full or underloaded, this happens when the transfer size $\Omega = \gamma^P$. When this happens, we are done for P. Thus, this scenario can only happen once for each source server P.

2. The underloaded server U in the transfer becomes full, this happens when transfer size $\Omega = \theta^U$. When this happens, U becomes full and will be full for the rest of the *pTrans* algorithm. Thus, this scenario can only happen $O(|\mathbf{S}|)$ times for all source servers.

3. An edge $\{j, k\}$ on the transfer path gets removed, this happens when transfer size $\Omega = w_{min}$. Based on Theorem 10, when $\{j, k\}$ reappears in a later configuration μ', all transfer paths from P to underloaded servers including $\{j, k\}$ will have distance $> l$. This implies that an edge can be removed then reappear at most $O(|\mathbf{S}|)$ times. Since the number of edges is bounded by $O(|\mathbf{S^2}|)$, this scenario can happen at most $O(|\mathbf{S^3}|)$ times for each source server.

Therefore, for each source server P, the number of prudent transfers can be made is bounded by $O(|\mathbf{S^3}|)$. □

4.4 Comparing *pTrans* with *Edmonds–Karp* Algorithm

The *Edmonds–Karp* [56] algorithm for finding the *max-flow* have some similarities with *pTrans*. Both works on directed graphs, and greedily keep finding profitable paths (*prudent transfer path* and *augmenting path* respectively) until no further progress is possible. The **max-flow min-cut theorem** establishes the optimal configuration for the *Edmonds–Karp*. An analogous result is the **fundamental pTrans optimality theorem** that characterizes the optimal configuration for *pTrans*, especially the idea using *BFS*.

However, there are also some differences between *pTrans* and *Edmonds–Karp*. Unlike *Edmonds–Karp* which works on the *residual graph*, *pTrans* works directly on the *prudent transfer graph*, which indicates the number of tokens can be transferred between servers. Moreover, unlike flows, the edge weights in *pTrans* cannot be added or split. For example, server A may be able to give 50 tokens to server B and 50 tokens to server C, but it may not be able to do both.

Chapter 5

Evaluation of Bandwidth Allocation QoS

5.1 Experimental Setup

To evaluate the performance of distributed bandwidth allocation QoS, we implemented the QoS framework using both simulation and direct evaluation on a small Linux cluster. For the former, we create a set of concurrent processes to simulate the storage servers and the token controller, and use a request generator process at each server to create the dynamic workload. The communication overhead is simulated by a built-in delay function. I/O service times are randomly drawn from a uniform distribution with mean equal to the reciprocal of the server IOPS capacity and limited variance.

For the actual implementation, we built a prototype on a small cluster of 9 Linux servers connected using QDR InfiniBand (40 Gb/s). Each server node is equipped with an *Intel® Xeon® Processor E5-2640 v4* [57] CPU with 10 two-way hyper-threaded cores. In our implementation, one thread on each server is responsible for inserting the generated requests to the client queues. A second thread at the server runs the Token Scheduler that implements the round-robin scheduling policy. Finally, each storage node uses an independent thread to communicate with the controller node. We use the *send* and *recv* primitives from the socket programming library to handle the communication between the controller and the storage nodes, and *OpenMP interface* to implement the parallel threads.

Two backend servers were used in the evaluation. The first is the well-known

distributed memory caching system *memcached* [58] and the second is a conventional block-based Linux storage server. In the first case, each server runs a *Memcached* daemon that is pre-populated with $10,000$ objects of size 4KB each. The requests on each server are generated by an independent *YCSB* workload generator [59], which generates the *core workload A* [60] that gives a $50-50$ mix of *gets* and *puts*. An initial profile run was used to determine that each server had an average throughput of roughly $50,000$ requests per second (RPS). All clients are continuously backlogged on their active servers with 5 outstanding requests. The scheduler chooses requests from the client queues and invokes the memcahced server with a *get* or *put* command. For the storage backend, requests consist of random 4KB reads from a 1GB file created on the server. Using 5 concurrent request threads, each server is initially profiled and found to have an average throughput of roughly 1000 IOPS.

We describe our experimental results below. In Section 5.2 we show that *pTrans* can meet reservations and enforce limits in the face of dynamically changing workloads and large numbers of clients. In Section 5.3 we report the measured run times of the parallelized controller algorithm on the Linux server for different numbers of threads and clients. In Section 5.4 results on the tradeoff between run times and accuracy for the approximation controller algorithm on the Linux server are reported. In Section 5.5 we show how inaccurate demand estimation could be resolved at runtime. Finally in Section 5.6 we report the results of the evaluation on Linux scheduler to show the workings of the *pTrans* approach in a real system.

5.2 QoS Evaluation

5.2.1 Bandwidth Allocation at Large Scale

We use the simulator to show how *pTrans* handles reservation QoS with a large number of clients and a dynamically changing workload. There are 64 servers and $10,000$ clients. Each server has an average capacity of $20,000$ IOPS, and we run the *pTrans* algorithm for a full QoS period of 5sec; the throughput per QoS period is therefore roughly $100,000$ I/Os. We divide each QoS period into 5 token redistribution intervals *i.e.* a token redistribution is triggered every 1sec using statistics gathered for the last interval.

Each server's throughput of $100,000$ I/Os (per QoS period) is fully reserved by all the clients. This causes the greatest stress on the scheduler since there is no spare capacity that can compensate for errors in the token distribution. The reservation of the clients follows a *Zipf distribution* with an exponent factor $s = 0.5$, as shown in Figure 5.1a. The *Zipf distribution* simulates a common scenario in practice where most clients have a relatively low reservation while a few highly-active clients have a much higher reservation. In the figure, there is a factor of 100 between the highest and lowest reservations. All clients are assumed to have unbounded limits. Each client is active on 8 servers at any time. The total demand of a client is set to 1.5 times to its reservation. The average request arrival rate for the client over all servers is the total demand divided by the length of the QoS period. To stress the *pTrans* algorithm, the demands of each client are also distributed among the eight servers using a *Zipf distribution* with an exponent factor of $s = 0.5$. I/O requests for a client on a server are generated at a uniform rate proportional to the demand on the server. Clients may change their demands at random times within the QoS period. When a demand change is triggered, the client randomly selects eight servers (which may or may not

intersect with the current set), and redistributes the total demand to them based on a *Zipf distribution*. In the initial experiment, a client may change its demands up to 2 times in the QoS period. Figure 5.1b shows the times of demand changes of the sample of the clients. For instance, client 6100 has its first demand change early in the 1st interval (around 0.065s).

Figure 5.2 shows the number of requests being completed by all clients in each of the redistribution intervals. From the figure we can see that, as expected, the number of requests completed by a client at the end of the last interval is highly consistent with its reservation. Quantitatively, 99.5% of the clients meet at least 95% of their reservation. Furthermore, since the servers perform reservation requests in a round-robin fashion, clients with smaller reservations will complete earlier and free up server capacity for use by clients with larger reservations. The effect can be seen clearly in the figure, where during the last two intervals, the servers are mainly processing requests of the clients with smaller indexes (*i.e.* those with higher reservations).

Figure 5.2 also shows the adaptivity of the algorithm to sharp demand changes. For instance, several red needles (representing I/Os in the 2nd interval) can be seen in the blue (1st interval) region. This means that these clients received less service than their peers in the first interval. This happens because of a sudden drop in the demands of this client at some servers and an increase in others because of locality changes. Servers with reduced demand will not be able to consume their reservation tokens in this interval. The unused capacity however is not wasted and will be used by clients which have both demand and tokens on the server.

Even if all tokens with demand at the server have been consumed, the additional capacity is used to serve requests without tokens. These opportunistic requests will still be counted towards the reservation requirements of the corresponding client, and the controller will correct for these additional I/Os by reducing its target remaining

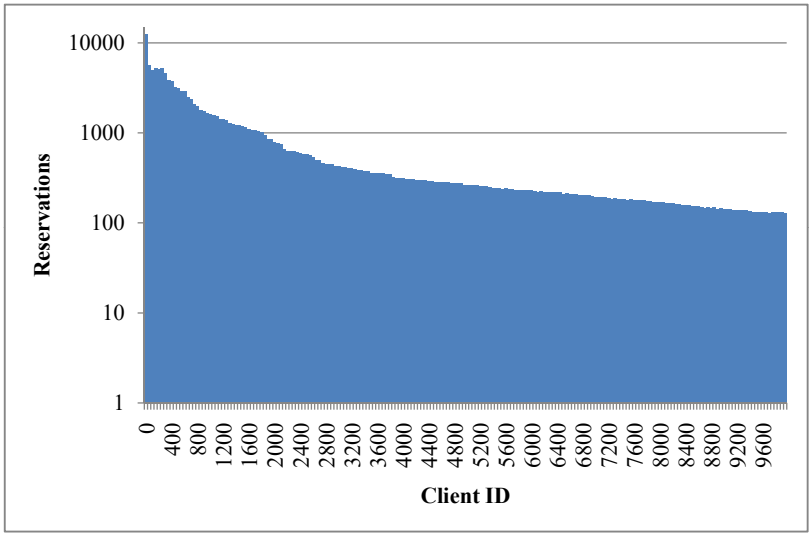

(a) The *Zipf distribution* of clients' reservation requirements with the exponent factor $s = 0.5$, sorted from high to low. Each client is assigned a weight $w_i = 1/i^{0.5}$ from the set of weights $\{w_j : j = 1, \cdots |C|\}$ with probability $(1/i^{0.5})/(\sum_i 1/i^{0.5})$. Then the aggregate capacity of the servers is distributed to the clients in proportional to their weights as their reservations. The client reservations are roughly in the range of $(120, 13000)$, and the y-axis has a logarithmic scale.

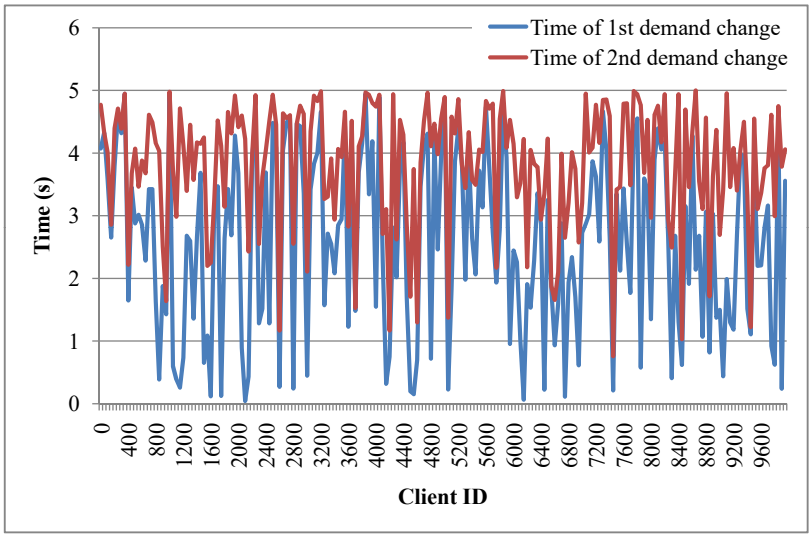

(b) The time that demand changes of the clients.

Figure 5.1 : The specifications of the simulator-based QoS evaluation: reservations and demand change times for a sample of the clients. The figures show the results for every 50^{th} client.

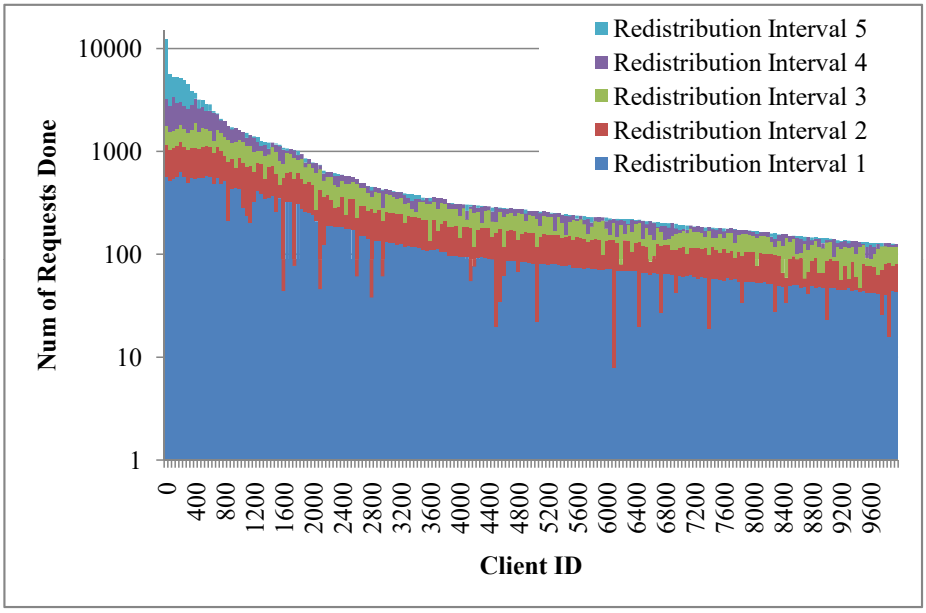

Figure 5.2 : The number of requests completed for each client in the 5 redistribution intervals. Each client is active (having non-zero demand) on a set of 8 servers. The figures show the results for every 50^{th} client.

reservation. In the next interval, the coordinator will allocate additional tokens to the clients that were underserved in the first interval and direct them to the new server, and reduce the total number of tokens to clients which received opportunistic I/Os. For instance, client 6100 that has its first demand change early in the 1st redistribution interval, receives less service in the first interval but catches up by the end of the second one.

5.2.2 Effect of Different Parameters

In this experiment we study the effect of two parameters on QoS accuracy: the number of servers on which the clients are active (N_A) and the number of times the demand of a client changes in a QoS period (N_D). The accuracy measure is the fraction of clients that miss 5% or more of their reservation in the QoS period.

Inaccuracy in the reservations achieved may arise due to *intrinsic error*. The intrinsic error arises because for certain data distributions it is *impossible* to meet the reservations irrespective of the scheduling strategy. For example, consider a situation where two clients with reservations of 100 IOPS each have a high demand on a single server and no demand on any of the other servers. If the capacity of the server is 100 IOPS then clearly at most one of the clients can meet its reservation, and the intrinsic error is greater than 0. Intrinsic errors are manifested in *pTrans* as weak excess tokens on some overloaded server(s) that cannot be moved to any underloaded server because of a lack of demand for the clients on the latter. When there is no runtime demand change, *pTrans* guarantees that all reservations will be met whenever such an allocation is possible. Hence, any error in this situation is an intrinsic error that cannot be avoided.

Figure 5.3 also shows the average measured error for $N_A = \{2, 4, 8\}$ and $N_D = \{0, 1, 2, 5, 10\}$. Each bar is the average of 5 runs; the variation was less than 10%. We found the error is almost always 0 for $N_A > 8$ and so are not reported. The bar for $N_D = 0$ represents intrinsic errors; in this case the optimal allocation determined by *pTrans* is still insufficient to meet all reservations. For a given number of active servers, the error grows initially as the number of demand changes increases, but levels off and becomes insensitive to additional demand changes. This is because demand changes that occur within a reallocation interval tend to average out or in any case have no worse an effect than one large demand change early in the interval. On the other hand, as the demands of a client get spread out over several servers, albeit in a skewed Zipf-like distribution, the error decreases. Note the errors also include intrinsic error, which no scheduling algorithm can avoid. It can be seen that a higher N_A reduces the intrinsic error. Characterization and bounds on intrinsic errors are deferred to future work.

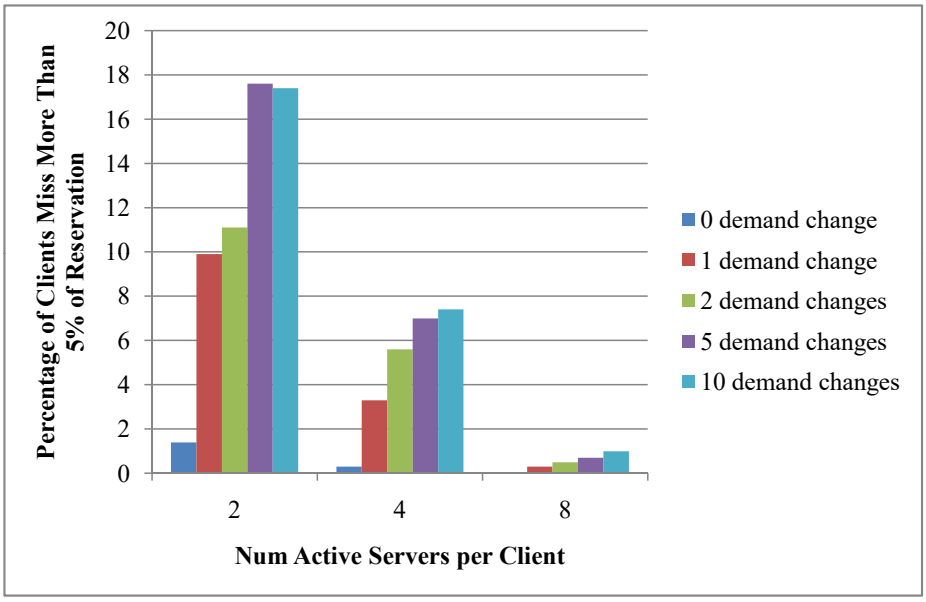

Figure 5.3 : The average error of *pTrans* with different number of demand changes and different number of active servers of each client.

5.3 Parallelization Evaluation

In this section, we show the speedup of the parallelization optimization for the *pTrans* algorithm. We used the **parallel for** primitive in *OpenMP* to parallelize the two hot-spot regions discussed in Section 3.4.4.1.

We use 64 servers and $10,000$ clients with the same *Zipf* demand and active server specification as in Section 5.2.1. Each server's throughput in the QoS period is $100,000$ and each client is active on 8 servers. However, we vary the following two variables:

- r : the fraction of the total cluster capacity being reserved, *i.e.* $(\sum_{i \in \mathbf{B}} R_i)/(\sum_{j \in \mathbf{S}} C^j)$. Note that $0 \leq r \leq 1$.
- m : the ratio of the total demand of each client to its reservation, *i.e.* D_i/R_i. Note that $m \geq 1$.

During the experiments, we found that the execution time of *pTrans* increases with higher r and smaller m. If m is small there will be less spare demands at a server reducing the number of tokens that can be moved along an edge. Similarly, if r is high, servers will overload more easily and underloaded servers will have less spare capacity to accept tokens. The execution times of *pTrans* with $r = 1.0$ and $r = 0.9$, with different number of working threads, and different m values are shown in Figure 5.4a and Figure 5.4b. From the figures we can see by using 12 threads, we can achieve up to 5× speedup and absolute runtimes in tens of milliseconds.

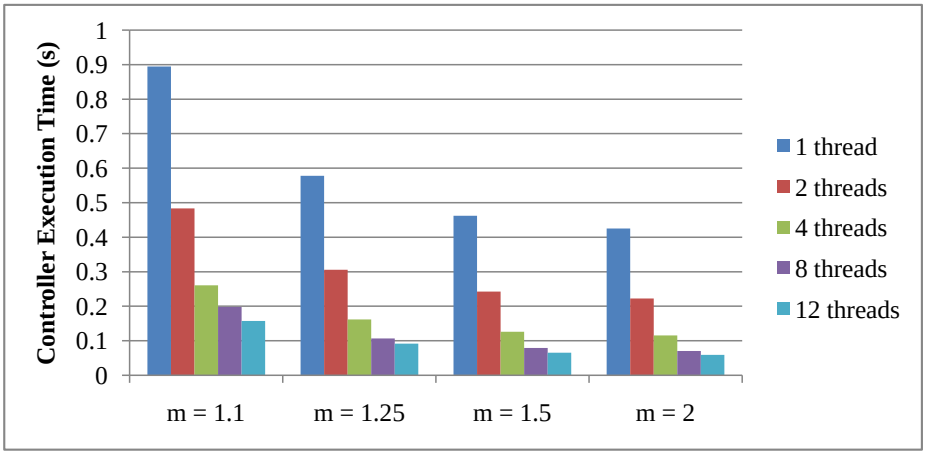

(a) Variation of the execution time of *pTrans* with m for $r = 1.0$.

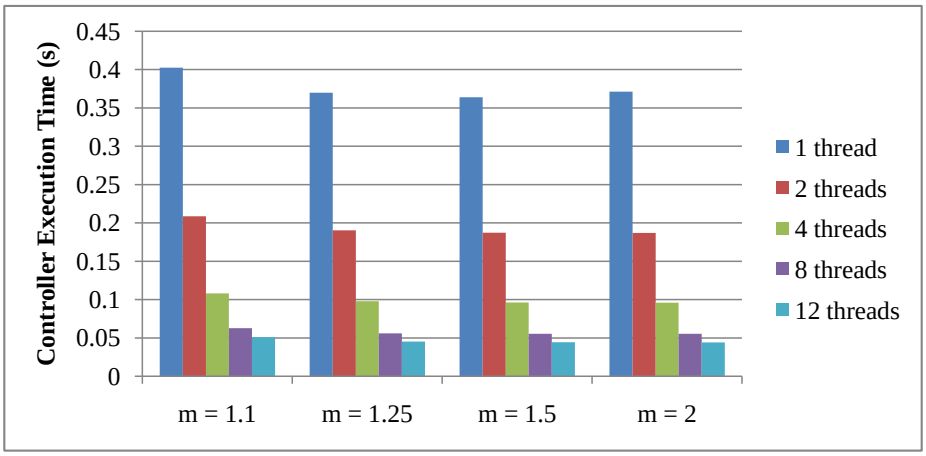

(b) Variation of the execution time of *pTrans* with m for $r = 0.9$.

Figure 5.4 : Execution time of *pTrans* with parallel threads.

Figure 5.5 : The execution time of linear programming for uniform and *Zipf* distribution ($s = 0.5$), with 100 to 1000 clients, 16 servers, $r = 1.0$ and $m = 1.1$. In comparison, even single-threaded *pTrans* can finish execution for such scale within 0.05 seconds.

5.3.1 Comparing *pTrans* with the LP and Max-flow Approaches

As a comparison, for the problem size of the scale in the parallel evaluation, both *Linear Programming (LP)* and *max-flow* take several minutes to complete, an overhead that renders it unusable in practice.

Figure 5.5 shows the execution time of *LP* for uniform and *Zipf* distributions ($s = 0.5$), with a smaller problem size: 16 servers and between 100 to 1000 clients, with $r = 1.0$, $m = 1.1$. From the figure, we can see *LP* is much slower than *pTrans*, and takes almost 30 seconds for 1000 clients. In contrast, even using a single thread, *pTrans* can finish execution for these problem sizes within 0.05 seconds.

On the other hand, Figure 5.6 shows the comparison of the controller's execution time of *pTrans* and *max-flow* with a smaller problem size of 100 to 1000 clients while keeping the number of servers to be 64, and $r = 1.0$, $m = 1.1$. From the figure, we can see with a fixed number of servers, *max-flow*'s execution time grows quadratically

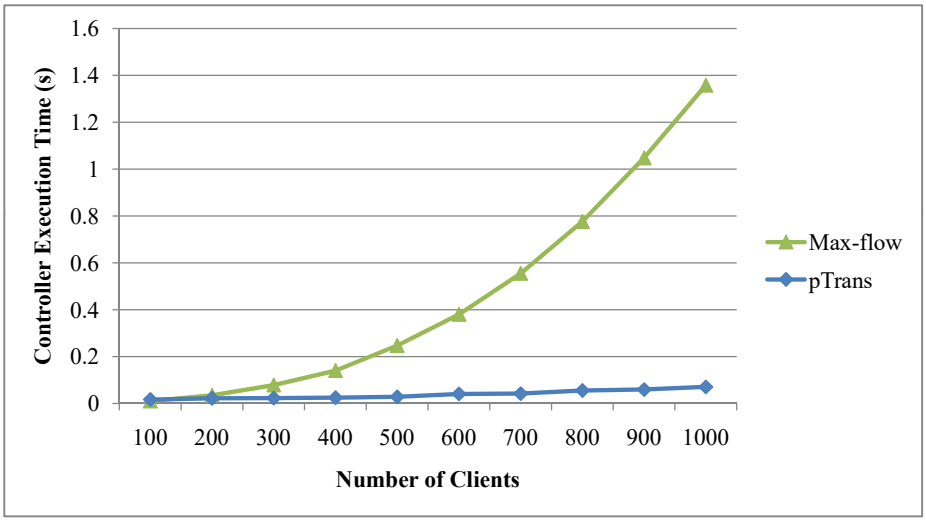

Figure 5.6 : The controller execution time of *pTrans* comparing against *max-flow*, with 100 to 1000 clients, 64 servers, $r = 1.0$ and $m = 1.1$.

with the number of clients, while *pTrans* only grows linearly. This is the main reason that *pTrans* runs faster than *max-flow*.

5.4 Approximation Evaluation

In this section, we evaluate the efficiency and accuracy of the approximation approach. To make a comparison, we maintain the configuration of Section 5.3. We choose $r = 1.0$ and $m = 1.1$ since this is the stress case that takes most execution time, and use 12 threads as well. Before beginning to shift the tokens we filter the data and retain only the top M clients with most tokens and the top M clients with the highest spare demands. We choose $M = \{100, 200, 500, 1000, 2000, 5000\}$. Moreover, we tried different reservation distributions by using different exponent factors s in generating the *Zipf* distribution. We tried $s = \{0, 0.1, 0.25, 0.5, 1, 2\}$, where a smaller s implies less variation in the reservations of different clients. In particular, $s = 0$ denotes a uniform distribution.

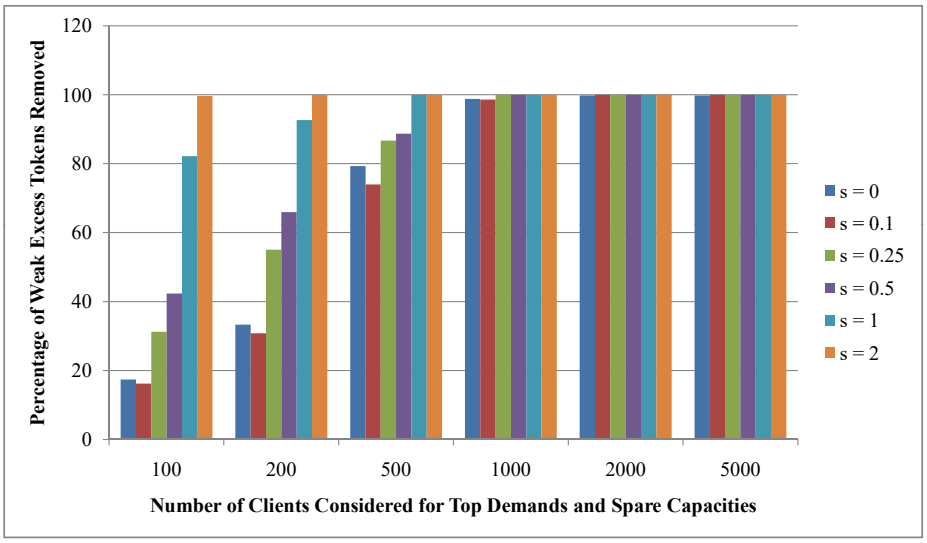

(a) Percentage of weak excess tokens removed with different M.

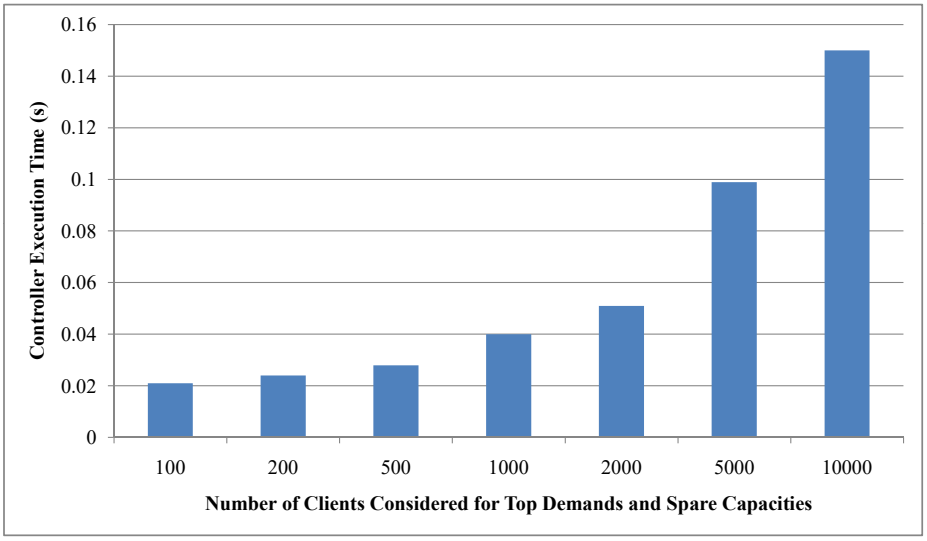

(b) Execution time with 12 threads and different M.

Figure 5.7 : Error and execution time with approximation.

Recall that the goal of the shift steps is to reduce the number of weak excess tokens. Figure 5.7a shows the percentage of weak excess tokens removed by using different M and s. Form the figure, we can see that though there are 10000 clients, considering only the top 2000 (20%) clients is enough to remove all the weak excess tokens, even with the uniform reservation distribution. Moreover, we can still remove

more than 70% weak excess tokens using only the top 500 (5%) clients. One can also see that for a fixed M we remove more weak excess tokens when the skew in the reservation distribution increases, reaching 100% success with just $1 - 5\%$ of the clients. Since skewed distributions are more likely in practice, the approximation will be especially useful in these cases.

The benefit of the approximation approach is that it can further accelerate the execution time of the *pTrans* algorithm. Figure 5.7b shows the running time of the *pTrans* algorithm with different M. It can be seen that we can achieve another $5\times$ speedup on top of the parallelization approach while still keeping the accuracy at a reasonable threshold.

5.5 Handling Demand Fluctuation

In our proposed QoS framework, the allocation of the tokens is based on the estimation of the future demand based on the recent history of request arrivals at a server. In this section, we therefore study how the framework adapts to demand fluctuations which cause incorrect demand estimates. In this experiment, there are two clients A, B with reservations 200 IOPS and unbounded limits, and two servers each capable of 200 IOPS. A is continuously backlogged on both servers and B alternates its demand between the servers. Specifically, it sends 20 requests to one of the servers on alternate 100ms intervals, starting with server 1.

Based on their capacities, each server can do 20 requests in a 100ms interval. An offline algorithm would observe that both reservations can be met by scheduling 20 requests of B on server 1 and 20 requests of A on server 2 in the first 100ms interval, and then flipping the servers of A and B in the next 100ms interval, and so on. After 1 second both clients will receive their reservations of 200 IOPS.

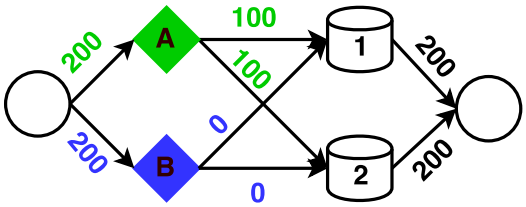

(a) Initial token allocation constraints at time 0.

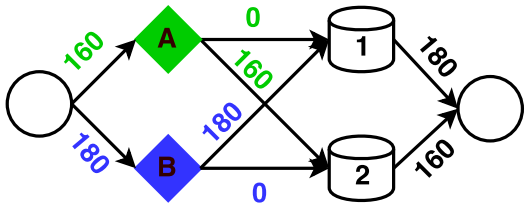

(b) The token allocation constraints at time 100ms.

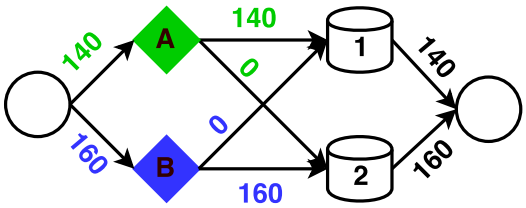

(c) The token allocation constraints at time 200ms.

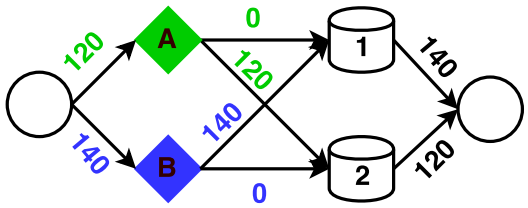

(d) The token allocation constraints at time 300ms.

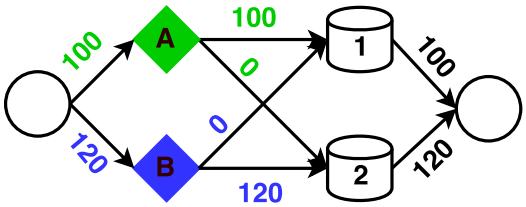

(e) The token allocation constraints at time 400ms.

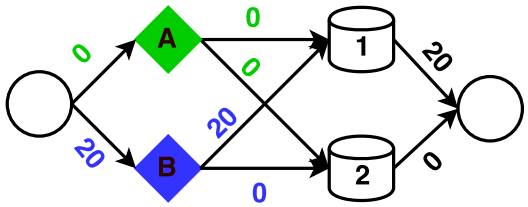

(f) The token allocation constraints at time 900ms.

Figure 5.8 : The token allocation constraints in the demand fluctuation experiment, with redistribution interval = 100ms.

However, an online algorithm that does not know of the arrival pattern can wrongly estimate the demand causing an inaccurate distribution of tokens. The pattern here is the worst-case for the demand estimation: it will always predict the demand incorrectly in every interval. However, we show that we are still able to come close to satisfying the reservations.

To better show the token allocation constraints, we show the **token allocation graph** in the *max-flow* model proposed in Section 3.3.2. The initial token allocation is shown in Figure 5.8a. Client A has its reservation divided equally between the two servers, while client B does not allocate any tokens since its predicted demand, based on its previous history, is zero. In the first 100ms interval, both A and B have requests at server 1; however B has no reservation tokens while A has enough reservation tokens to saturate the server. Hence A will get 20 requests at server 1 while B will not get any. B will have a pending queue of 20 requests which together with the arrival of 20 requests will be projected to an estimated demand of $20+20\times 9$ = 200 requests for the next allocation. Meanwhile, server 2 which only has requests from A will complete 20 of its requests as well. Also since there are no pending requests or arrivals for B on server 2, its estimated demand will be zero. The token allocation at 100ms is shown in Figure 5.8b. Based on the predicted demand, the controller moves all 180 tokens of B to server 1, and all 160 tokens of A to server 2.

The process repeats in every interval, and the pattern follows that of the offline algorithm except that it is one interval behind, serving queued requests of B on the server on which it has no current request arrivals (see Figures 5.8c - 5.8e). The final token allocation is shown in Figure 5.8f at 900 ms, where client A has consumed all its reservation tokens. As a result, A does 10 normal requests on server 2 while B finishes 10 of its 20 reservation requests on server 1. Totally, A finishes 210 requests, while B finishes 190 requests. Figure 5.9a shows the number of requests scheduled of

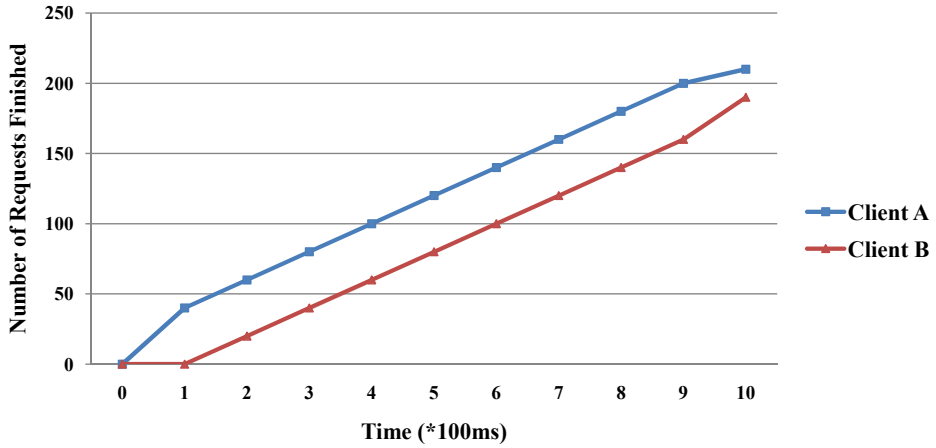

(a) Redistribution interval = 100ms.

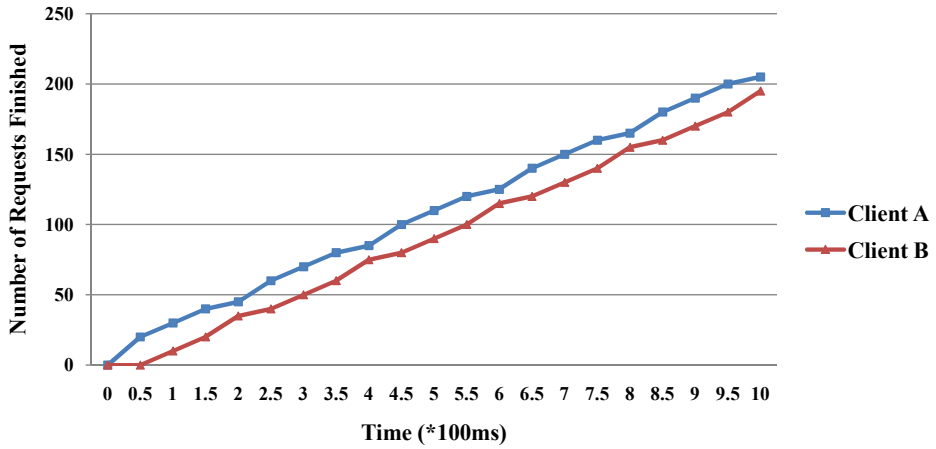

(b) Redistribution interval = 50ms.

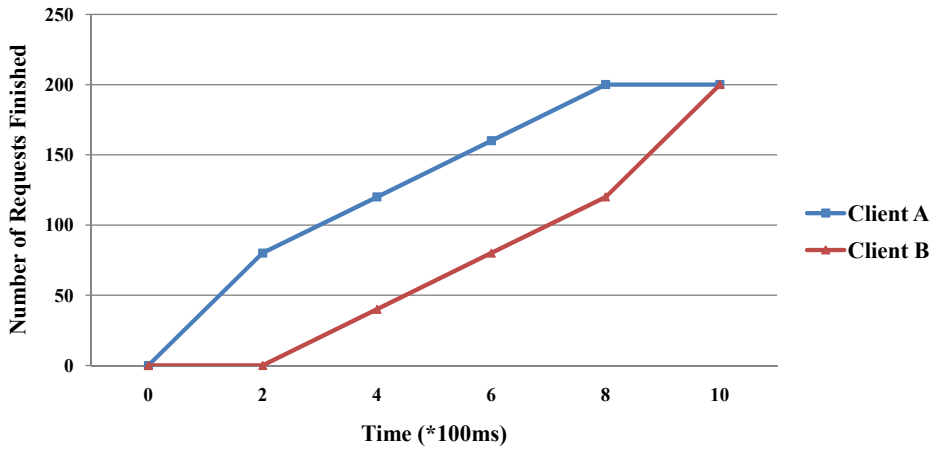

(c) Redistribution interval = 200ms.

Figure 5.9 : Number of Requests vs Time with Demand Fluctuation.

both clients against time.

Next, we change the redistribution interval to 50ms, to see if redistributing more frequently can handle the demand fluctuation better. Figure 5.9b shows the number of requests scheduled for both clients, where we see that B's reservation is still not met. On the other hand, if we change the redistribution interval to 200ms, the controller can handle the demand fluctuation better, since the interval is large enough to absorb and accurately smooth out the rapid demand fluctuation of B. Figure 5.9c shows the number of requests scheduled. We can see this time both clients meet their reservations, since the controller has accurately estimated the demand.

5.6 Linux Evaluation

In this section, we describe results on the Linux cluster in three experiments. In Section 5.6.1 we use a small configuration with static demands to show how *pTrans* meets reservations and limits. We then consider dynamically varying demands in Section 5.6.2. These experiments are done using *Memcached* as the backend server. Finally, Section 5.6.3 shows the evaluation results using file I/O.

5.6.1 *Memcached* Evaluation with Static Demand

In this experiment, we show how *pTrans* handles reservations and limits with a simple and steady configuration of 4 clients and 4 servers. We initially focus on reservations; each client has a reservation of $30,000$ RPS and an essentially unbounded limit ($200,000$ RPS was used in the experiment). Clients 1, 2, 3, 4 are continuously backlogged on servers $\{1\}$, $\{1,2\}$, $\{1,2,3\}$ and $\{1,2,3,4\}$ respectively with 5 outstanding requests. We choose a QoS period of 1 second. For the token allocation, we redistribute tokens every 200ms *i.e.* we have 5 token redistributions in each QoS

period. Theoretically, if no QoS controls are applied, the round-robin scheduler will give clients 1, 2, 3, 4 throughputs in the ratio of (1/4) : (1/4+1/3) : (1/4+1/3+1/2) : $(1/4 + 1/3 + 1/2 + 1) = 3 : 7 : 13 : 25$, which results in average throughputs of 12500, 29166, 54166, and 104166 RPS, respectively. On the other hand, when QoS controls are applied, the reservations of all clients are expected to be met.

Figures 5.10a and 5.10b show the results of the execution, which matches our theoretical analysis. Figure 5.10a shows the throughput of the clients without QoS controls and the results match the predicted throughputs closely. In Figure 5.10b the throughputs with reservation controls are shown. Client 1's throughput, which was well below its reservation, now increases to match the required $30,000$ RPS. Looking at Figure 5.10b we can see that client 4 reaches its reservation first (at roughly 400ms) since it gets service on all servers. At that point it loses priority in scheduling and the other clients get increased service; this can be seen most dramatically by the change in the slope of client 1 at that time.

Finally, we set the limit of each client to be $60,000$ RPS. Figure 5.11 shows the execution results. We can see that both reservations and limits are met by all the clients. Figure 5.11 looks similar to Figure 5.10b in the interval 0 to 0.6s, where the servers are basically doing reservation requests. Beyond this time client 4 gradually slows down as it meets its limit threshold in each sub-interval, yielding to clients that are further away from their limit.

5.6.2 *Memcached* Evaluation with Dynamic Demand

We now show how *pTrans* guarantees QoS on the cluster when demands change dynamically. We use a larger configuration of 8 servers and 10 clients. Each client has a reservation of $30,000$ RPS and a limit of $50,000$ RPS. Each client randomly chooses a number between 2 to 6 active servers; at every demand change instant, a

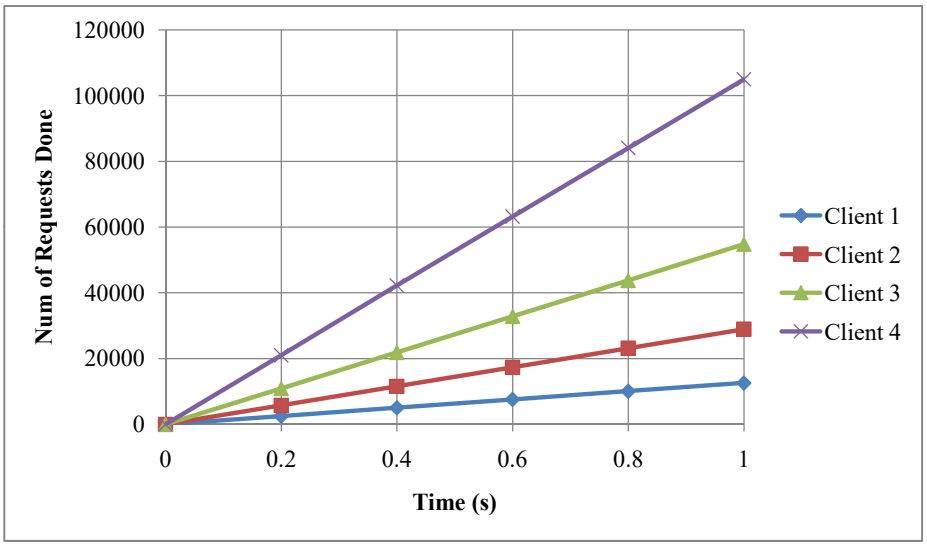

(a) The number of requests being completed with simple round-robin scheduler.

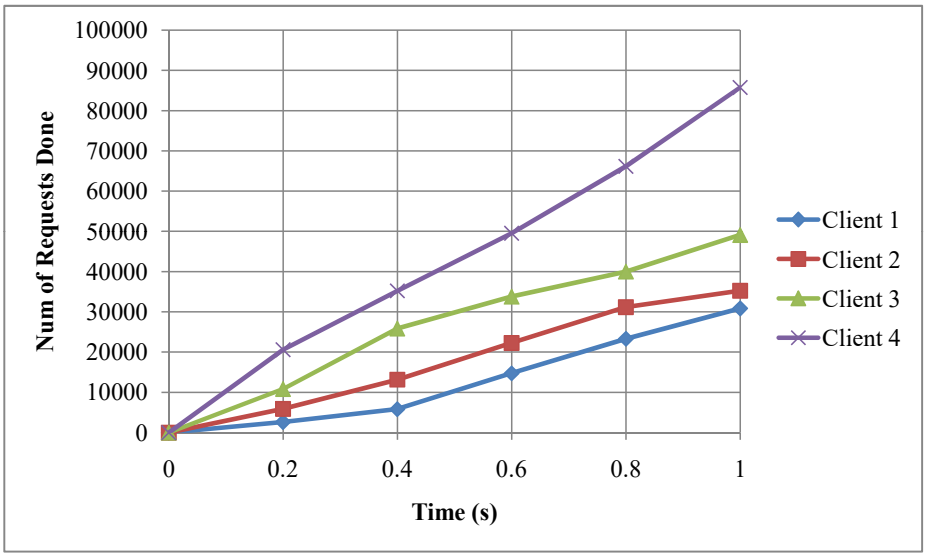

(b) The number of requests being completed with *pTrans* scheduler with only reservations.

Figure 5.10 : The number of requests done for *pTrans* and simple round robin schedulers.

fresh set of active servers (between 2 and 6) is chosen. We allow 5 demand changes for each client. We run 4 consecutive QoS periods with 5 redistributions in each period.

Figures 5.12a and 5.12b show the dynamic throughput for both scenarios. From

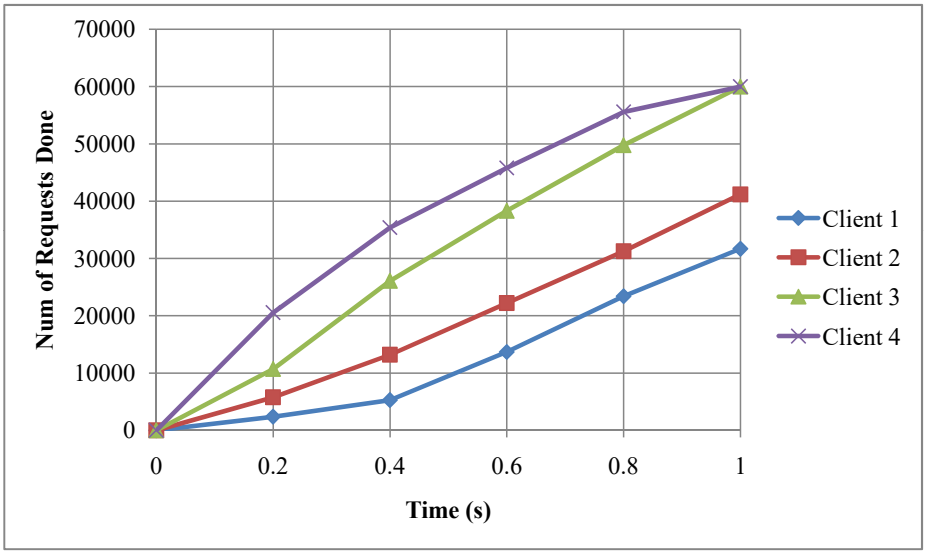

Figure 5.11 : The number of requests being completed with *pTrans* scheduler with reservations and limits.

the figures, we can see with the simple round-robin scheduler, the QoS is not guaranteed, as some clients (*e.g.* clients $5, 7$ and 8) in QoS period 1 did not meet their reservations, and some clients (*e.g.* clients 3 and 4) received throughput exceeding their limits. In contrast, by using the *pTrans* scheduler, both reservation and limit QoS was guaranteed in all intervals for all clients.

Finally, we tested a bigger problem size using 200 clients. On average without QoS controls, 68.5% of the clients met their reservations and 83.5% did not go beyond their limits. In contrast, when using *pTrans*, 99.6% of the clients met their reservations and none exceeded their limits. By running the QoS controller for 15 minutes, we found on average, the communication in every 1s QoS period takes 9ms, *i.e.* the average communication overhead is around 0.9%.

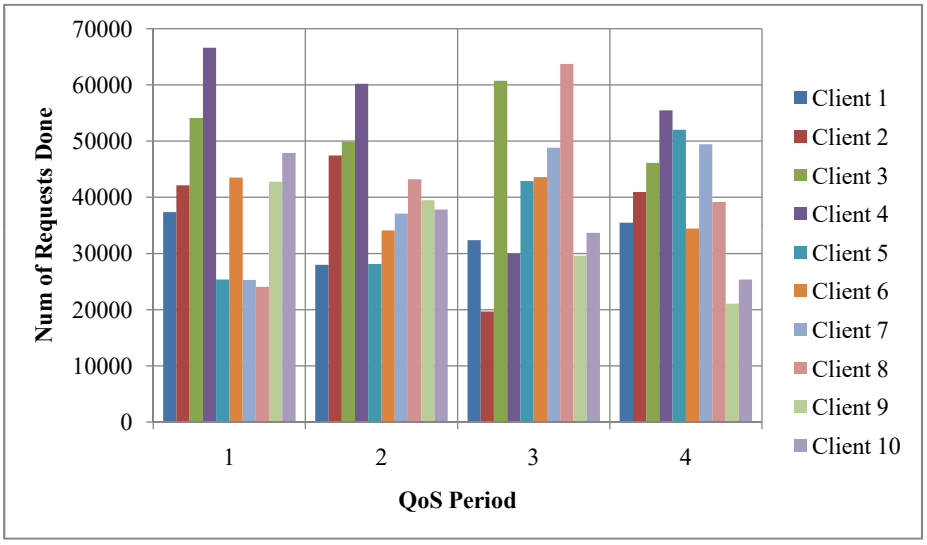

(a) The number of requests being completed with simple round-robin scheduler.

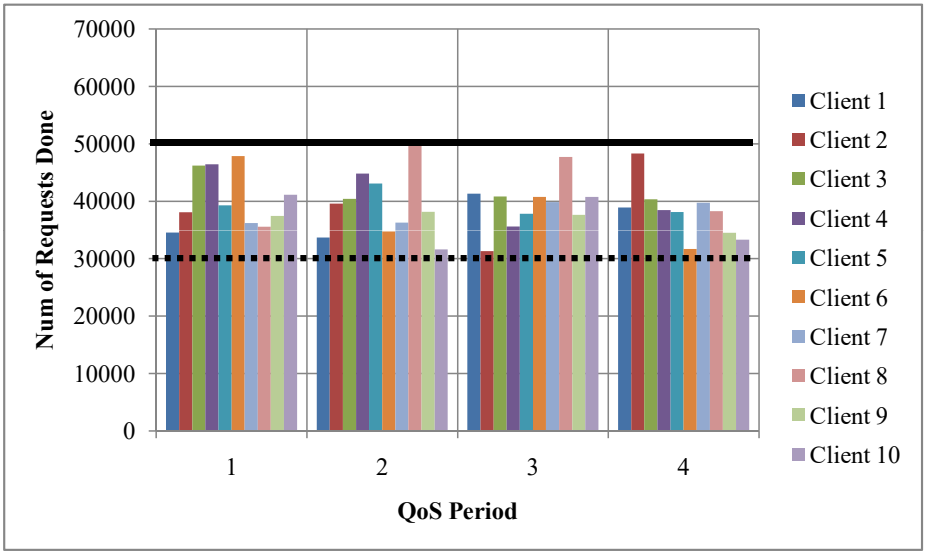

(b) The number of requests being completed with *pTrans* scheduler.

Figure 5.12 : Total number of request completed for *pTrans* and simple round-robin scheduler.

5.6.3 File I/O Evaluation

Finally, we show how our storage prototype with *pTrans* guarantees reservation and limit QoS when doing block file I/O. In this experiment, we have 8 servers and

200 clients, and 80% of the total server capacities are being reserved, *i.e.* $r = (\sum_{i \in \mathbf{B}} R_i)/(\sum_{j \in \mathbf{S}} C^j) = 0.8$. The client reservations (shown in Figure 5.13) and demands follow the same *Zipf distribution* that we used in the simulation, and each client allows 2 demand changes in the QoS period as before. Here we also assign each client a *limit* equal to 1.5 times its reservation.

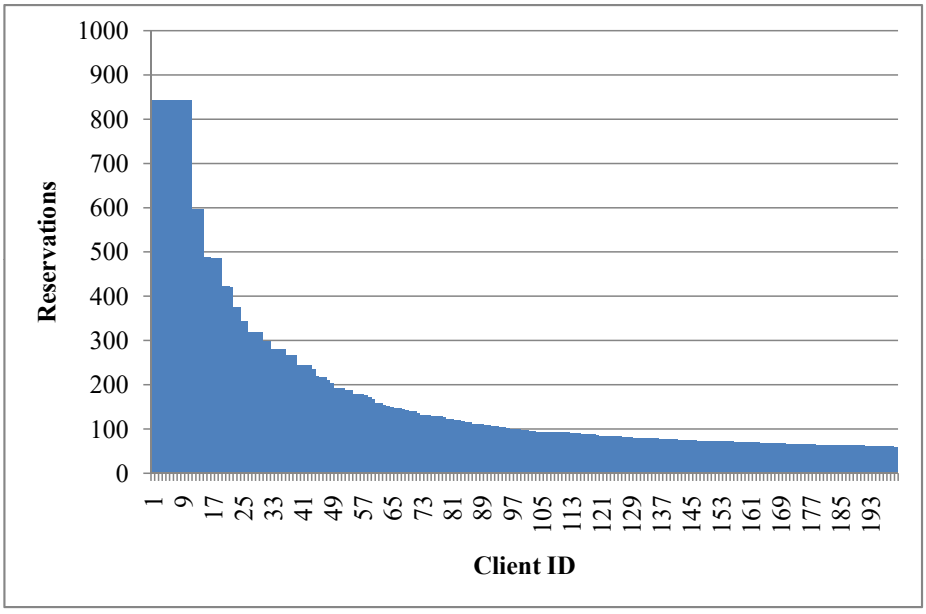

Figure 5.13 : The *Zipf distribution* of clients' reservation requirements in Linux QoS evaluation.

We set the QoS periods to be 5 seconds, and in each QoS period we do 5 token allocations, *i.e.* each redistribution interval is 1 second. We run the server for two QoS periods (*i.e.* 10 seconds) and record the QoS result as the number of requests being completed in each redistribution interval. Servers continue to serve I/Os as the controller is computing new token allocations.

Figure 5.14a and Figure 5.14b shows the number of requests being done in both QoS periods. From the figures, we can see *pTrans* provides the reservation and limit QoS in a reasonable manner. The needles, similar to those shown in the simulation,

indicate how *pTrans* handles demand changes. Quantitatively, only one client (0.5%) missed its reservation by more than 1%, and no client exceeded its limit.

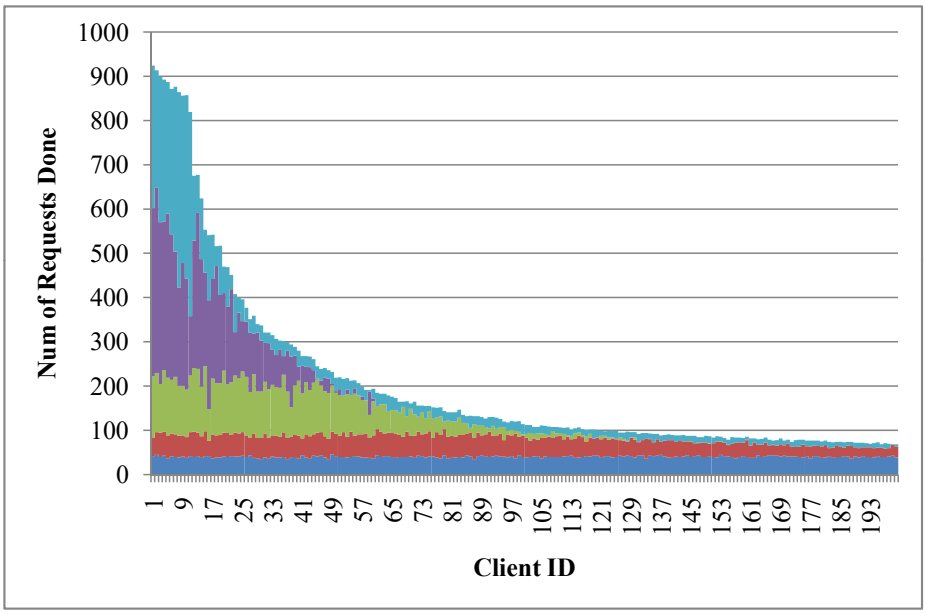

(a) The number of requests being completed in the first QoS period.

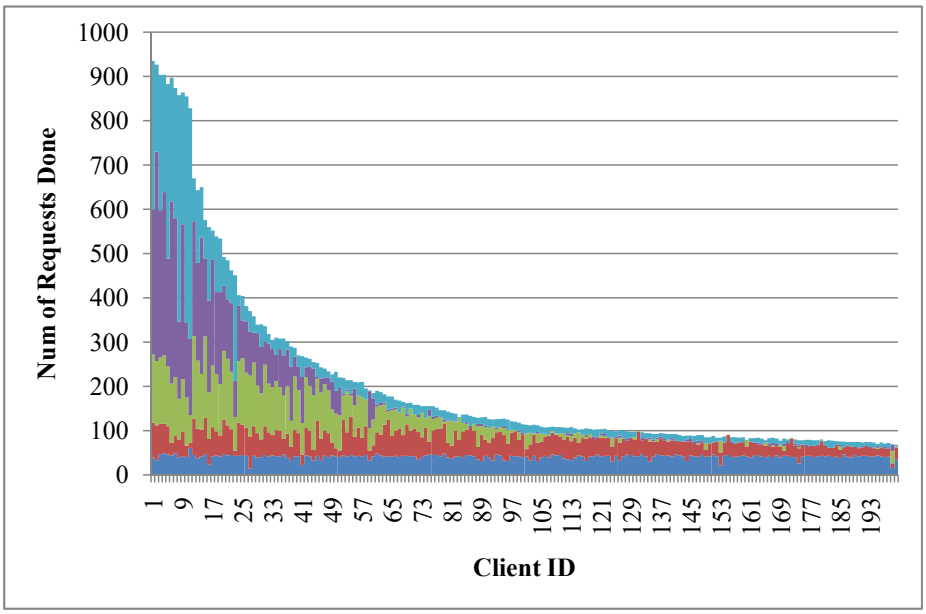

(b) The number of requests being completed in the second QoS period.

Figure 5.14 : The the number of requests being completed in Linux QoS evaluation.

Chapter 6

Response Time QoS

6.1 Chapter Overview

In this chapter, we introduce *Fair-EDF*, a framework for providing fairness to clients in a shared storage server, while guaranteeing their latencies. *Fair-EDF* aims to schedule requests to meet their specified deadlines. When it detects that the server is overloaded, it drops some requests so that the remaining requests can meet their deadlines. *Fair-EDF* drops the minimum number of requests while trying to balance this penalty among the clients.

Fair-EDF uses the *earliest deadline first* (EDF) [61] scheduling policy at the back-end, while adding a front-end *controller* that selects and drops requests in the scheduling queue when it detects that latency violations will occur. It extends the idea of the offline *RT-OPT* [62] framework to work in an online situation and adds fairness. *Fair-EDF* assumes an OS such as *MittOS* [41] is already in place which provides system support for dropped requests. In practice, *Fair-EDF* would be especially useful in streaming applications, such as streaming video from object storage.

6.2 Problem Statement

In this section, we present the latency fairness QoS problem. We focus on a single server for developing our *Fair-EDF* algorithm. In a distributed cluster, we propose a solution where QoS enforcement is done independently by each server; periodically,

the servers coordinate to adjust the QoS targets to satisfy the global fairness requirements. In this thesis, we concentrate on the latency QoS algorithm at each server. The coordination of QoS controls between servers will be studied in future work.

The storage server is shared by a number of clients that send I/O requests to the server. Each request has a stipulated latency (response time) bound. Large I/O operations are assumed to be chunked into fixed-size I/O requests. The service time of all requests is upper-bounded by σ. The service time is the interval between the time the request is dispatched to the storage device and its completion time. A request must complete its execution in σ time after being scheduled; else it is assumed to time-out and abort. A request r that arrives at time t_r is assigned a *deadline* d_r equal to the sum of its arrival time and latency bound. A request is said to be *successful* if it completes execution before its deadline, and *missed* otherwise *i.e.* if it was dropped (not scheduled), or scheduled but aborted after σ time. Each request can have its own latency bound $d_r - t_r$ based on some classification. On the other hand, a client i can also choose to specify a single latency bound δ_i for all its requests, which implies that $d_r = t_r + \delta_i$. However, this situation is covered by the more general specification. Finally, we require that the latency bound is at least the service time bound σ; *i.e.* $t_r + \sigma \leq d_r$ is always true.

Furthermore, we define the *client success ratio*, s_i, as the fraction of client i's requests that succeed. The *system success ratio* S is the fraction of the total number of requests that succeed. The goal of our framework is to shape the s_i subject to maximizing S. In this thesis, we let each client i specify its *required success ratio* q_i as its SLO, and the algorithm will try to ensure each client i has $s_i \geq q_i$. In our model, a client can specify any success ratio, but in practice, the success ratios would shadow the priorities of the clients. For example, premium clients with higher priorities are able to specify higher required success ratios.

Example 6.2.1. We motivate the latency fairness framework with the following example. Suppose a server of 100 IOPS capacity is shared by two clients A and B, which send uniformly-sized I/O requests with a service time of 10ms each. At time 0, A sends a burst of 100 requests with deadlines all at 1s. Client B sends I/O requests at a uniform rate every 10ms apart and all request have a latency bound of 40ms, *i.e.* B sends requests at times $0, 10, 20, ...$, with deadlines of $40, 50, 60, ...$ respectively.

Almost all of the 200 requests arriving at the server in one second have deadlines of 1 second or less. Meeting these deadlines would require at least double the server IOPS capacity. An *EDF* [61] scheduler, which is commonly used for supporting latency requirements, will do almost all of B's requests first, followed by those of A. Most requests of B will meet their deadlines and almost no requests of A will do so, resulting in poor fairness. Furthermore, all new requests arriving in the next second will also miss their deadlines. □

6.3 Basic Fair-EDF Framework

In this section, we describe our basic *Fair-EDF* framework. Figure 6.1 shows the components of the framework. When any request arrives at the server, the request is tentatively *accepted* for scheduling by adding it to a *taken queue*. If service demands of the requests in the taken queue exceed the system capacity, then one or more pending requests needs to be *dropped*. Requests in the taken queue wait for their turn to be dispatched by the scheduler; during its wait, the request may still be dropped as new requests arrive. The system provides fairness by selecting requests to drop so that each client meets its latency SLO. The *Fair-EDF controller* decides when to discard a request and which request to drop based on the QoS requirements. Different fairness criteria can be substituted in the controller without changing the framework.

A standard *EDF* scheduler is used to dispatch requests in deadline order. All requests that remain in the *taken queue* are guaranteed to meet their deadlines even in the worst case. The *Fair-EDF* controller extends the idea of the offline *RT-OPT* [62] framework to work in an online situation and add fairness.

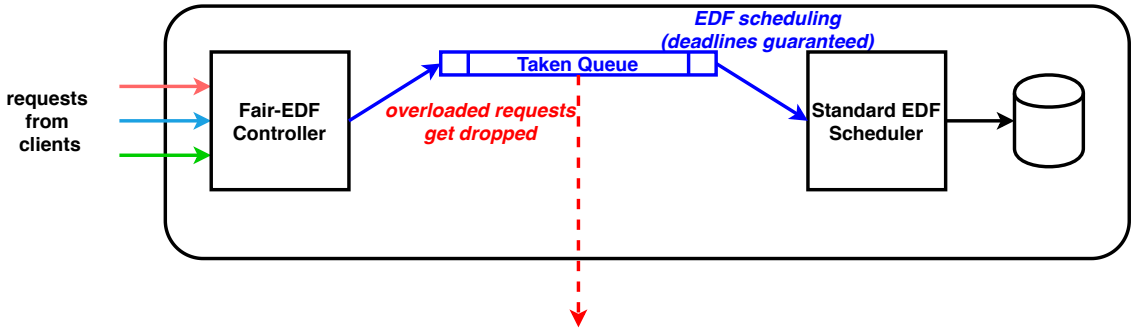

Figure 6.1 : The basic *Fair-EDF* framework.

6.4 Fair-EDF Controller

The *Fair-EDF* Controller determines whether a new request is added to the taken queue or gets dropped. If it is added to the taken queue, an existing request may sometimes be dropped in order to guarantee that all deadlines in the taken queue can be met.

6.4.1 Occupancy Chart

We first discuss the idea behind the algorithm followed by some implementation details. Let σ denote an upper bound on the service time of a request r and d_r denote its deadline. The current set of accepted requests are conceptually placed on a timeline called an *occupancy chart*. Request r occupies the *interval* $[t_r,\ t_r + \sigma]$ on the timeline where t_r is the *latest time* it can begin execution while ensuring that it

and all requests with deadlines later than d_r are successful. The occupancy chart is naturally partitioned into alternating *busy* and *idle* segments; a *busy segment* consists of a continuous sequence of intervals while an *idle segment* is not covered by any interval. As long as no interval crosses the current time T_{now}, all requests will meet their deadlines when scheduled in *EDF* order.

Example 6.4.1. Consider two clients A and B. Each request has a worst-case service time of $\sigma = 10$ms. Client A has 4 requests a_1, a_2, a_3, a_4 with deadlines 30, 100, 100, and 140ms respectively, and Client B has 3 requests b_1, b_2, b_3 with deadlines 50, 145 and 150ms. Suppose the current time is 10ms. Figure 6.2a shows the occupancy chart. Request b_3 occupies the interval $[140,\ 150]$; b_2 cannot be scheduled at 135 as it would conflict with b_3, and occupies the interval $[130,\ 140]$. Similarly a_4 must occupy the interval $[120,\ 130]$, resulting in the busy segment $[120,\ 150]$ comprising requests $\{a_4, b_2, b_3\}$. In the same way $\{a_2, a_3\}$ comprises busy segment $[80,\ 100]$, $\{a_1\}$ forms segment $[20,\ 30]$, and $\{b_1\}$ forms segment $[40,\ 50]$. □

In the implementation, we do not keep track of the interval for each request in the occupancy chart. Instead, we maintain the current busy segments in the occupancy chart, and for each request, we keep track of the busy segment it belongs to. In particular, we use $S_1, S_2, \cdots S_n$ to denote the current set of busy segments and let S_i span the time range $[L_i,\ R_i]$. We also let $S_{n+1} = [\infty,\ \infty]$ as a sentinel. Since we employ a standard *EDF* scheduler for the backend, requests in each busy segment are implicitly organized by the *EDF* order.

Example 6.4.2. We use the same setup of Example 6.4.1 in Figure 6.2a. For the occupancy chart, we maintain 4 busy segments: $S_1 = \{a_1\}$, $[L_1,\ R_1] = [20,\ 30]$; $S_2 = \{b_1\}$, $[L_2,\ R_2] = [40,\ 50]$; $S_3 = \{a_2, a_3\}$, $[L_3,\ R_3] = [80,\ 100]$; $S_4 = \{a_4, b_2, b_3\}$, $[L_4,\ R_4] = [120,\ 150]$. Within a segment the requests are arranged in *EDF* order as

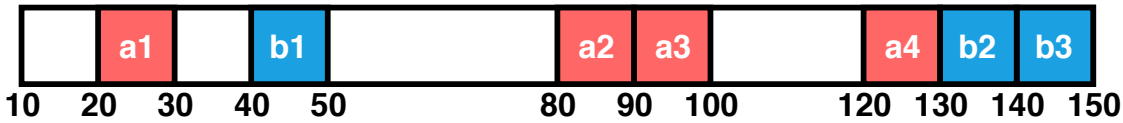

(a) The initial occupancy chart in Examples 6.4.1 and 6.4.2.

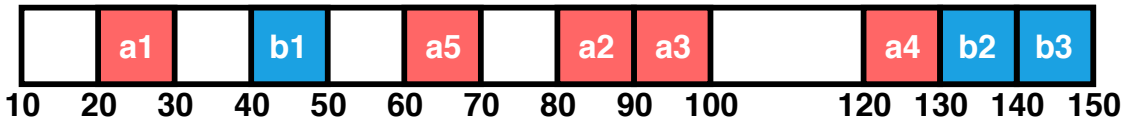

(b) The occupancy chart in Example 6.4.3 after accepting a_5.

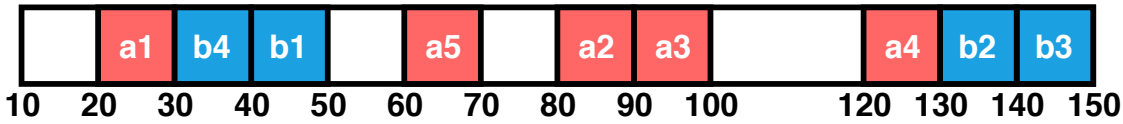

(c) The occupancy chart in Example 6.4.3 after accepting b_4.

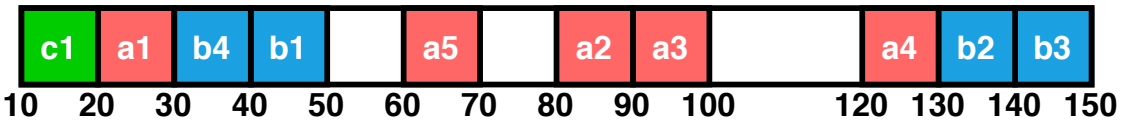

(d) The occupancy chart in Example 6.4.4 after accepting c_1.

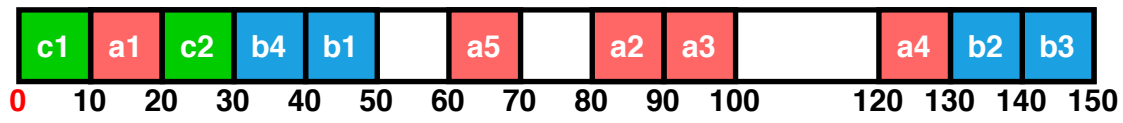

(e) The occupancy chart in Example 6.4.4 after accepting c_2.

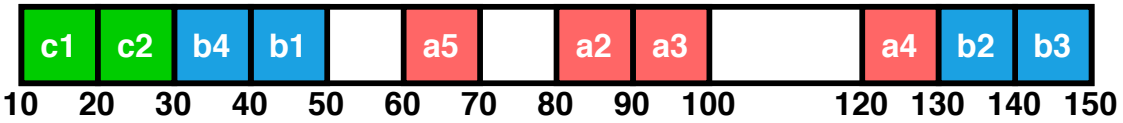

(f) The occupancy chart in Example 6.4.5 after dropping a_1.

Figure 6.2 : An illustration of the occupancy chart in Examples 6.4.1, 6.4.2, 6.4.3, 6.4.4 and 6.4.5.

shown in Figure 6.2a. For instance, by organizing the requests in $S_4 = \{a_4, b_2, b_3\}$ in *EDF* order in the busy interval $[L_4,\ R_4] = [120,\ 150]$, they will occupy the intervals $[120,\ 130]$, $[130,\ 140]$ and $[140,\ 150]$, respectively. □

It has been proved that for a set of independent jobs with arbitrary release times and deadlines, the standard *EDF* scheduler will always find a feasible* schedule if and only if there exists one [63, 64]. Therefore, as long as we can ensure there exists a feasible schedule for the requests in the occupancy chart, then by scheduling them using the standard *EDF* scheduler, the deadlines of those requests can be guaranteed.

6.4.2 Handling New Requests

When a new request r arrives, we must identify the busy segment containing its deadline, followed by updating the boundaries for the segment. This may now cause some segments to overlap, leading to a cascade of boundary changes and segment merges. If the start time of the earliest (leftmost) segment (*i.e.* L_1) is smaller than the current time T_{now}, then the current set of requests in the taken queue cannot all meet their deadlines, and one or more will need to be dropped so that the rest can be successful.

Let d_r denote the deadline of the new request r:

Case 1: d_r lies *between* two consecutive segments S_k and S_{k+1} *i.e.* $R_k < d_r < L_{k+1}$. Request r is assigned the interval $[d_r - \sigma,\ d_r]$. If $d_r - \sigma > R_k$ then we create a new segment $[d_r - \sigma,\ d_r]$ for r that lies between S_k and S_{k+1}. Otherwise, r is assigned to S_k by merging the interval $[d_r - \sigma,\ d_r]$ with the segment S_k: L_k is reduced by $\sigma - (d_r - R_k)$ (the amount of overlap) and R_k is changed to d_r. Note that changing

*Given a set of requests, a schedule is feasible if it meets all deadlines of the requests.

L_k may cause S_k to overlap segment S_{k-1}, potentially causing a cascade of merges of adjacent segments.

Case 2: d_r lies *within* a segment S_k *i.e.* $L_k \leq d_r \leq R_k$. In this case, r is assigned to segment S_k and L_k is reduced by σ. Once again, reducing L_k may cause segments S_k and S_{k-1} to overlap, potentially triggering a cascade of merges of adjacent segments.

In general, when a request arrives it is placed on the timeline using case 1 or 2 above. If the first segment now begins at a time less than the current time (this can happen only if the left boundary of the first segment S_1 changes), we say the occupancy chart is *overloaded*, and some request in S_1 has to be dropped.

Example 6.4.3. Continuing Example 6.4.1, suppose there is a new request a_5 with deadline 70ms. The request's deadline 70 falls between two segments [40, 50] and [80, 90] (*i.e.* Case 1), and it can be assigned as the new segment [60, 70], since it will not conflict with existing requests (see Figure 6.2b). Next a new request b_4 with deadline 45ms arrives. Since its deadline 45 falls inside the second segment [40, 50] (*i.e.* Case 2), it will be assigned to the second segment, and will be assigned the interval [30, 40]. Now the two adjacent segments [20, 30] and [40, 50] will merge into a single segment [20, 50], as shown in Figure 6.2c. □

Example 6.4.4. In Figure 6.2c, suppose two new requests c_1 and c_2 from client C, with deadlines 25 and 40, arrive at time 10. From Case 2 above, c_1 will be assigned to the first segment and occupy the interval [10, 20] (see Figure 6.2d). Since the current time is 10, this is a feasible schedule in which all requests will meet their deadlines if they are executed in *EDF* order. Next c_2 will be assigned to the first segment as well. Now the first segment S_1 spans the interval [0, 50], which contains requests c_1, a_1, c_2, b_4 and b_1, with deadlines 25, 30, 40, 45 and 50, respectively. These will

occupy the intervals [0, 10], [10, 20], [20, 30], [30, 40] and [40, 50], respectively (see Figure 6.2e). Now the first segment S_1 starts at time 0, which is smaller than the current time 10, which means the occupancy chart now become overloaded. □

Example 6.4.5. Continuing Example 6.4.4, we must drop one request to create a feasible schedule. A set of candidate requests is $\{c_1, a_1, b_4, c_2\}$. The choice of which of these requests to drop is governed by the QoS policy. Among the candidate requests for dropping, we will drop a request from the client i with maximum s_i/q_i value, *i.e.* the client that has the highest current fulfillment ratio. Say we dropped a_1, then the resulting occupancy chart becomes in Figure 6.2f which is no longer overloaded. □

Algorithm 10 shows the pseudo-code of the *Fair-EDF* controller algorithm. In Section 6.4.3, we formally describe the set of candidate requests which can be dropped when there is a server overflow, and give a proof of the correctness of the algorithm. We also prove that this is a sufficient condition to ensure that the removal of any such request will result in a feasible schedule. We leave as an open question for future work the derivation of the necessary and sufficient conditions for a request to be a candidate for dropping, and efficient implementations of the same.

6.4.3 Candidate Set Identification

Consider a snapshot of the first segment of the occupancy chart at time t_0. For notational convenience, we normalize the chart so that each interval is of length 1 (rather than σ), and denote the first segment by Σ.

Let there be n requests $r_1, r_2, \cdots r_n$ at time t_0 arranged in deadline order; that is if d_i denotes the deadline of r_i then $d_1 \leq d_2 \leq d3 \cdots \leq d_n$. Without loss of generality, let r_1 occupy the interval (slot) $[s,\ s+1]$ in Σ; since all the slots in Σ are occupied with no gaps, request r_i occupies the slot $[s+i-1,\ s+i]$.

Algorithm 10: *Fair-EDF* **Controller Algorithm**

```
// A new request r with deadline d_r arrives
// Adjusting the occupancy chart according to T_now
while R_1 ≤ T_now do
    Remove S_1 and re-number segments;
if L_1 < T_now then
    L_1 = T_now;
// Adding r to the occupancy chart
Add r to the taken queue;
Find S_k, where R_k < d_r < L_{k+1} or L_k ≤ d_r ≤ R_k;
if R_k < d_r < L_{k+1} then
    // Case 1
    Create and insert new segment S'_k = [d_r − σ, d_r] between S_k and S_{k+1};
    Assign r to S'_k;
    k = k';
else
    // Case 2
    L_k = L_k − σ;
    Assign r to S_k;
// Merging the overlapping segments
while k > 1 and R_{k−1} ≥ L_k do
    L_{k−1} = L_{k−1} − (L_k − R_{k−1});
    R_{k−1} = R_k;
    Remove S_k;
    k = k − 1;
// Handling request overloading
if L_1 < T_now then
    Let i be the client with the highest s_i/q_i value that has a request r̂ ∈ C,
      where C is defined in Section 6.4.3;
    // Note: r̂ may be same as r. In basic Fair-EDF (Section 6.3), r̂
      is discarded and marked as missed. With best-effort scheduling
      (Section 6.5), r̂ is put into the dropped queue.
    Drop r̂;
    L_1 = L_1 + σ;
```

Observation 6.1: If r_i is scheduled no later than $s + i - 1$ (that is the left-endpoint of the interval it occupies) it will meet its deadline.

Observation 6.2: Σ has a *feasible schedule* in which all requests can meet their deadline, if and only if if $s \geq t_0$.

Suppose Σ has a feasible schedule. Now a new request r^* with deadline d_{r^*} is inserted into Σ, and assume that $d_k \leq d_{r^*} < d_{k+1}$. Σ is modified to a segment Σ^* for the $(n+1)$-request sequence: $r_1 \cdots r_k, r^*, r_{k+1}, \cdots r_n$. Each request $r_i, 1 \leq i \leq k$, is shifted one slot to the left and occupies the slot $[s + i - 2,\ s + i - 1]$ in Σ^*. The requests $r_i, k + 1 \leq i \leq n$, occupy the same slots as they did in Σ, and r^* occupies the slot $[s + k - 1,\ s + k]$.

If Σ^* does not have a feasible schedule the controller needs to discard one of the requests to ensure a feasible schedule. We need to identify as many requests that can be discarded while guaranteeing that the remaining requests have a feasible schedule. We call the set of requests that can be discarded as the *candidate set*. A larger candidate set implies a larger pool from which to select a victim.

Some obvious possibilities for candidate requests are readily apparent. Discarding the new request r^* will allow Σ^* to revert to the feasible schedule of Σ; similarly, discarding the request occupying the first slot $[s - 1,\ s]$ where $t_0 < s$, will also solve the problem. To completely characterize the candidate set we introduce the following definitions.

Definition 6.1: Define the *slack* of a request in Σ^* as the amount of time it can be delayed while still meeting its deadline. If a request with slack $\rho \geq 1$ currently occupies slot $[u,\ u + 1]$ then it will still meets its deadline if scheduled in any of the later slots $[u + 1,\ u + 2]$, $[u + 2,\ u + 3] \cdots\ [u + \rho,\ u + \rho + 1]$.

Definition 6.2: Define λ to be the largest integer such that $s + \lambda \leq d_{r^*}$, where d_{r^*} is the deadline of the new request r^*.

Note that r^* occupies slot $[s+k-1,\ s+k]$ in Σ^*. If $\lambda = k$ then r^* occupies slot $[s+\lambda-1,\ s+\lambda]$.

Lemma 12. If $\lambda - 1 \geq k+1$, all requests $r_{k+1}, r_{k+2}, \cdots, r_{\lambda-1}$ have a slack of at least 1 in Σ^*.

Proof. A request $r_i,\ k+1 \leq i \leq \lambda-1$, has a deadline $d_i > d_{r^*} \geq (s+\lambda)$. Hence it can meet its deadlines if it is scheduled in the slot $[s+\lambda-1,\ s+\lambda]$. Since $r_{\lambda-1}$ currently occupies slot $[s+\lambda-2,\ s+\lambda-1]$, it has a slack of 1. All remaining $r_i,\ k+1 \leq i < \lambda-1$, have slack greater than 1. □

Corollary 12.1. If $\lambda - 1 \geq k$, request r^* has a slack of 1 in Σ^*.

Lemma 13. All requests $r_1, r_2, \cdots, r_k$ have a slack at least 1 in Σ^*.

Proof. Any request $r_i,\ 1 \leq i \leq k$ that occupies a slot $[u,\ u+1]$ in Σ, will occupy the slot $[u-1,\ u]$ in Σ^*. Since Σ had a feasible schedule, r_i must have a slack of 0 or higher in Σ, and hence a slack of 1 or more in Σ^*. □

Theorem 14. Let $\mathcal{C} = \{r_i,\ \ i = 1 \cdots \lambda\} \cup \{r^*\}$. Then if any request $r \in \mathcal{C}$ is dropped, the remaining requests have a feasible schedule.

Proof. Whichever request from $\mathcal{C}$ is dropped, the remaining requests have a slack of at least 1. Hence all requests occupying slots earlier than that of the dropped request can be moved forward by one slot, and no request will required to be scheduled before t_0. □

6.5 Fair-EDF Scheduler for Best-Effort Scheduling

Since in practice, the upper bound on service time, σ, overestimates the actual service time, the basic *Fair-EDF* may unnecessarily drop some requests because of the

pessimistic assumption. Therefore, we are motivated to add a second-chance policy to the basic scheme. In this approach, the requests dropped from the *taken queue* are not discarded immediately but queued and executed opportunistically if there is free bandwidth before their deadlines. We therefore add a best-effort scheduling component to *Fair-EDF*. The new framework is shown in Figure 6.3, where a *dropped queue* is added. Similar to the *taken queue*, the *dropped queue* is also a priority queue based on request deadlines, and all dropped requests are moved to the *dropped queue* for best-effort scheduling.

Accordingly, instead of having the standard *EDF* scheduler in Figure 6.1, we introduce our *Fair-EDF scheduler*. It keeps fetching and scheduling requests from the taken queue and dropped queue. Requests in the taken queue are guaranteed to meet their deadlines if their actual service times do not exceed σ. The dropped queue is used for best-effort scheduling through work-stealing.

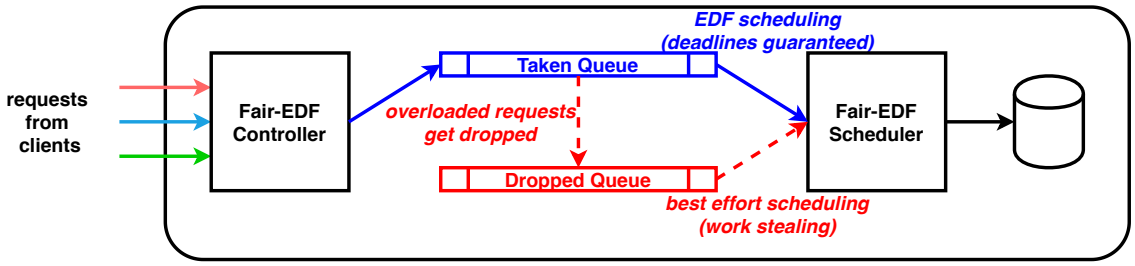

Figure 6.3 : The *Fair-EDF* framework with best-effort scheduling.

The request scheduling process is as follows: the *Fair-EDF* scheduler first removes the requests in the dropped queue whose deadlines can no longer be guaranteed even if they are scheduled immediately *i.e.* it removes all requests r for which $T_{now} + \sigma > d_r$. These removed requests will be counted as missed. Now let tq and dq to be the requests with earliest deadlines in the taken queue and dropped queue respectively. *Fair-EDF* scheduler will perform work-stealing for dq if it can guarantee that scheduling dq will

not disrupt the guaranteed deadlines of requests in the taken queue, *i.e.* $T_{now}+\sigma \leq d_{dq}$ and $T_{now}+\sigma \leq L_1$ where L_1 is the left boundary of the first segment of the occupancy chart defined in Section 6.4.1. If work-stealing cannot be performed, the scheduler will schedule tq instead. If the first of the conditions is violated the request dq is discarded and marked as missed. The opportunity for work-stealing arises because not all requests will use their worst-case allocated service time, and the excess is returned to the system as credit; when the total credit reaches σ, we will have the chance to schedule requests from the dropped queue.

Algorithm 11 shows the pseudo-code of the *Fair-EDF* scheduler algorithm for best-effort scheduling.

6.6 Chapter Summary

In this chapter, we presented *Fair-EDF*, a framework providing fairness QoS for latency guarantees in shared storage systems. *Fair-EDF* combines the idea of the offline algorithm *RT-OPT* with the *EDF* scheduler, and employs a work-stealing mechanism for best-effort scheduling. In the next chapter, we will show in the evaluation that *Fair-EDF* gives reasonable fairness control with different runtime workload behaviors, and the runtime overhead is relatively small.

Algorithm 11: *Fair-EDF* **Scheduler Algorithm for Best-Effort Scheduling**

```
while TRUE do
    // Removing requests in the dropped queue with deadlines
     cannot be guaranteed
    while DroppedQueue is not empty do
        dq = DroppedQueue.top();
        if T_now + σ > d_dq then
            dq = DroppedQueue.pop();
            count dq as missed;
        else
            break;
    L_1 = the left boundary of the first segment of the occupancy chart;
    if DroppedQueue is not empty and T_now + σ ≤ L_1 then
        // Work-stealing
        dq = DroppedQueue.pop();
        Schedule dq;
        if dq finishes within its deadline then
            count dq as successful;
        else
            count dq as missed;
    else
        if TakenQueue is not empty then
            // Normal scheduling
            tq = TakenQueue.pop();
            Schedule tq;
            if tq finishes within its deadline then
                count tq as successful;
            else
                count tq as missed;
```

Chapter 7

Evaluation of Response Time QoS

7.1 Experimental Setup

In the evaluation, we compare *Fair-EDF* with a standard *EDF* scheduler, as well as a variant of *EDF* we call *Prudent-EDF*. The problem with standard *EDF* is that a capacity overload will cause the deadlines of future requests, those following the overloaded period, to be missed as well. By contrast, *Prudent-EDF* drops requests that it recognizes will miss their deadline, thereby preventing them from affecting future request deadlines. *Prudent-EDF* drops a request at the latest possible time and consequently, like an immediate-drop policy, cannot shape the QoS profile by selecting an appropriate victim request to discard. However, like *Fair-EDF*, it will drop the minimal number of requests in the worst case.

We implemented a prototype of the *Fair-EDF* framework in *OpenMP*. We use different threads to handle the request controller and request scheduler and keep them pinned on different cores. The arrival pattern and deadlines of the clients are explicitly specified using external input files. The controller generates requests at desired times. With *Prudent-EDF*, the scheduler chooses requests in deadline order but will discard the request at the head of the queue if its deadline cannot be guaranteed. For *Fair-EDF*, the controller maintains taken and dropped queues as discussed in Section 6.5. The scheduler chooses a request from one of the queues depending on whether it can perform work stealing or not and discards requests from the head of the dropped queue that cannot be guaranteed.

The workload in our evaluation consists of random 4KB direct reads from a 1GB file. We run our experiments on a standard Linux server. The server node is equipped with an Intel® SSD DC S3700 hard disk [65] and an Intel® Xeon® E5-2697 CPU [66]. We profiled the service time using the standard *EDF* scheduler and a closed loop client which keeps the server always busy. The average profiled service time for each request is $142\mu s$, *i.e.* the server has an average throughput of around 7050 IOPS.

7.2 Linux Evaluation

7.2.1 QoS Evaluation

In this evaluation, we have 2 clients. Client 1 sends one request every 0.15ms, with a latency bound of 0.5ms. Client 2 sends a burst of 10 requests every 10ms, with a latency bound of 25ms for each request. Client 1 has a request rate of 6667 IOPS, and Client 2 a rate of 1000 IOPS. The load on the server is 7667 IOPS which exceeds its capacity of 7050 IOPS. The specified success ratios for clients 1 and 2 are 0.9 and 0.8, respectively.

We ran the system for a second, and Figure 7.1 shows the success ratio of both clients using the three policies. Figure 7.2a and 7.2b show the average response time for both clients. We can see that *EDF* gradually misses the deadlines of both clients, and the response times start to increase. Due to the chain effect of missed deadlines for simple *EDF* scheduling under overload, it results in a poor success ratio for both clients. For *Prudent-EDF*, technically no deadlines will be missed (since they are proactively dropped). However, for this workload it keeps doing requests of client 1 and drops most of the requests of bursty client 2, resulting in poor fairness between clients. Finally, *Fair-EDF* also guarantees that no deadlines will be missed and will

drop the same (minimal) number of requests as *Prudent-EDF*. However, it tries to fairly distribute the pain of dropped requests according to the required success ratios.

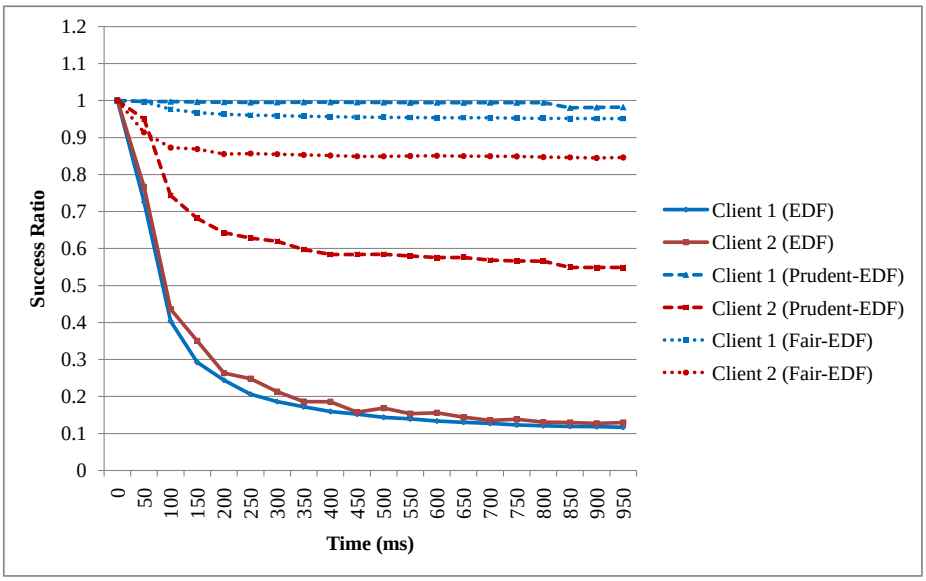

Figure 7.1 : The success ratio of both clients using three policies.

7.2.2 Effect of Overestimated Service Time

In practice, the actual service time is not fixed and the exact value may be unknown. The σ we choose must be a strict upper bound of the service time and so we must use an overestimate. To avoid losing throughput due to the conservative assumption we use the dropped queue to pick up overflowing requests based on the estimated service time. In this evaluation, we show how *Fair-EDF* handles overestimated σ, especially how the dropped queue is used for utilizing the time credits caused by the overestimation. We keep the same arrival pattern of the clients as Experiment 1. However, we vary σ from 2× to 20× of the profiled average cost of 142μs. We set the latency bound to be 10ms for both clients' requests, which is greater than the maximum service time as required (see Section 6.2).

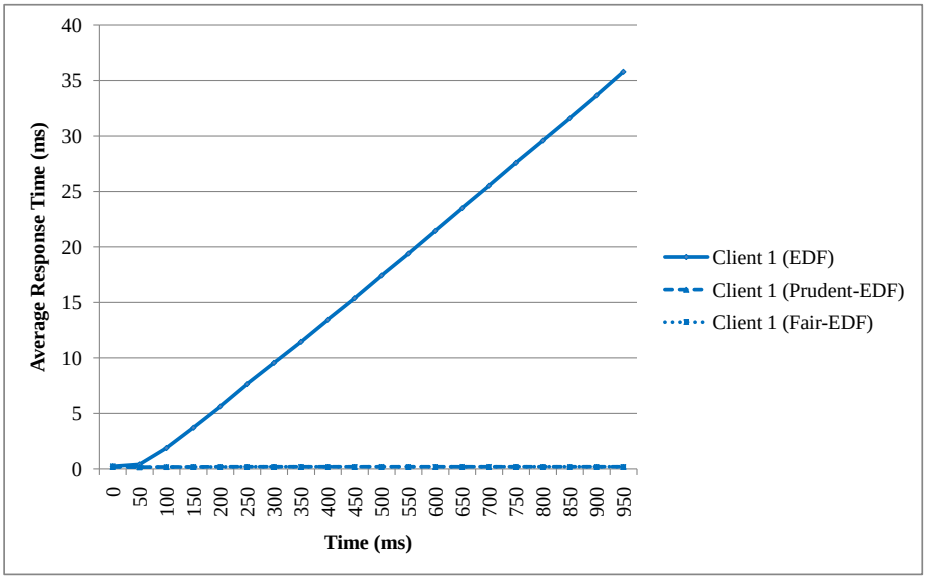

(a) The average response time for Client 1 using three policies.

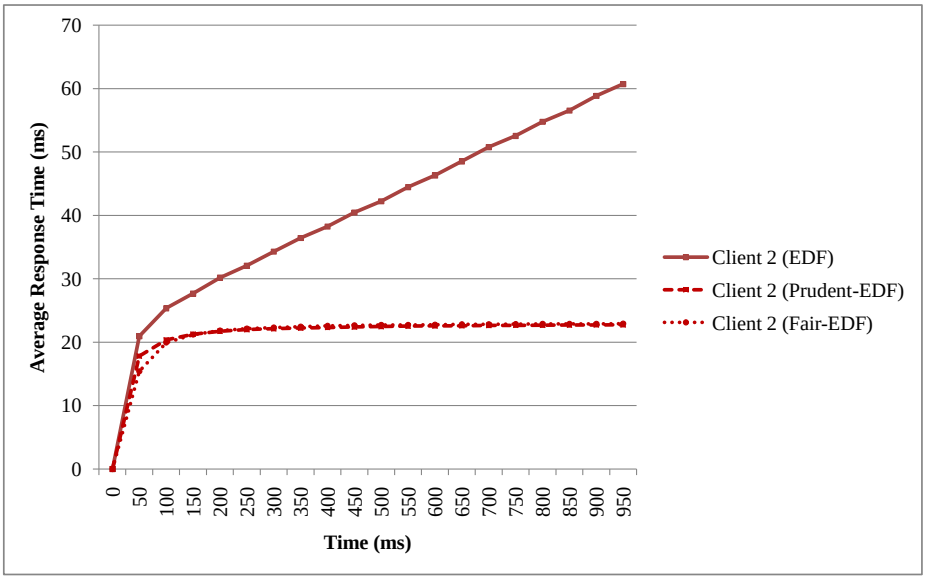

(b) The average response time for Client 2 using three policies.

Figure 7.2 : The average response time for both clients using three policies.

We run *Fair-EDF* for one second with different σ, and use *Prudent-EDF* as a comparison. The success ratios are shown in Figure 7.3. From the figure, we can see the system success ratio (green bar) does not decrease with the overestimation factor.

The reason is that with a higher σ, although fewer requests are placed in the taken queue, each request finishes much earlier than σ and provides greater opportunities for work-stealing in the dropped queue. Similarly, until σ gets very high (overestimate by 10× the real cost), the QoS result is also good. With a high value of σ, the fairness starts getting worse and approaches that of *Prudent-EDF*. The reason is that with a high σ, many more requests are put into the dropped queue, making the controller unable to catch up the changes. In the extreme case, with σ tending the ∞, all requests are put into the dropped queue, and the scheduler essentially becomes *Prudent-EDF*. The experiment illustrates this predicted behavior.

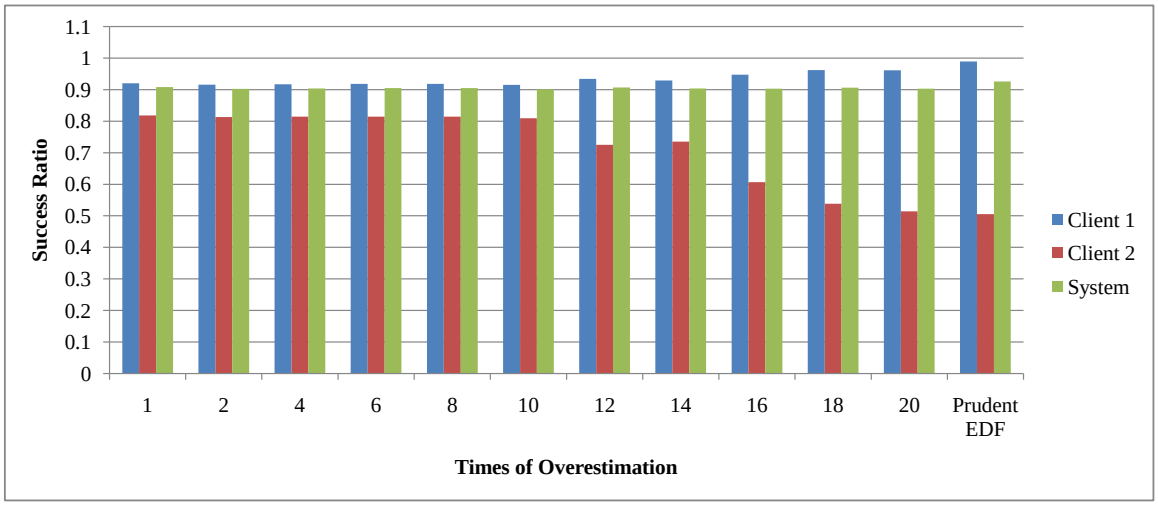

Figure 7.3 : Evaluation result for different overestimated service times.

7.2.3 QoS Result for More Clients

In this evaluation, we have 10 clients sharing the server. The arrival patterns and deadline specifications are shown in Table 7.1. Clients 1 to 8 send requests at different fixed rates, and clients 9 and 10 are very bursty. The total load is again 7750 IOPS exceeding the server capacity of 7050 IOPS.

Client	Inter-Arrival Time (ms)	Burst Size	Demand (IOPS)	Deadline Time (ms)
1	0.4	1	2500	0.5
2	1	1	1000	1
3	1	1	1000	1
4	2	1	500	2
5	2	1	500	2
6	2	1	500	2
7	2	1	500	4
8	4	1	250	4
9	40	20	500	40
10	50	25	500	50

Table 7.1 : The arrival pattern and deadline specifications of the clients.

For *Fair-EDF*, we introduce a grouping policy consisting of two groups: *gold* and *silver*. The *gold* group has a required success ratio of 0.9, and the *silver* group has a required success ratio of 0.8. We show the results of two grouping policies. Policy 1 groups clients 1 to 8 as *gold* and the rest as *silver*, and policy 2 does the opposite, *i.e.* grouping clients 1 to 8 as *silver* and the rest as *gold*.

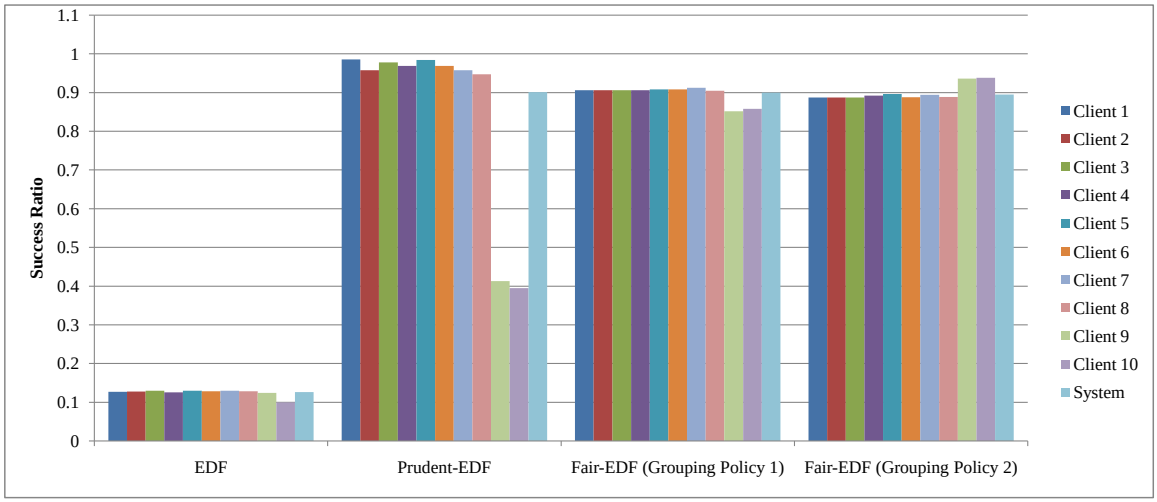

Figure 7.4 : Evaluation result for the experiment with ten-clients and two-groups.

We run the three schedulers for one second, and the success ratio for all clients as well as the system is shown in Figure 7.4. From the figure, we can see that *EDF* has poor success ratios for all clients since it gradually misses all deadlines if the capacity is not enough. Both *Prudent-EDF* and *Fair-EDF* have a good system success ratio. However, in *Prudent-EDF*, most requests of bursty clients 9 and 10 are dropped, making their success ratios below the other clients and the system's ratio. In contrast, by using *Fair-EDF*, the success ratios of clients 9 and 10 go up to the required success ratio of the group, while the success ratios of other clients do not decrease significantly, resulting in better fairness. Moreover, *Fair-EDF* achieves a similar system throughput as *Prudent-EDF*. This indicates *Fair-EDF* does not introduce much runtime overhead compared with *Prudent-EDF*.

Chapter 8

Conclusions and Open Problems

8.1 Conclusions

In this thesis, we studied the problem of providing QoS in distributed storage systems, and developed novel algorithms for providing bandwidth and latency guarantees. For bandwidth allocation, we proposed *bQueue*, a novel coarse-grained scheduling framework for reservation and limit QoS controls in distributed storage systems. *bQueue* uses token allocation to control the number of high-priority reservation requests, and to cap the maximum number of requests served for each client. To accommodate demand and server capacity variations due to workload changes, token allocations are recomputed at fixed intervals using dynamic demand and capacity estimates. Optimization problem formulations based on Integer Linear Programming and Maximum Network Flow were developed for token allocation. A simple token-sensitive round-robin scheduler that executes at each server was developed to enforce the reservation and limit requirements. Compared to fine-grained QoS solutions, *bQueue* does not incur the extra overhead of using a centralized metadata server for tagging all requests of a client, and uses a simple round-robin scheduler at the servers. Our performance results show that *bQueue* is able to handle run-time variations in demands and service rates, and provide reasonable and accurate QoS to the clients.

We developed *pTrans*, a fast and scalable algorithm for solving the token allocation problem. *pTrans* models the problem as distributing tokens on a small graph (number of vertices equal to the number of servers) augmented with per-edge vectors reflecting

current client token allocations. *pTrans* greedily transfers tokens from overloaded to underloaded servers while avoiding the creation of wasteful strong-excess tokens that cannot be consumed due to insufficient demand. We formally proved that *pTrans* converges to the global optimal in a polynomial number of steps. Furthermore, it has a much smaller run time than existing approaches, and can be further accelerated using parallelization. Empirical performance results show that *pTrans* achieves orders-of-magnitude improvement in execution time over the alternative *ILP* and *max-flow* based approaches.

For response time QoS we introduce *Fair-EDF*, a framework providing fairness in latency tail distributions of concurrent clients. *Fair-EDF* combines the idea of the offline algorithm *RT-OPT* with the standard *EDF* scheduler to identify overload conditions at a server. It uses a data structure called *occupancy chart* for identifying candidate requests that can be dropped to alleviate the overload. *Fair-EDF* also incorporates a work-stealing mechanism for best-effort scheduling of dropped requests. The evaluation results show that *Fair-EDF* is effective in meeting QoS guarantees for different dynamic workload behaviors.

8.2 Open Problems

In this section, we discuss some open problems identified in the course of this research.

8.2.1 Bandwidth Allocation QoS

Demand and Capacity Estimation: In many practical situations, the demand of the clients may not change too frequently. In such cases, recomputing token allocations in fixed redistribution intervals may be unnecessary. Instead, we can use a dynamic window to monitor the demand changes, and trigger token allocation only

if demands change beyond a threshold. A similar approach can be applied for server capacity estimation. By using dynamic estimation, we can reduce the communication overhead as well.

Additional QoS Controls: A broad open problem is how to provide QoS controls such as weight-proportional bandwidth allocation in a distributed environment. We will also study the token allocation problem for distributed systems which employ data replication. In one such model, any server can be used to satisfy a read request, leading to additional choices in the token distributions. Dealing with writes in this environment creates additional challenges and depends heavily on the write protocols and consistency models in place.

Distributed Token Controller: In the current design, the token controller is centralized. An open problem is to investigate ways to distribute the token control algorithm to further improve the scalability.

8.2.2 Response Time QoS

In this section, we discuss some open issues and challenges for *Fair-EDF*.

Average service time estimation: Estimating the service time of a request once it is dispatched to the back-end server is a challenging problem. By improving the estimated upper-bound, *Fair-EDF* can reduce the number of requests that need to be served on a best-effort basis, and thereby increase the fairness of the tail latency distributions. This is an orthogonal issue to our results. MittOS [41] studied predicting the request costs for better handling requests latencies.

Variable request service times: A difficult problem is to adapt *Fair-EDF* to efficiently support requests with highly variable service times, so a single upper-bound σ is unreasonable. The current algorithm will need to be generalized to handle this

situation. For instance, in the substitution, one long request may cause several short requests to be dropped, and a single substitution may involve requests of multiple clients. Thus, there are more choices in the substitution, which increases algorithmic complexity and implementation overheads. Furthermore, with variable service times, we may need a different policy for fairness. For instance, we may want to give different weights to requests based on their service times; otherwise, longer requests are more likely to be dropped.

Scalability improvement: The scalability of *fair-EDF* as the number of clients and requests increases, and the storage system processes requests faster, warrants further research. Possible avenues for improvement are implementations using better data structures such as priority queues or balanced binary search trees (e.g. *AVL tree*, *Red-black tree* and *interval trees*) which handle insertion, modification and deletion in worst-case logarithmic time. In addition, more efficient data structures for QoS selection on subsets of the requests need to be designed.

Fairness in distributed clusters: The original motivation for the work was the difficulty of shaping the workload at individual servers of a clustered storage system. Combining the individual server schedulers with a global QoS policy where the performance of a client in aggregate across all servers is optimized, is an interesting avenue for further research.

Bibliography

[1] S. A. Weil, S. A. Brandt, E. L. Miller, D. D. Long, and C. Maltzahn, "Ceph: A Scalable, High-Performance Distributed File System," in *Proceedings of the 7th symposium on Operating systems design and implementation*, pp. 307–320, USENIX Association, 2006.

[2] B. Sakshi, "GlusterFS : A Dependable Distributed File System." `http://opensourceforu.com/2017/01/glusterfs-a-dependable-distributed-file-system/`, 2017.

[3] M. R. Palankar, A. Iamnitchi, M. Ripeanu, and S. Garfinkel, "Amazon S3 for Science Grids: a Viable Solution?," in *Proceedings of the 2008 international workshop on Data-aware distributed computing*, pp. 55–64, ACM, 2008.

[4] Y. Saito, S. Frølund, A. Veitch, A. Merchant, and S. Spence, "FAB: Building Distributed Enterprise Disk Arrays from Commodity Components," in *ACM SIGARCH Computer Architecture News*, vol. 32, pp. 48–58, ACM, 2004.

[5] T. Lipcon, D. Alves, D. Burkert, J.-D. Cryans, A. Dembo, M. Percy, S. Rus, D. Wang, M. Bertozzi, C. P. McCabe, *et al.*, "Kudu: Storage for Fast Analytics on Fast Data," *Cloudera, inc*, 2015.

[6] G. DeCandia, D. Hastorun, M. Jampani, G. Kakulapati, A. Lakshman, A. Pilchin, S. Sivasubramanian, P. Vosshall, and W. Vogels, "Dynamo: Amazon's Highly Available Key-value Store," in *ACM SIGOPS operating systems*

review, vol. 41, pp. 205–220, ACM, 2007.

[7] A. Lakshman and P. Malik, "Cassandra: A Decentralized Structured Storage System," *ACM SIGOPS Operating Systems Review*, vol. 44, no. 2, pp. 35–40, 2010.

[8] K. Shvachko, H. Kuang, S. Radia, and R. Chansler, "The Hadoop Distributed File System," in *2010 IEEE 26th symposium on mass storage systems and technologies (MSST)*, pp. 1–10, IEEE, 2010.

[9] VMWare, "What is VMware vSAN?." `https://www.vmware.com/products/vsan.html`.

[10] A. Gulati, A. Holler, M. Ji, G. Shanmuganathan, C. Waldspurger, and X. Zhu, "VMware Distributed Resource Management: Design, Implementation, and Lessons Learned," *VMware Technical Journal*, vol. 1, no. 1, pp. 45–64, 2012.

[11] A. Tavakkol, M. Sadrosadati, S. Ghose, J. Kim, Y. Luo, Y. Wang, N. M. Ghiasi, L. Orosa, J. Gómez-Luna, and O. Mutlu, "FLIN: Enabling Fairness and Enhancing Performance in Modern NVMe Solid State Drives," in *2018 ACM/IEEE 45th Annual International Symposium on Computer Architecture (ISCA)*, pp. 397–410, IEEE, 2018.

[12] A. Tavakkol, J. Gómez-Luna, M. Sadrosadati, S. Ghose, and O. Mutlu, "MQSim: A Framework for Enabling Realistic Studies of Modern Multi-Queue {SSD} Devices," in *16th {USENIX} Conference on File and Storage Technologies ({FAST} 18)*, pp. 49–66, 2018.

[13] C. A. Waldspurger, "Memory Resource Management in VMware ESX Server," *ACM SIGOPS Operating Systems Review*, vol. 36, no. SI, pp. 181–194, 2002.

[14] C. R. Lumb, A. Merchant, and G. A. Alvarez, "Façade: Virtual Storage Devices with Performance Guarantees," in *FAST*, vol. 3, pp. 131–144, 2003.

[15] L. Huang, G. Peng, and T.-c. Chiueh, "Multi-Dimensional Storage Virtualization," in *ACM SIGMETRICS Performance Evaluation Review*, vol. 32, pp. 14–24, ACM, 2004.

[16] J. C. Wu and S. A. Brandt, "QoS support in Object-Based Storage Devices," in *Proceedings of the 3rd international workshop on storage network architecture and parallel I/Os (SNAPI'05)*, vol. 329, pp. 41–48, 2005.

[17] T. M. Wong, R. A. Golding, C. Lin, and R. A. Becker-Szendy, "Zygaria: Storage Performance as a Managed Resource," in *Real-Time and Embedded Technology and Applications Symposium, 2006. Proceedings of the 12th IEEE*, pp. 125–134, IEEE, 2006.

[18] A. Gulati, A. Merchant, and P. Varman, "d-clock: Distributed QoS in Heterogeneous Resource Environments," in *Proceedings of the twenty-sixth annual ACM symposium on Principles of distributed computing*, pp. 330–331, ACM, 2007.

[19] A. Povzner, D. Sawyer, and S. Brandt, "Horizon: Efficient Deadline-Driven Disk I/O Management for Distributed Storage Systems," in *Proceedings of the 19th ACM International Symposium on High Performance Distributed Computing*, pp. 1–12, ACM, 2010.

[20] A. Gulati, A. Merchant, and P. J. Varman, "mClock: Handling Throughput Variability for Hypervisor IO Scheduling," in *Proceedings of the 9th USENIX Conference on Operating Systems Design and Implementation*, pp. 437–450, USENIX Association, 2010.

[21] A. Gulati, G. Shanmuganathan, X. Zhang, and P. J. Varman, "Demand Based Hierarchical QoS Using Storage Resource Pools," in *USENIX Annual Technical Conference*, pp. 1–13, 2012.

[22] Y. Wang and A. Merchant, "Proportional-Share Scheduling for Distributed Storage Systems," in *FAST*, vol. 7, pp. 4–4, 2007.

[23] J. Zhang, A. Sivasubramaniam, Q. Wang, A. Riska, and E. Riedel, "Storage Performance Virtualization via Throughput and Latency Control," *ACM Transactions on Storage (TOS)*, vol. 2, no. 3, pp. 283–308, 2006.

[24] A. Gulati, A. Merchant, and P. J. Varman, "pClock: An Arrival Curve Based Approach For QoS. Guarantees In Shared Storage Systems," in *ACM SIGMETRICS Performance Evaluation Review*, vol. 35, pp. 13–24, ACM, 2007.

[25] A. Merchant, M. Uysal, P. Padala, X. Zhu, S. Singhal, and K. Shin, "Maestro: Quality-of-Service in Large Disk Arrays," in *Proceedings of the 8th ACM international conference on Autonomic computing*, pp. 245–254, ACM, 2011.

[26] X. Ling, H. Jin, S. Ibrahim, W. Cao, and S. Wu, "Efficient Disk I/O Scheduling with QoS Guarantee for Xen-based Hosting Platforms," in *Proceedings of the 2012 12th IEEE/ACM International Symposium on Cluster, Cloud and Grid Computing (CCGrid 2012)*, pp. 81–89, IEEE Computer Society, 2012.

[27] P. E. Rocha and L. C. Bona, "A QoS Aware Non-work-conserving Disk Scheduler," in *012 IEEE 28th Symposium on Mass Storage Systems and Technologies (MSST)*, pp. 1–5, IEEE, 2012.

[28] A. Wang, S. Venkataraman, S. Alspaugh, R. Katz, and I. Stoica, "Cake: Enabling High-level SLOs on Shared Storage Systems," in *Proceedings of the Third ACM*

Symposium on Cloud Computing, p. 14, ACM, 2012.

[29] H. Wang, K. Doshi, and P. Varman, "Nested QoS: Adaptive Burst Decomposition for SLO Guarantees in Virtualized Servers," *Intel Technology Journal*, vol. 16, no. 2, 2012.

[30] T. Zhu, A. Tumanov, M. A. Kozuch, M. Harchol-Balter, and G. R. Ganger, "Prioritymeister: Tail Latency QoS for Shared Networked Storage," in *Proceedings of the ACM Symposium on Cloud Computing*, pp. 1–14, ACM, 2014.

[31] N. Jain and J. Lakshmi, "PriDyn: Enabling Differentiated I/O Services in Cloud Using Dynamic Priorities," *IEEE Transactions on Services Computing*, vol. 8, no. 2, pp. 212–224, 2015.

[32] H. Lu, B. Saltaformaggio, R. Kompella, and D. Xu, "vFair: Latency-Aware Fair Storage Scheduling via Per-IO Cost-Based Differentiation," in *Proceedings of the Sixth ACM Symposium on Cloud Computing*, pp. 125–138, ACM, 2015.

[33] N. Li, H. Jiang, D. Feng, and Z. Shi, "PSLO: Enforcing the Xth Percentile Latency and Throughput SLOs for Consolidated VM Storage," in *Proceedings of the Eleventh European Conference on Computer Systems*, p. 28, ACM, 2016.

[34] C. Staelin, G. Amir, D. Ben-Ovadia, R. Dagan, M. Melamed, and D. Staas, "CSched: Real-time Disk Scheduling with Concurrent I/O Requests," tech. rep., Citeseer, 2011.

[35] L. Suresh, M. Canini, S. Schmid, and A. Feldmann, "C3: Cutting Tail Latency in Cloud Data Stores via Adaptive Replica Selection," in *12th USENIX Symposium on Networked Systems Design and Implementation (NSDI 15)*, pp. 513–527, 2015.

[36] Z. Lai, Y. Cui, M. Li, Z. Li, N. Dai, and Y. Chen, "TailCutter: Wisely Cutting Tail Latency in Cloud CDNs Under Cost Constraints," in *IEEE INFOCOM 2016-The 35th Annual IEEE International Conference on Computer Communications*, pp. 1–9, IEEE, 2016.

[37] J. Mace, P. Bodik, M. Musuvathi, R. Fonseca, and K. Varadarajan, "2DFQ: Two-Dimensional Fair Queuing for Multi-Tenant Cloud Services," in *Proceedings of the 2016 ACM SIGCOMM Conference*, pp. 144–159, ACM, 2016.

[38] H. Zhu and M. Erez, "Dirigent: Enforcing QoS for Latency-Critical Tasks on Shared Multicore Systems," *ACM SIGARCH Computer Architecture News*, vol. 44, no. 2, pp. 33–47, 2016.

[39] W. Reda, M. Canini, L. Suresh, D. Kostić, and S. Braithwaite, "Rein: Taming Tail Latency in Key-Value Stores via Multiget Scheduling," in *Proceedings of the Twelfth European Conference on Computer Systems*, pp. 95–110, ACM, 2017.

[40] V. Jaiman, S. B. Mokhtar, V. Quéma, L. Y. Chen, and E. Rivière, "Héron: Taming Tail Latencies in Key-Value Stores Under Heterogeneous Workloads," in *2018 IEEE 37th Symposium on Reliable Distributed Systems (SRDS)*, pp. 191–200, IEEE, 2018.

[41] M. Hao, H. Li, M. H. Tong, C. Pakha, R. O. Suminto, C. A. Stuardo, A. A. Chien, and H. S. Gunawi, "MittOS: Supporting Millisecond Tail Tolerance with Fast Rejecting SLO-Aware OS Interface," in *Proceedings of the 26th Symposium on Operating Systems Principles*, pp. 168–183, ACM, 2017.

[42] VMWare, "VMware vSphere 5.5 Release Notes." `https://www.vmware.com/support/vsphere5/doc/vsphere-esx-vcenter-server-55-release-notes.html`.

[43] "Code that Implements the dmClock Distributed Quality of Service Algorithm." `https://github.com/ceph/dmclock`.

[44] E. Jugwan, K. Taewoong, and P. Byungsu, "Implementing Distributed mClock in Ceph." `https://www.slideshare.net/ssusercee823/implementing-distributed-mclock-in-ceph`.

[45] H. Wang and P. Varman, "A Flexible Approach to Efficient Resource Sharing in Virtualized Environments," in *Proceedings of the 8th ACM International Conference on Computing Frontiers*, p. 39, ACM, 2011.

[46] Y. Peng and P. Varman, "bQueue: A Coarse-Grained Bucket QoS Scheduler," in *2018 18th IEEE/ACM International Symposium on Cluster, Cloud and Grid Computing (CCGrid)*, pp. 93–102, IEEE, 2018.

[47] Y. Peng, Q. Liu, and P. Varman, "Scalable QoS for Distributed Storage Clusters using Dynamic Token Allocation," in *35th International Conference on Massive Storage Systems and Technology (MSST)*, 2019.

[48] Y. Peng and P. Varman, "pTrans: A Scalable Algorithm for Reservation Guarantees in Distributed Systems," in *Proceedings of the 32nd ACM Symposium on Parallelism in Algorithms and Architectures*, pp. 441–452, 2020.

[49] Y. Peng and P. Varman, "Fair-EDF: A Latency Fairness Framework for Shared Storage Systems," in *11th USENIX Workshop on Hot Topics in Storage and File Systems (HotStorage)*, 2019.

[50] Y. Peng, Q. Liu, and P. Varman, "Latency Fairness Scheduling for Shared Storage Systems," in *14th IEEE International Conference on Networking, Architecture, and Storage (NAS)*, 2019.

[51] C. H. Papadimitriou, "On the Complexity of Integer Programming," *Journal of the ACM (JACM)*, vol. 28, no. 4, pp. 765–768, 1981.

[52] N. Karmarkar, "A New Polynomial-time Algorithm for Linear Programming," in *Proceedings of the sixteenth annual ACM symposium on Theory of computing*, pp. 302–311, 1984.

[53] J. Renegar, "A Polynomial-time Algorithm, Based on Newton's Method, for Linear Programming," *Mathematical programming*, vol. 40, no. 1-3, pp. 59–93, 1988.

[54] R. M. Freund, "Polynomial-time Algorithms for Linear Programming Based Only on Primal Scaling and Projected Gradients of a Potential Function," *Mathematical Programming*, vol. 51, no. 1-3, pp. 203–222, 1991.

[55] L. R. Ford and D. R. Fulkerson, "Maximal Flow Through a Network," *Canadian Journal of Mathematics*, vol. 8, no. 3, pp. 399–404, 1956.

[56] J. Edmonds and R. M. Karp, "Theoretical Improvements in Algorithmic Efficiency for Network Flow Problems," *Journal of the ACM (JACM)*, vol. 19, no. 2, pp. 248–264, 1972.

[57] Intel, "Intel® Xeon® Processor E5-2640 v4 (25M Cache, 2.40 GHz) Product Specifications." `https://ark.intel.com/products/92984/Intel-Xeon-Processor-E5-2640-v4-25M-Cache-2_40-GHz`.

[58] B. Fitzpatrick, "Distributed Caching with Memcached," *Linux journal*, vol. 2004, no. 124, p. 5, 2004.

[59] B. F. Cooper, A. Silberstein, E. Tam, R. Ramakrishnan, and R. Sears, "Benchmarking Cloud Serving Systems with YCSB," in *Proceedings of the 1st ACM*

symposium on Cloud computing, pp. 143–154, ACM, 2010.

[60] "YCSB Core Workloads." `https://github.com/brianfrankcooper/YCSB/wiki/Core-Workloads`.

[61] C. Lu, J. A. Stankovic, G. Tao, and S. H. Son, "Design and Evaluation of a Feedback Control EDF Scheduling Algorithm," in *Proceedings 20th IEEE Real-Time Systems Symposium (Cat. No. 99CB37054)*, pp. 56–67, IEEE, 1999.

[62] Ö. Ertug, M. Kallahalla, and P. J. Varman, "Real-Time Parallel I/O Stream Scheduling," in *Proceedings 2nd Intl. Workshop. on Compiler and Architecture Support for Embedded Systems*, 1999.

[63] C. L. Liu and J. W. Layland, "Scheduling Algorithms for Multiprogramming in a Hard-Real-Time Environment," *Journal of the ACM (JACM)*, vol. 20, no. 1, pp. 46–61, 1973.

[64] J. Xu and D. L. Parnas, "Scheduling Processes with Release Times, Deadlines, Precedence and Exclusion Relations," *IEEE Transactions on software engineering*, vol. 16, no. 3, pp. 360–369, 1990.

[65] Intel, "Intel® SSD DC S3700 Series." `https://ark.intel.com/content/www/us/en/ark/products/71915/intel-ssd-dc-s3700-series-400gb-2-5in-sata-6gb-s-25nm-mlc.html`.

[66] Intel, "Intel® Xeon® Processor E5-2697 v2." `https://ark.intel.com/content/www/us/en/ark/products/75283/intel-xeon-processor-e5-2697-v2-30m-cache-2-70-ghz.html`.